Star Formation in Galaxies and the “Bathtub” Model

ASTR:6782

Hai Fu

Star-Forming Regions in M51, a nearby grand-design spiral galaxy

Formation of Molecular Clouds and Stars in a Disk Galaxy

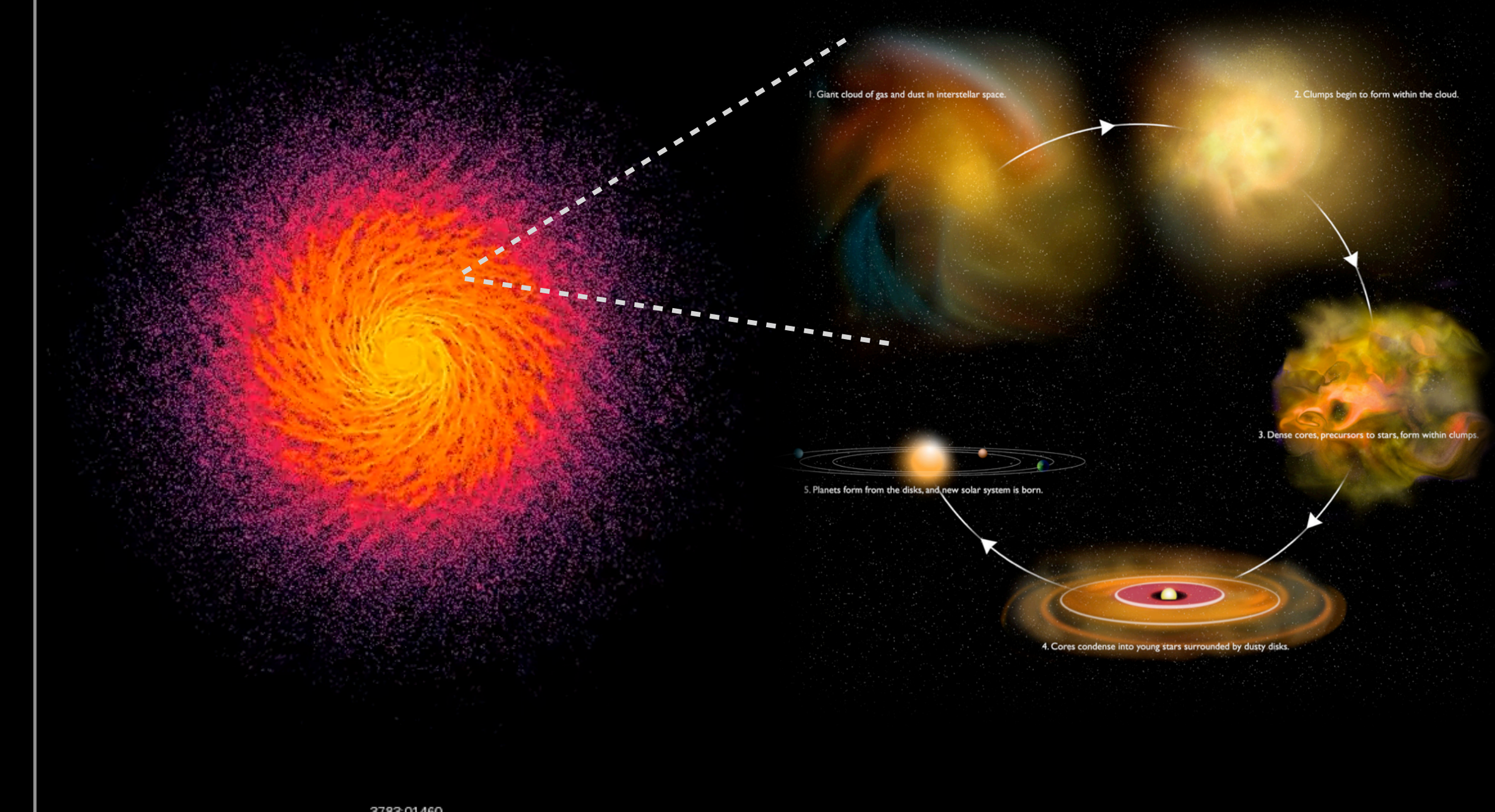

3783:01460

M51 - WHIRLPOOL GALAXY

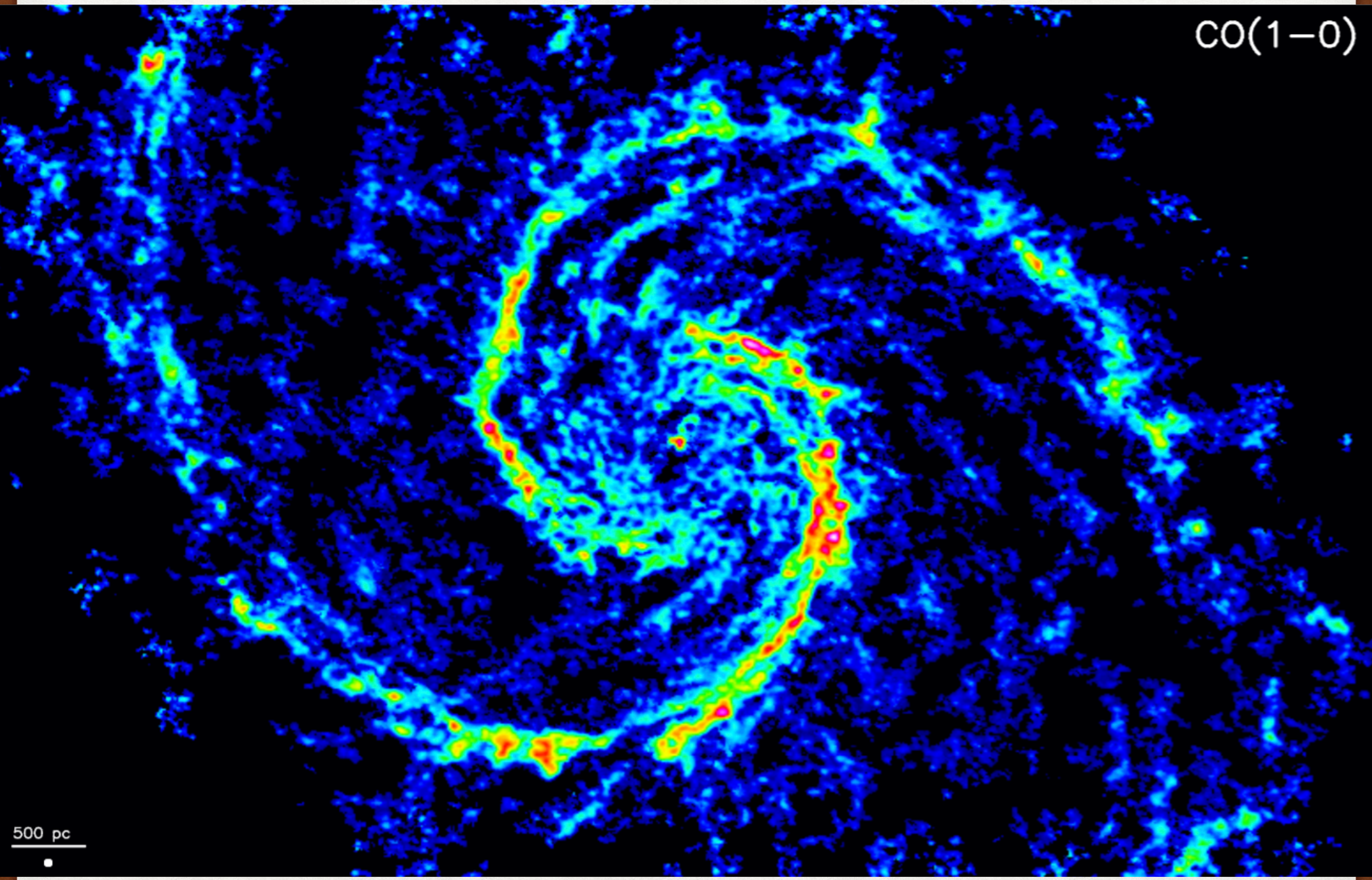

M51 - WHIRLPOOL GALAXY

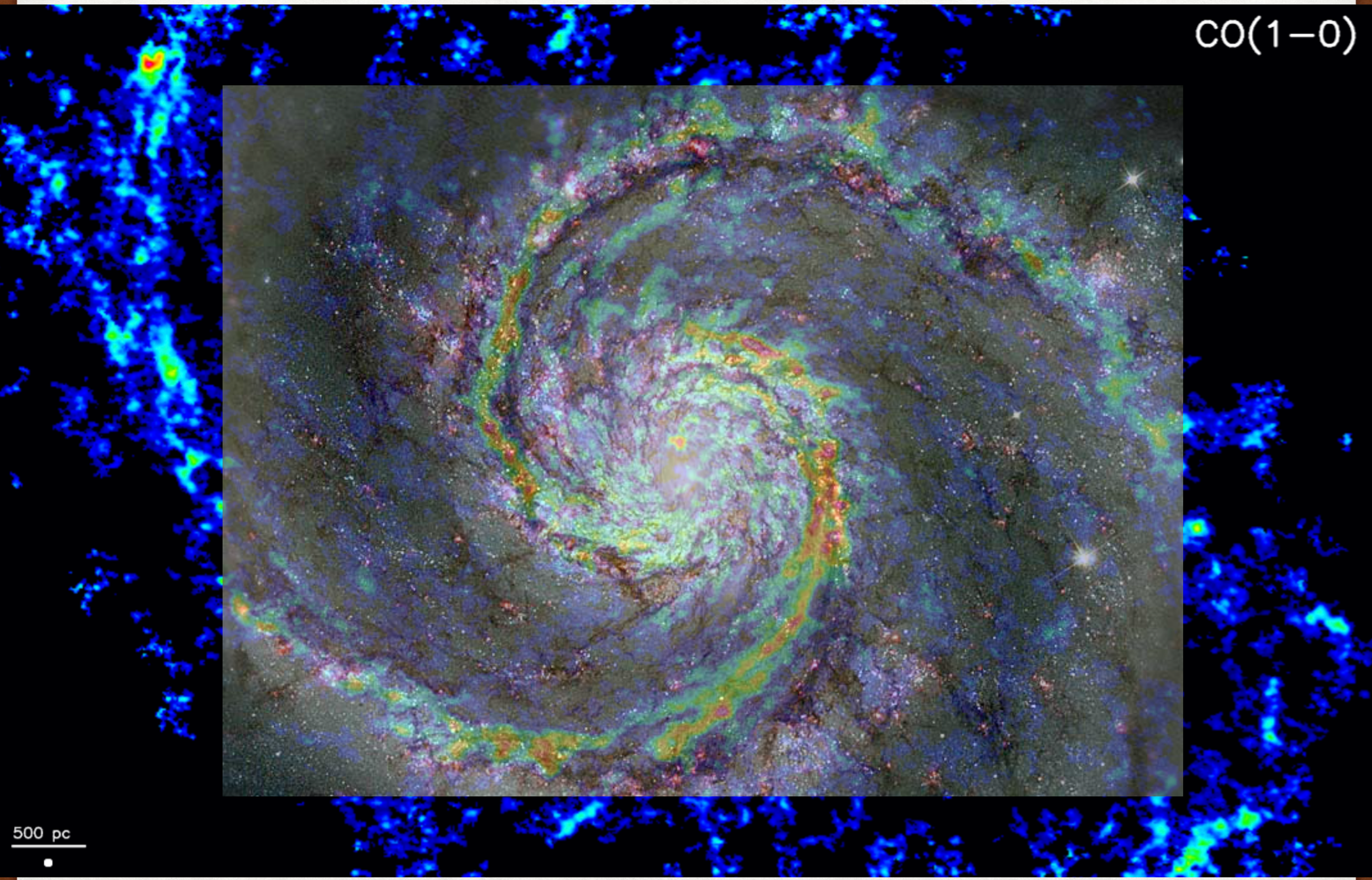

The Orion Star Forming Region

The Orion Star-Forming Region
(Optical Image)

The Orion Star-Forming Region
(Continuum + H-alpha)

Molecular Gas seen in CO J=1-0 transition

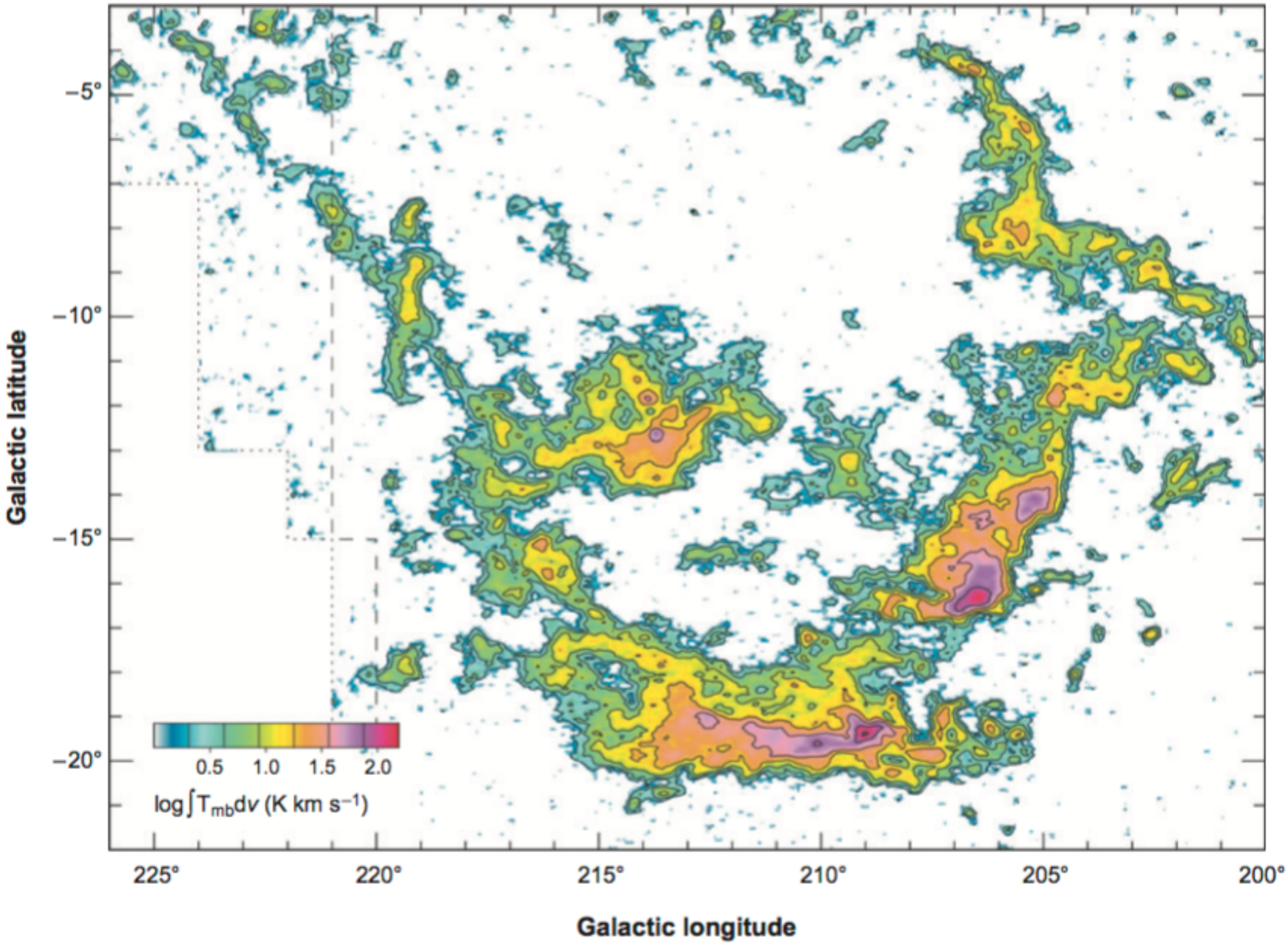

Molecular Gas (contours) vs. Ionized Gas (hue map)

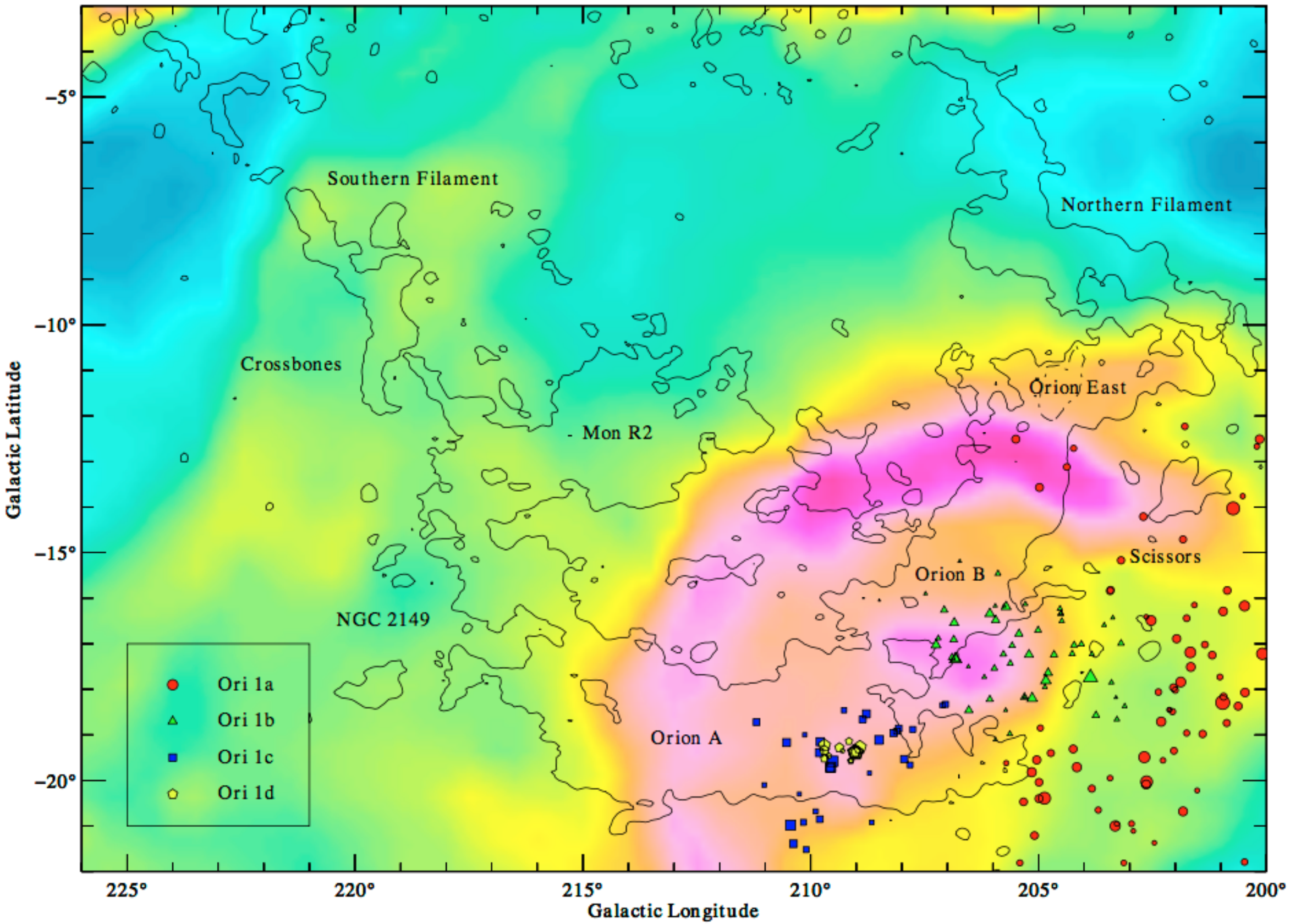

Cold Molecular Cores
(Boner-Elbert Spheres)

Bergin & Tafalla 2007

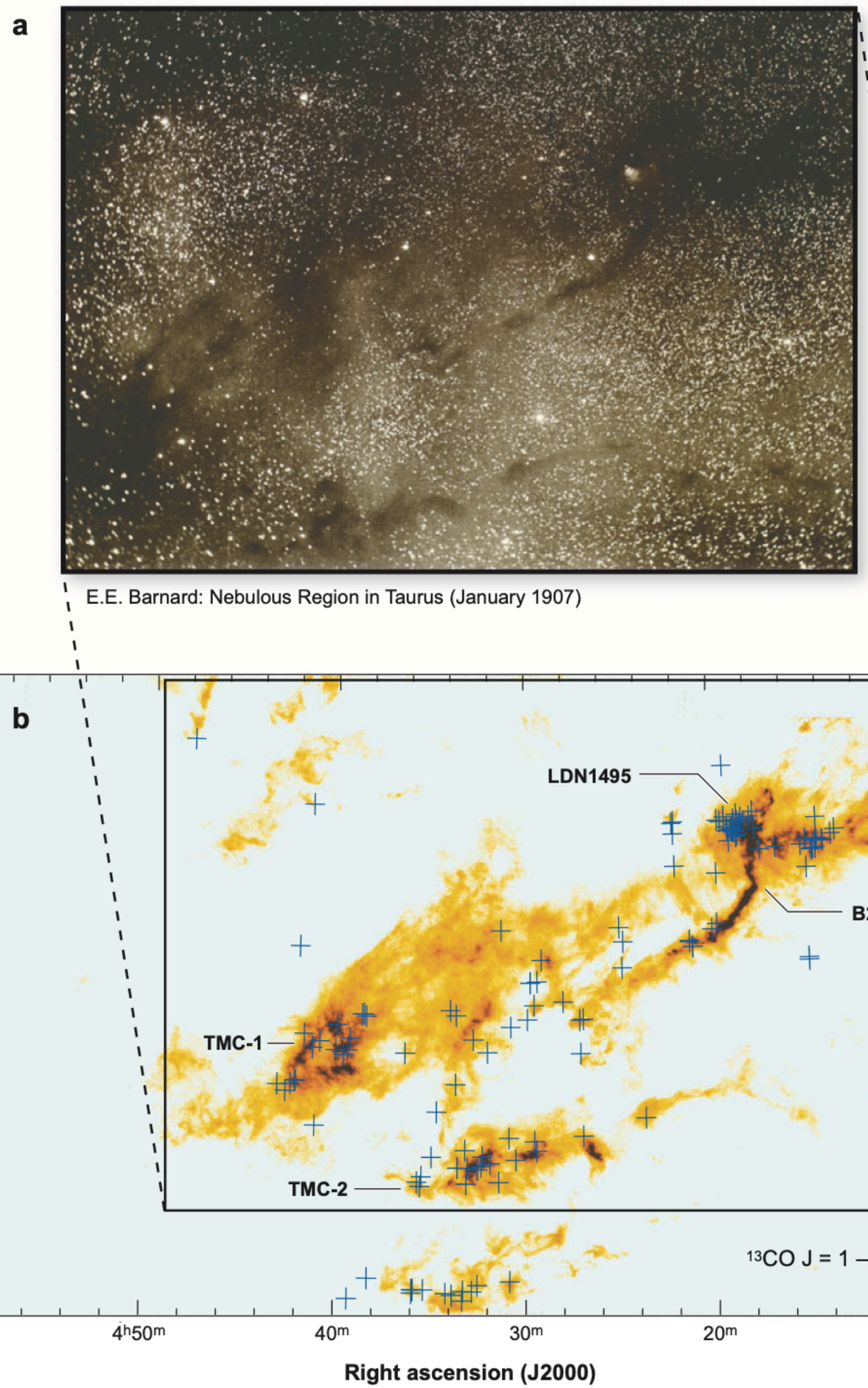

Optical photographic image of the Taurus molecular cloud, taken in 1907

CO(1-0) emission crosses indicate known stellar and protostellar objects

Bergin & Tafalla 2007

Table 1 Properties of dark clouds, clumps, and cores

	Clouds[a]	Clumps[b]	Cores[c]
Mass ($M_\odot$)	$10^3 - 10^4$	50–500	0.5–5
Size (pc)	2–15	0.3–3	0.03–0.2
Mean density (cm^{-3})	50–500	10^3–10^4	10^4–10^5
Velocity extent (km s^{-1})	2–5	0.3–3	0.1–0.3
Crossing time (Myr)	2–4	≈1	0.5–1
Gas temperature (K)	≈10	10–20	8–12
Examples	Taurus, Oph, Musca	B213, L1709	L1544, L1498, B68

[a]Cloud masses and sizes from the extinction maps by Cambrésy (1999), velocities and temperatures from individual cloud CO studies.
[b]Clump properties from Loren (1989) (^{13}CO data) and Williams, de Geus & Blitz (1994) (CO data).
[c]Core properties from Jijina, Myers & Adams (1999), Caselli et al. (2002a), Motte, André & Neri (1998), and individual studies using NH_3 and N_2H^+.

Barnard 68
dark core

Bergin & Tafalla 2007

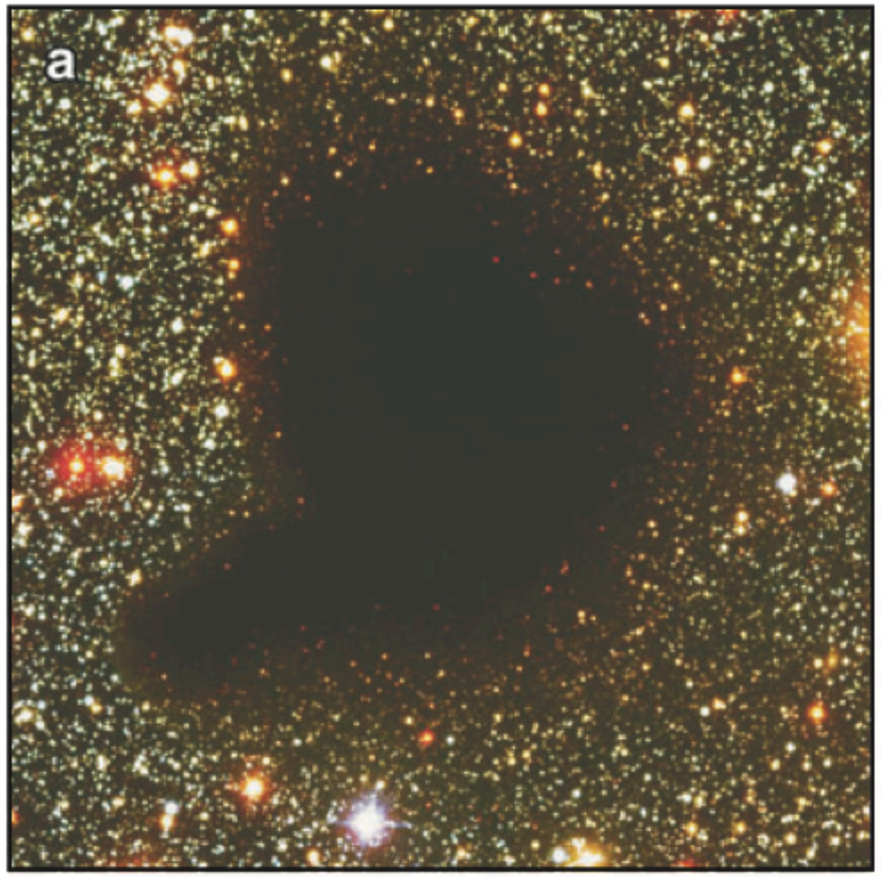

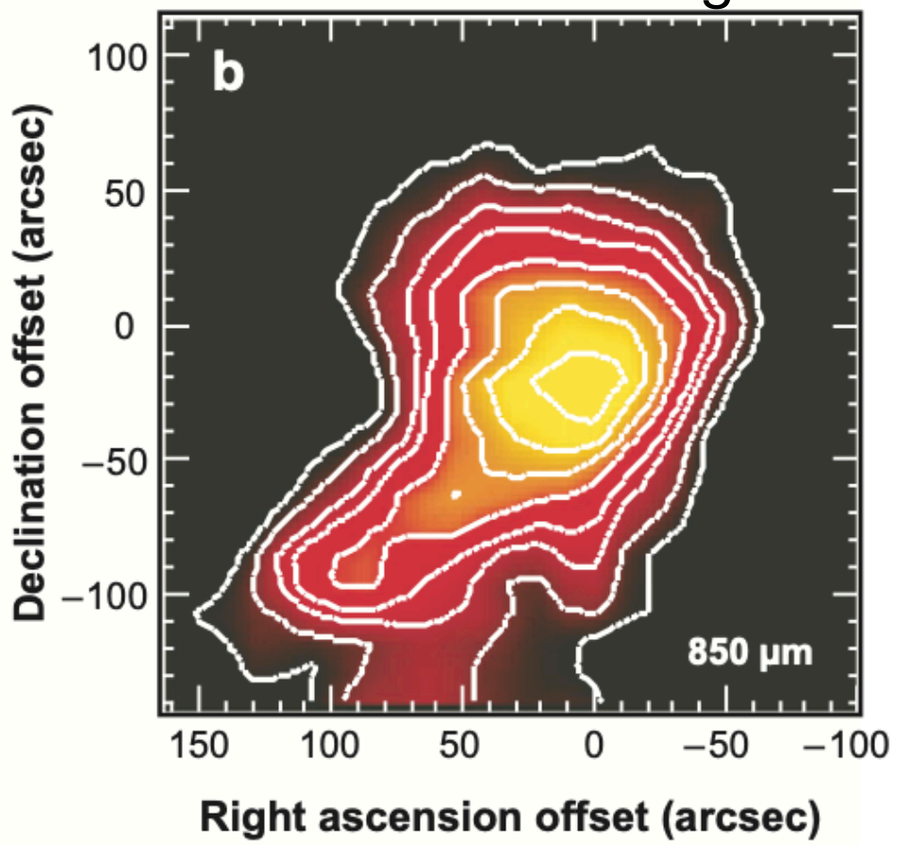

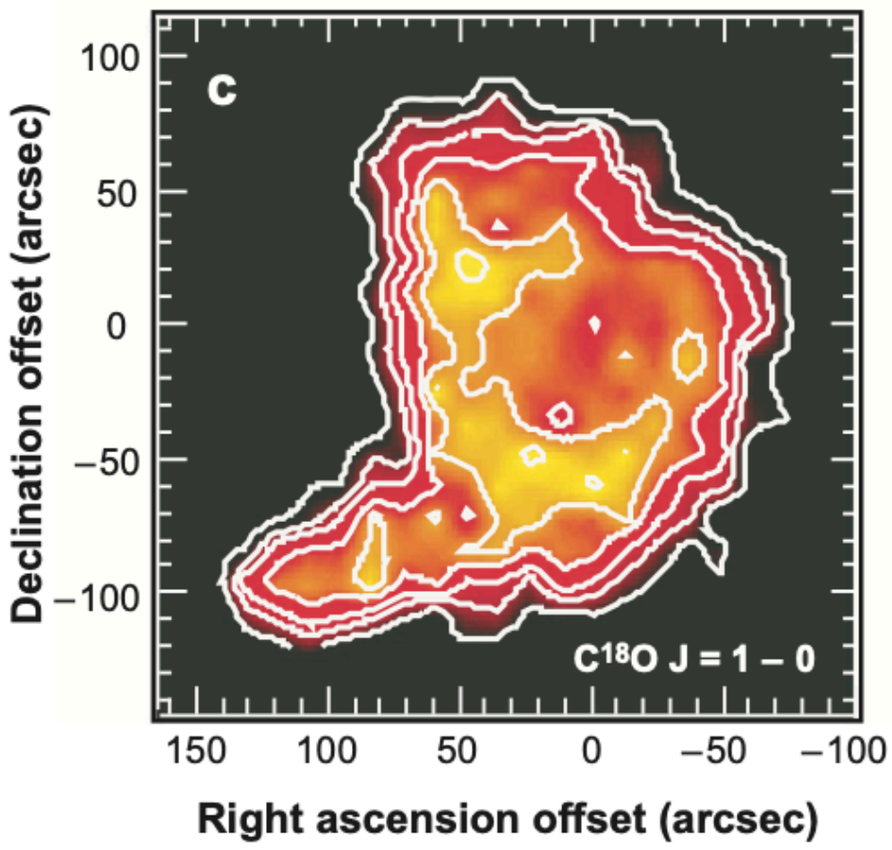

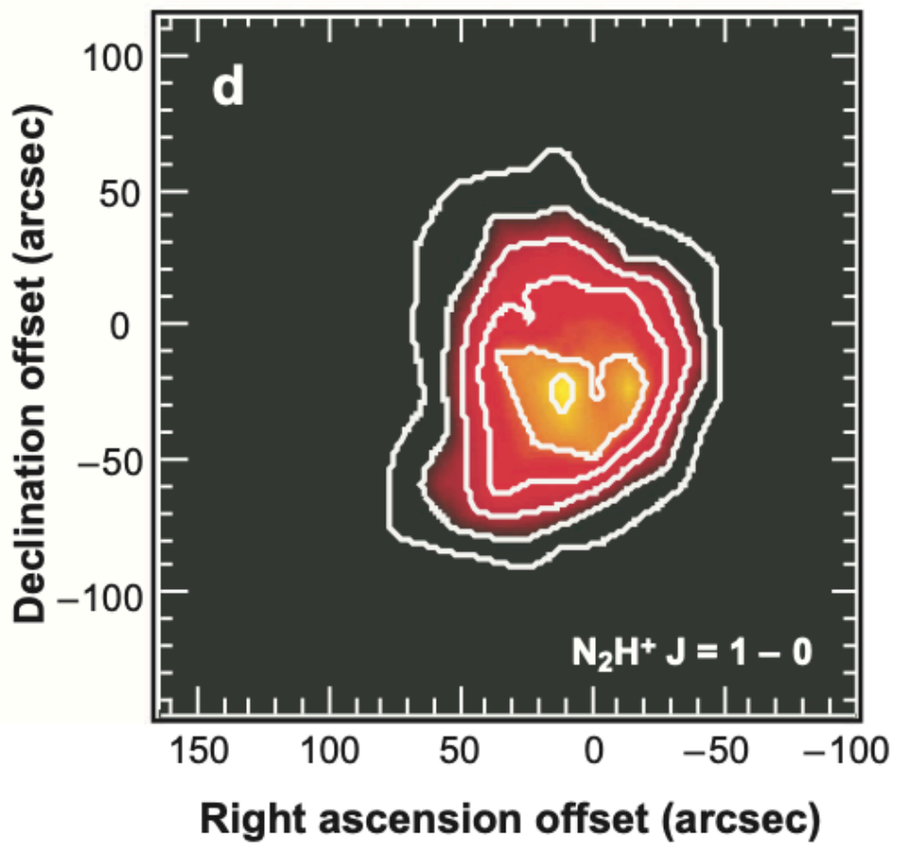

Bergin & Tafalla 2007

a Barnard 68 K band

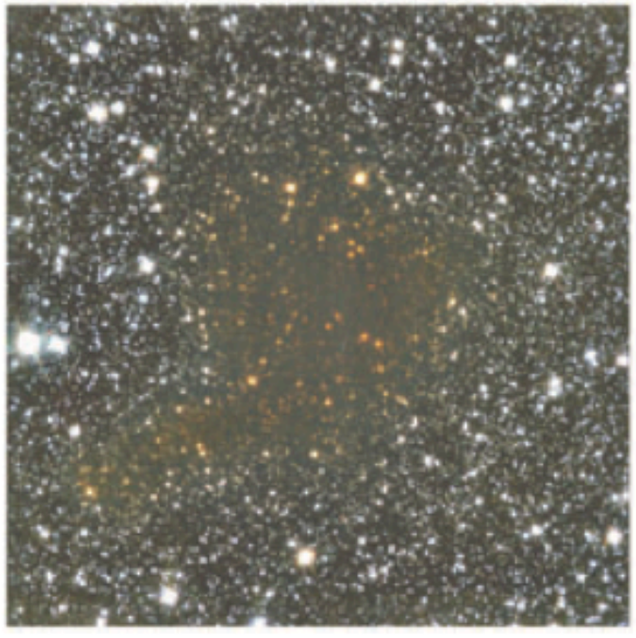

$A_V = r_V^{H,K} E(H-K)$

$A_V = f N_H$

$N_H = (r_V^{H,K} f^{-1}) \cdot E(H-K)$

b L1544 1.2 mm continuum

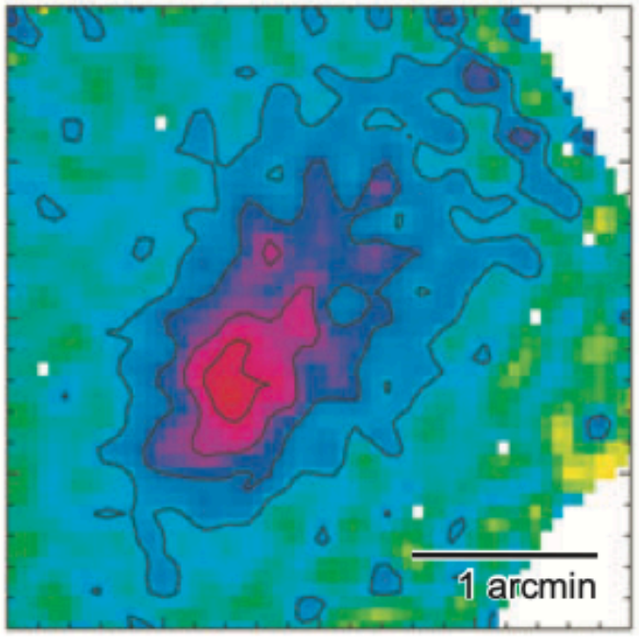

For optically thin emission:

$I_\nu = \int \kappa_\nu \rho \, B_\nu(T_d) dl$

$I_\nu = m \langle \kappa_\nu B_\nu(T_d) \rangle N_H$

$N_H = I_\nu \, [\langle m \kappa_\nu B_\nu(T_d) \rangle]^{-1}$

c ρ Oph core D 7 μm image

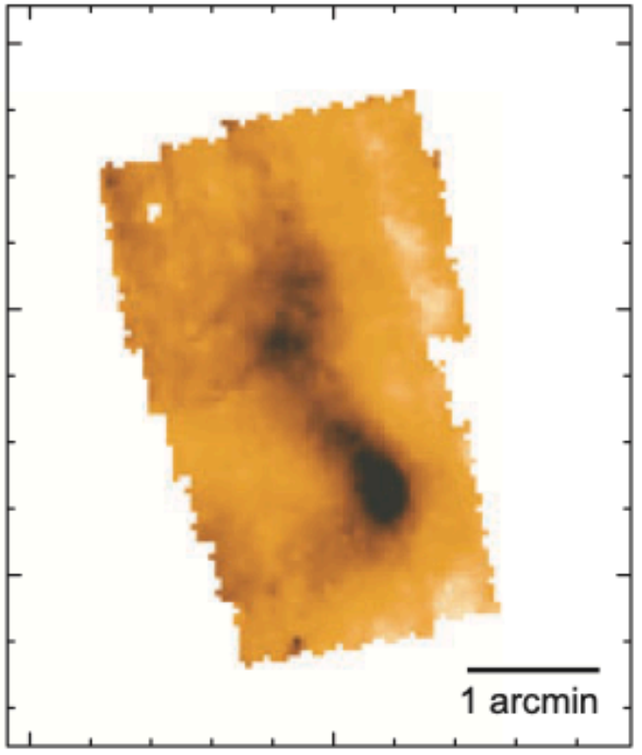

$I_\nu = I_\nu^{bg} \exp(-\tau_\lambda) + I_\nu^{fg}$

$\tau_\lambda = \sigma_\lambda N_H$

$$N_H = \frac{1}{\sigma_\lambda} \, ln\left[\frac{I_\nu^{bg}}{I_\nu - I_\nu^{fg}}\right]$$

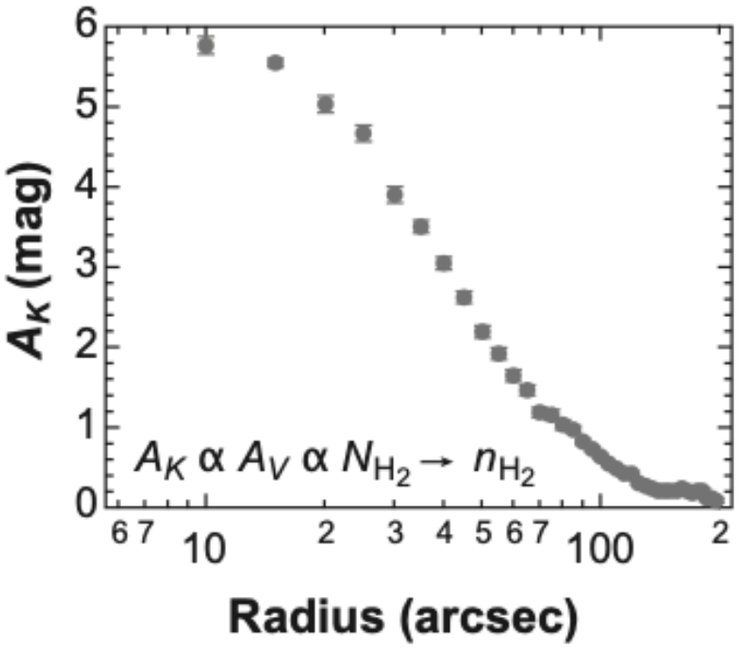

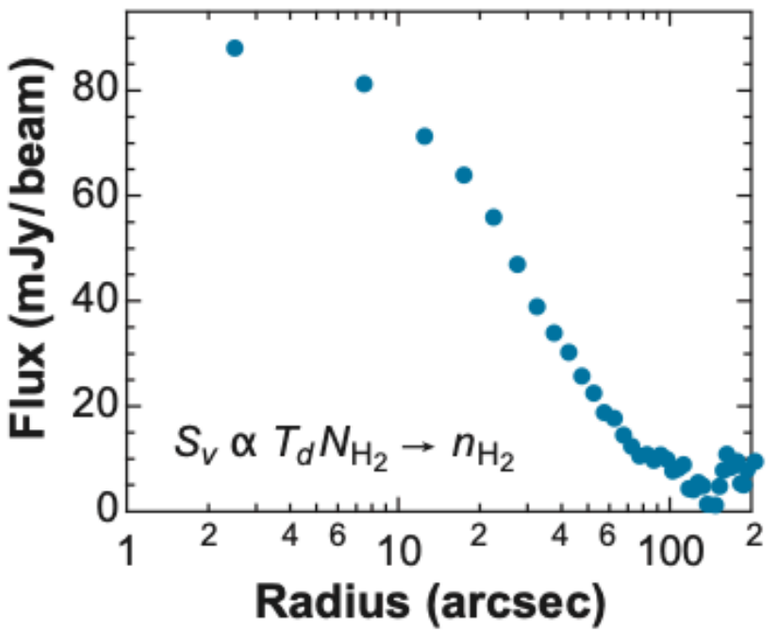

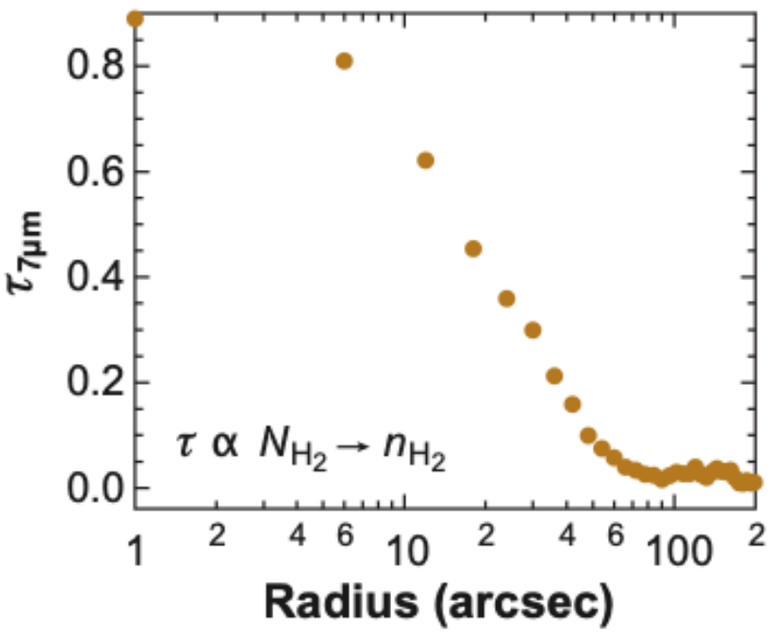

Bonnor-Ebert Sphere Fit to Extinction Data of the Barnard 68 Core

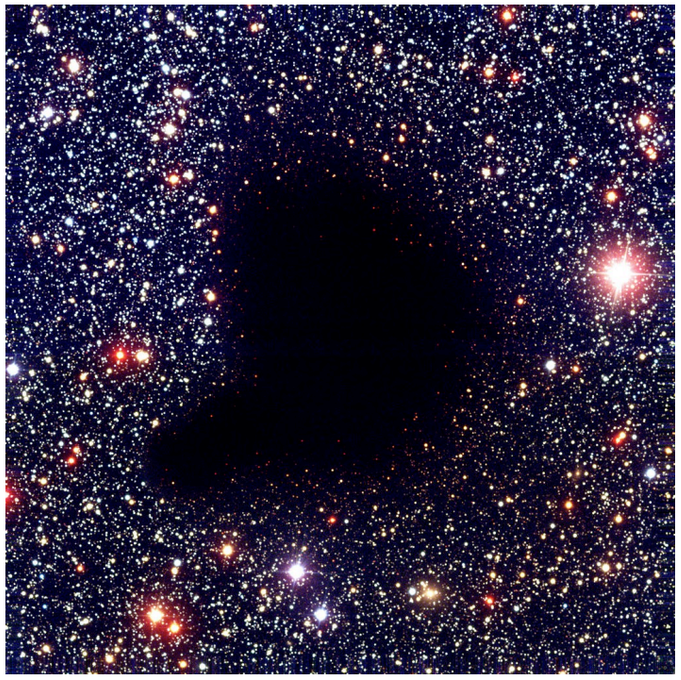

B68 visual extinction

Observations

Bonnor Ebert profile

A_V (mag)

30

10

3

1

10

30

100

Projected radius ('')

Williams 2021

Isothermal Lane-Emden Equation

hydrostatic equilibrium: $\frac{dP}{dr} = c_s^2 \frac{d\rho}{dr} = -\rho \frac{d\Phi}{dr}$ $\Rightarrow \rho = \rho_c \exp\left(-\frac{\Phi - \Phi_c}{c_s^2}\right)$

ideal gas law: $P = \rho \frac{kT}{\mu m_p} = \rho c_s^2$

isothermal sound speed: $c_s = \sqrt{\frac{dP}{d\rho}} = \sqrt{\frac{kT}{\mu m_p}}$

Poisson Equation: $\nabla^2 \Phi = \frac{1}{r^2}\frac{d}{dr}\left(r^2 \frac{d\Phi}{dr}\right) = 4\pi G\rho$

Define dimensionless radius and potential: $x = \left(\frac{4\pi G\rho_c}{c_s^2}\right) r$ $y \equiv \frac{\Phi - \Phi_c}{c_s^2} = \ln(\rho_c/\rho)$

one obtains LEE: $\frac{1}{x^2}\frac{d}{dx}\left(x^2 \frac{dy}{dx}\right) = e^{-y}$

or: $\frac{d^2y}{dx^2} = e^{-y} - \frac{2}{x}\frac{dy}{dx}$

Bonnor-Ebert Spheres: Non-Singular Solution of LEE

Define dimensionless radius and potential:

$$x = \left(\frac{4\pi G\rho_c}{c_s^2}\right) r \qquad y \equiv \frac{\Phi - \Phi_c}{c_s^2} = \ln(\rho_c/\rho)$$

one obtains LEE:

$$\frac{1}{x^2}\frac{d}{dx}\left(x^2\frac{dy}{dx}\right) = e^{-y} \quad \text{or} \quad \frac{d^2y}{dx^2} = e^{-y} - \frac{2}{x}\frac{dy}{dx}$$

boundary condition:

$$\text{at } x = 0, y = 0, \frac{dy}{dx} = 0, \rho = \rho_c \text{ at a finite value}$$

Taylor expansion:

$$y(x_0 + h) = y(x_0) + hy'(x_0) + \frac{h^2}{2}y''(x_0)$$

Solve by applying **Euler's method** to the LEE:

- $x_i = x_{i-1} + h$
- $y_i = y_{i-1} + y'_{i-1}h + y''_{i-1}h^2/2$
- $y'_i = y'_{i-1} + y''_{i-1}h$
- $y''_i = e^{-y_i} - 2y'_i/x_i$

Bonnor-Ebert Spheres

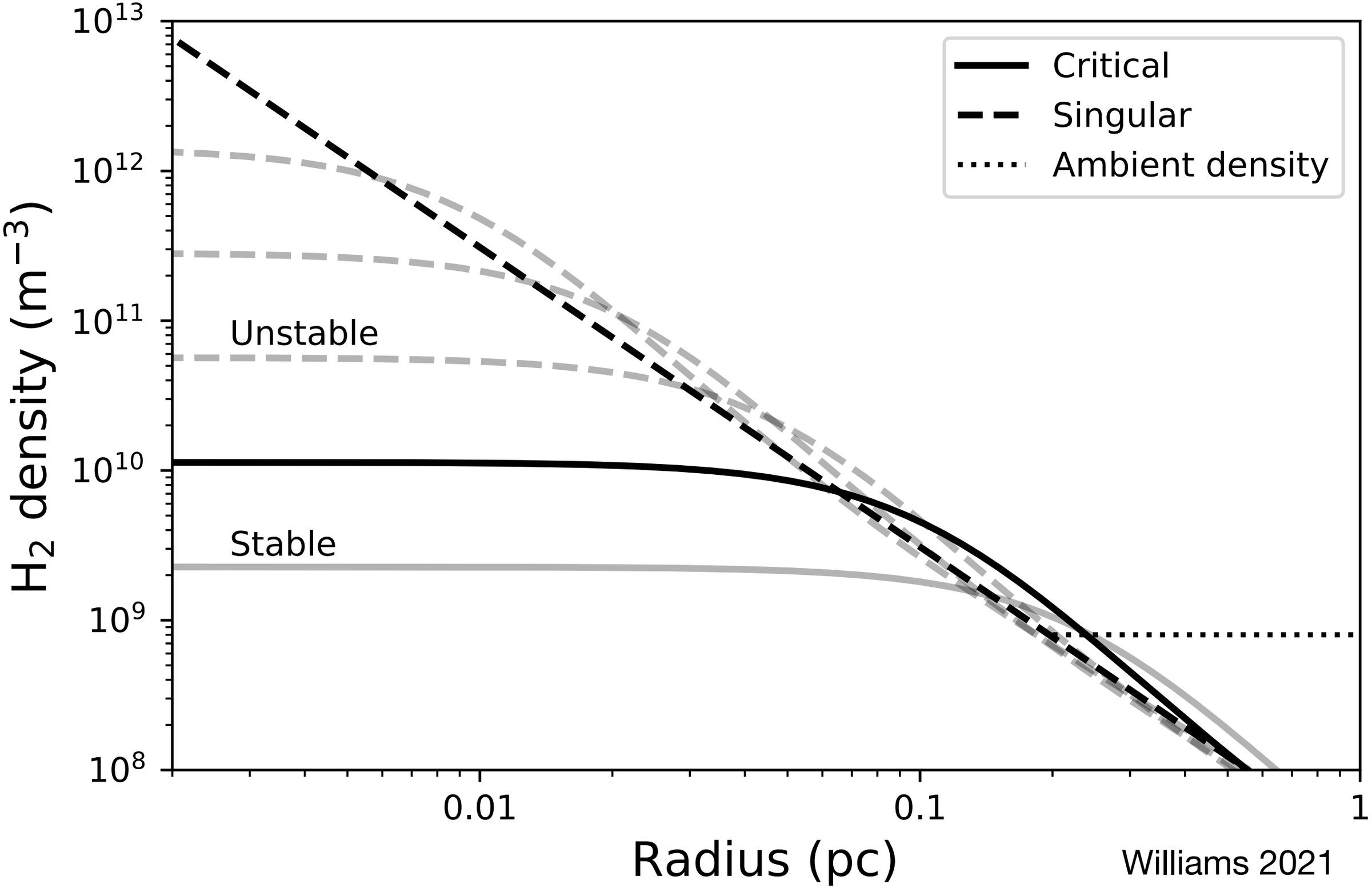

The Maximum Mass and the Stability of Bonnor-Ebert Sphere

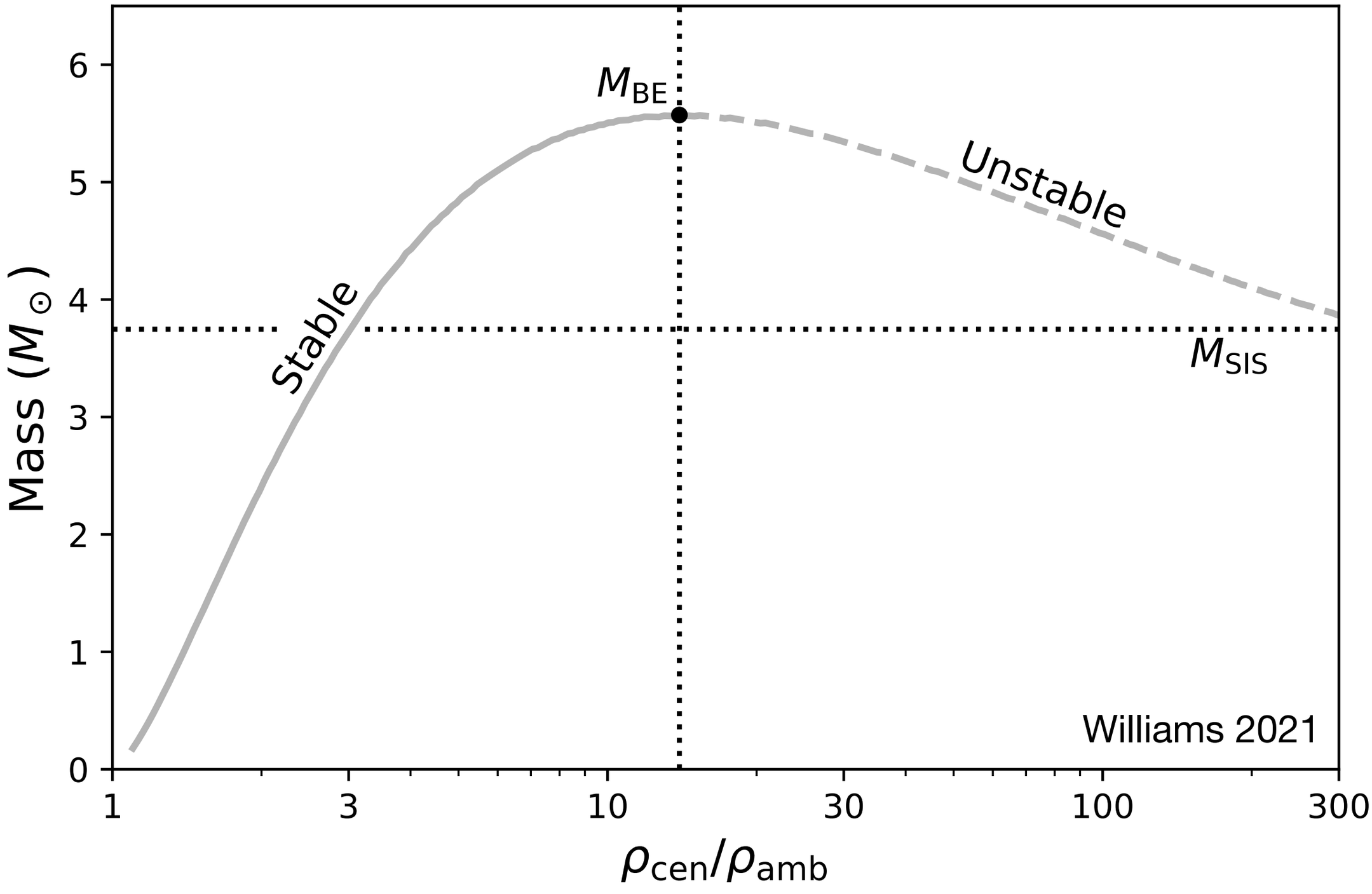

Constructing a simple analytical model

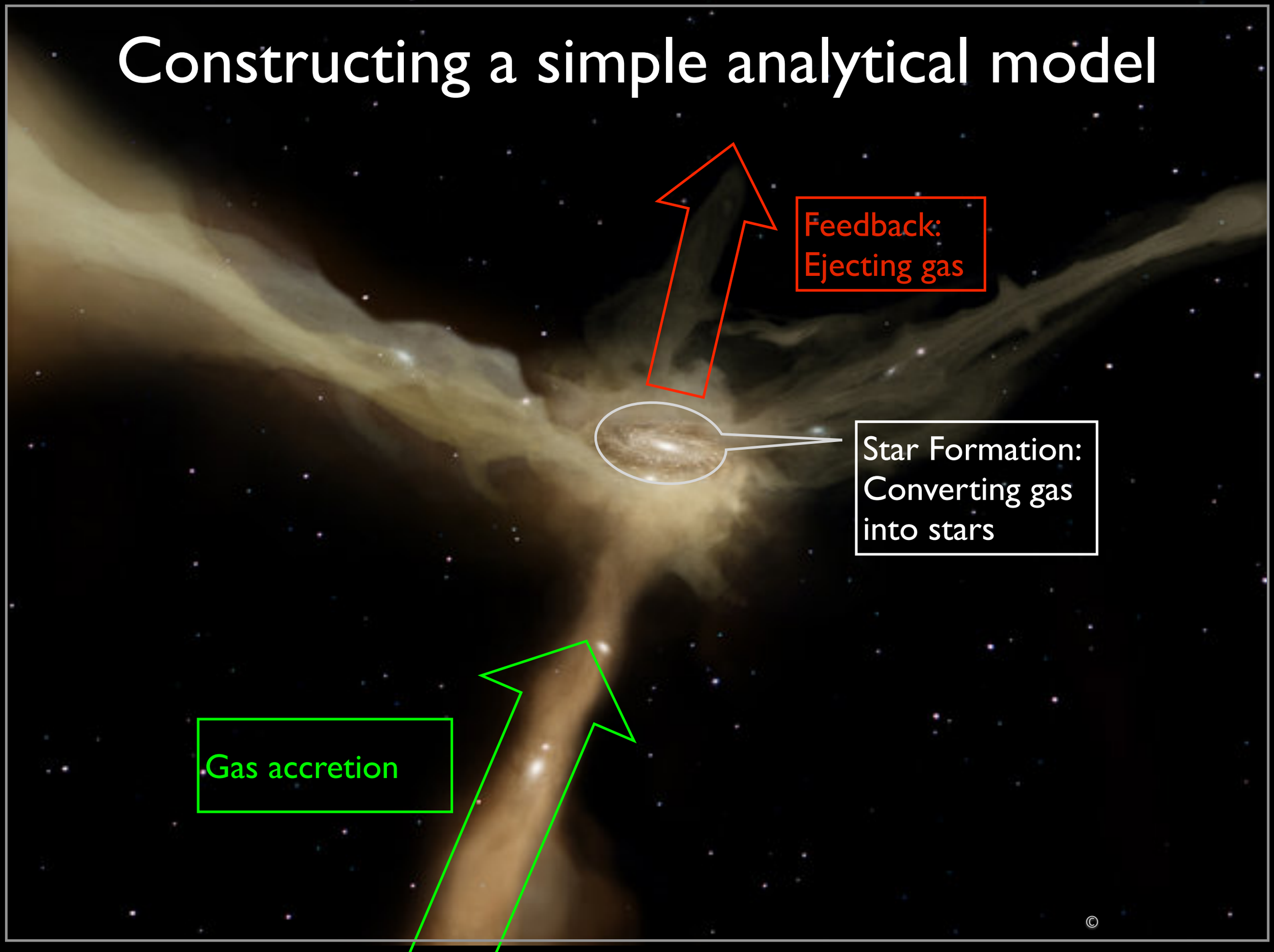

The “Bathtub” Model

Bouche+2010
see also Lilly+2013
Cattaneo+2006
Dekel & Birnboim 2006

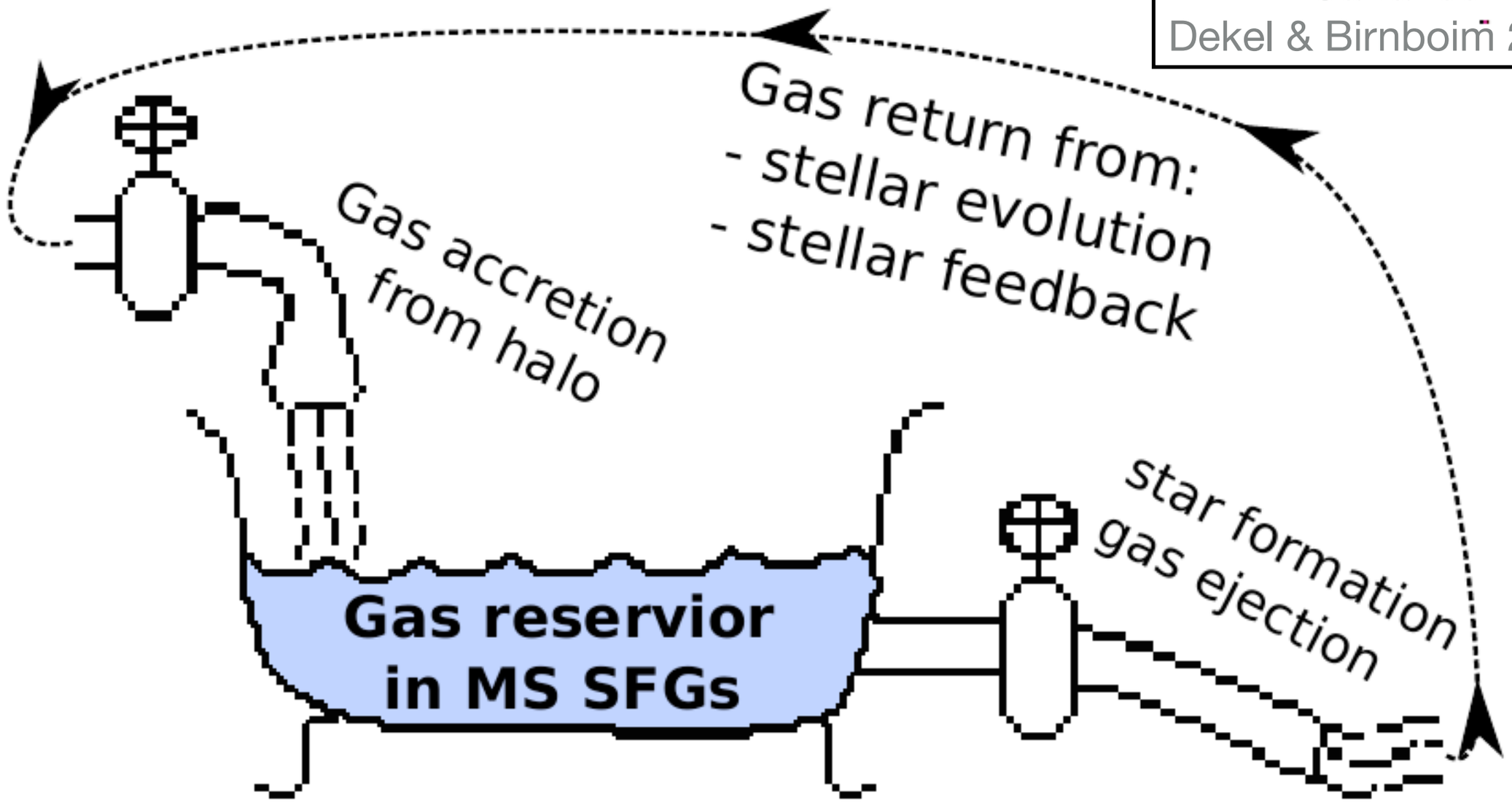

A Simple Analytical Model

(1) a continuity equation:

Change in Cold Gas Reservoir = **Accretion Rate** ∝ **Halo Growth Rate** − **Gas Consumption Rate** ∝ **Star Formation Rate**

$$\frac{dM_{\rm gas}}{dt} = \epsilon_{\rm cold} f_{\rm baryon} \frac{dM_{\rm halo}}{dt} - (1 - f_{\rm recycle} + f_{\rm outflow}) \frac{dM_{\rm star}}{dt}$$

where stellar growth decouples from halo growth, as specified by the cold gas accretion efficiency ($\epsilon_{\rm cold}$) that depends on halo mass

Virialized halo gas cools effectively only in the mass range where $t_{cool} < t_{ff}$

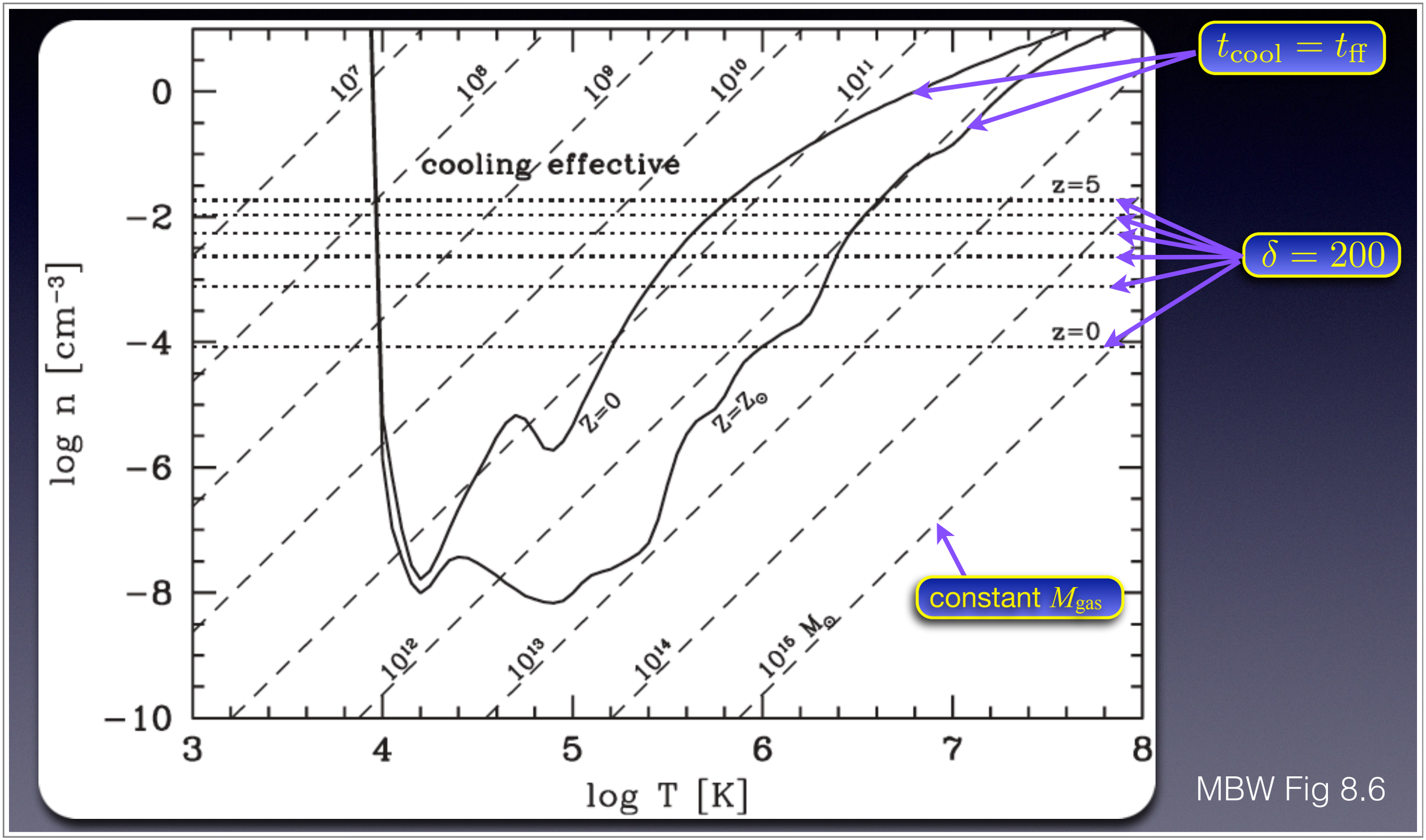

MBW Fig 8.6

The Cold Gas Accretion Rate

$$\frac{dM_{\rm gas}}{dt} = \epsilon_{\rm cold} f_{\rm baryon} \frac{dM_{\rm halo}}{dt}$$

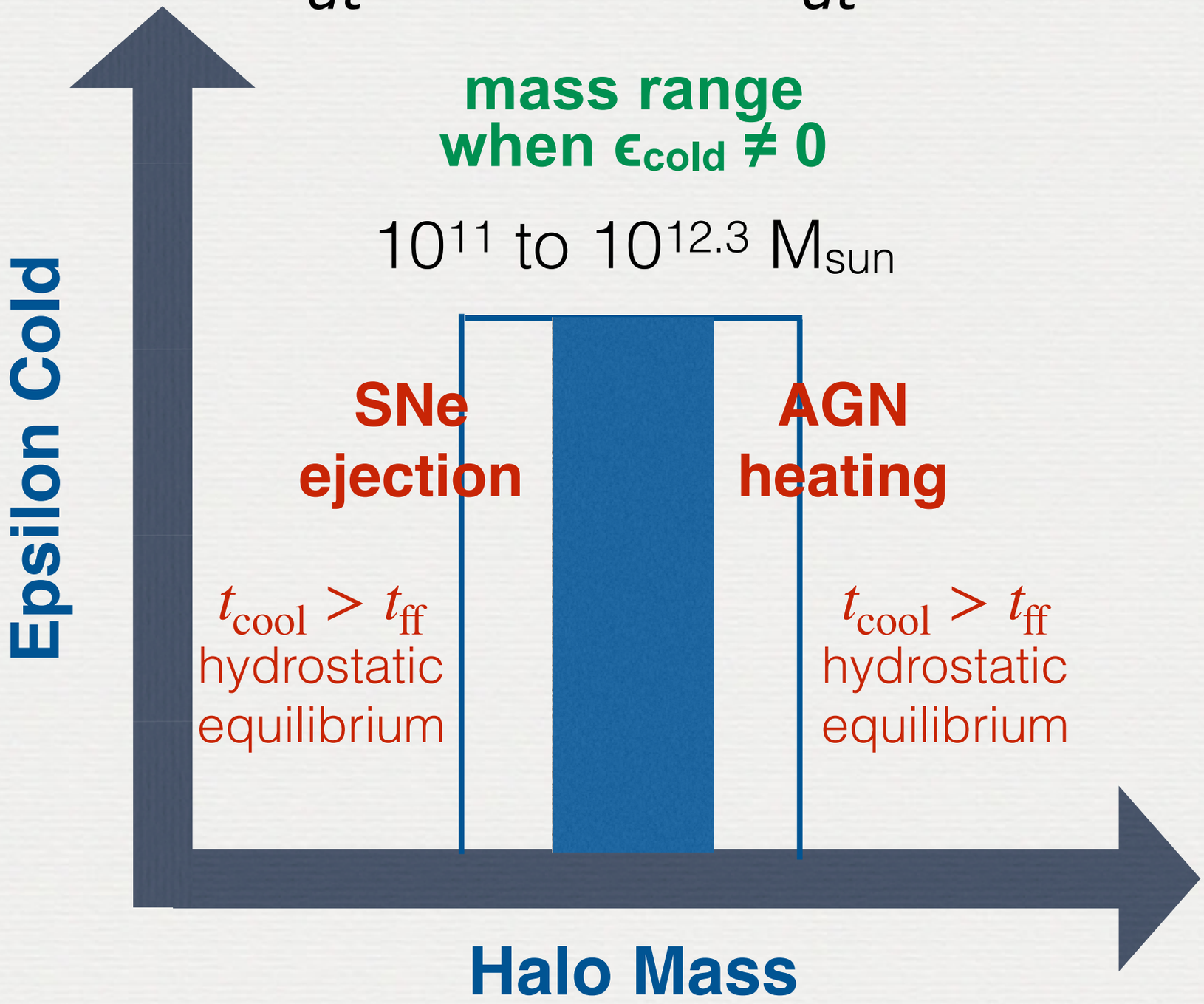

The `Bathtub'' Model

(1) a continuity equation:

Change in Cold Gas Reservoir **Accretion Rate ∝ Halo Growth Rate** **Gas Consumption Rate ∝ Star Formation Rate**

$$\frac{dM_{\rm gas}}{dt} = \epsilon_{\rm cold} f_{\rm baryon} \frac{dM_{\rm halo}}{dt} - (1 - f_{\rm recycle} + f_{\rm outflow}) \frac{dM_{\rm star}}{dt}$$

Where stellar growth decouples from halo growth is specified by the cold gas accretion efficiency ($\epsilon_{\rm cold}$)

$$\begin{cases} \epsilon_{\rm cold} = 0.0 \text{ if } M_{\rm halo} < 10^{11} M_{\odot} \\ \epsilon_{\rm cold} = 0.7 \text{ if } 10^{11} < M_{\rm halo} < 10^{12.3} M_{\odot} \\ \epsilon_{\rm cold} = 0.0 \text{ if } M_{\rm halo} > 10^{12.3} M_{\odot} \end{cases}$$

But we need two additional equations to solve the continuity equation.

The `Bathtub'' Model

(2) halo growth from PS formalism: $\frac{dM_{\rm halo}}{dt} \propto M_{\rm halo}^{1.1}(1+z)^{2.2}$

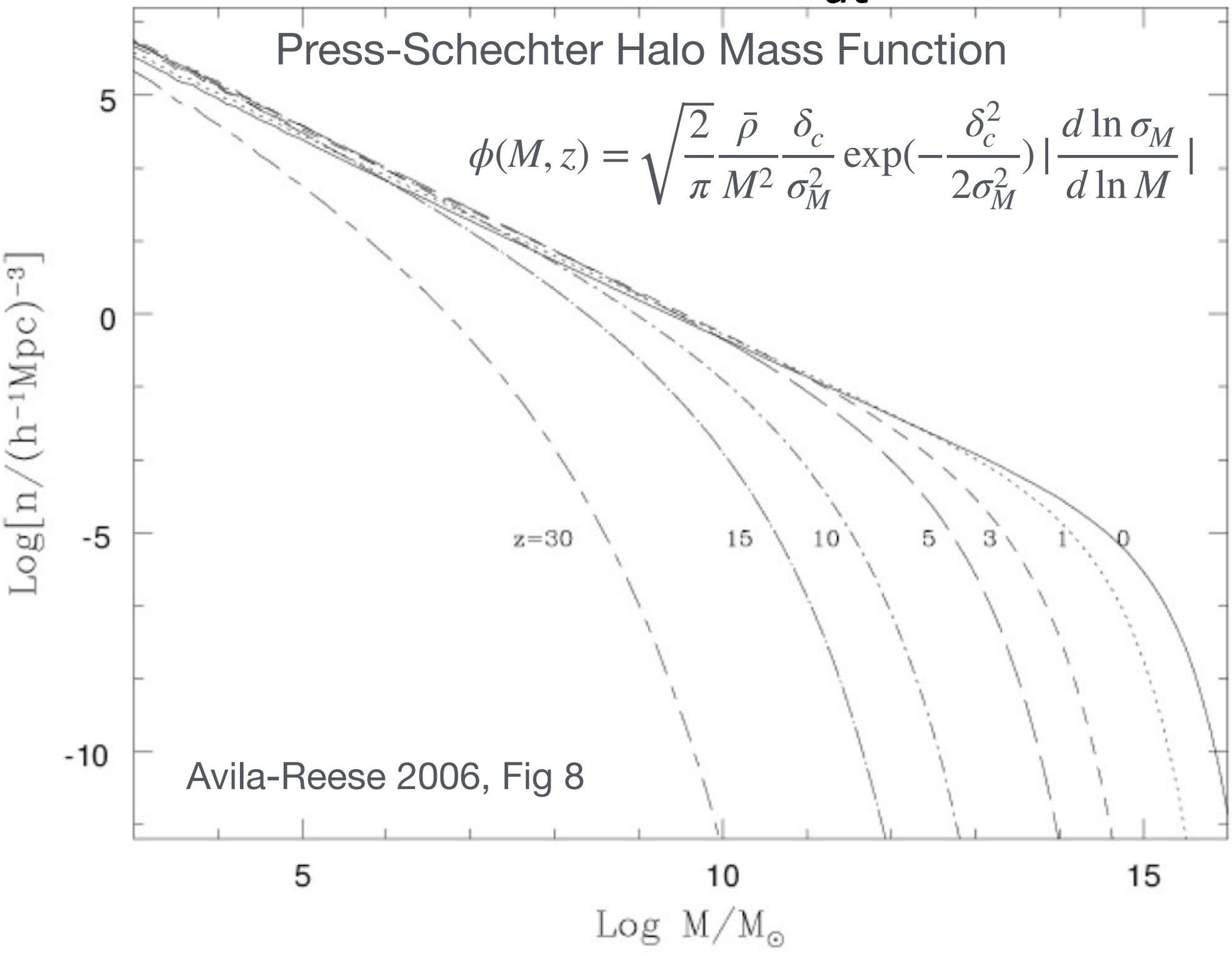

Avila-Reese 2006, Fig 8

Halo mass vs. redshift & time

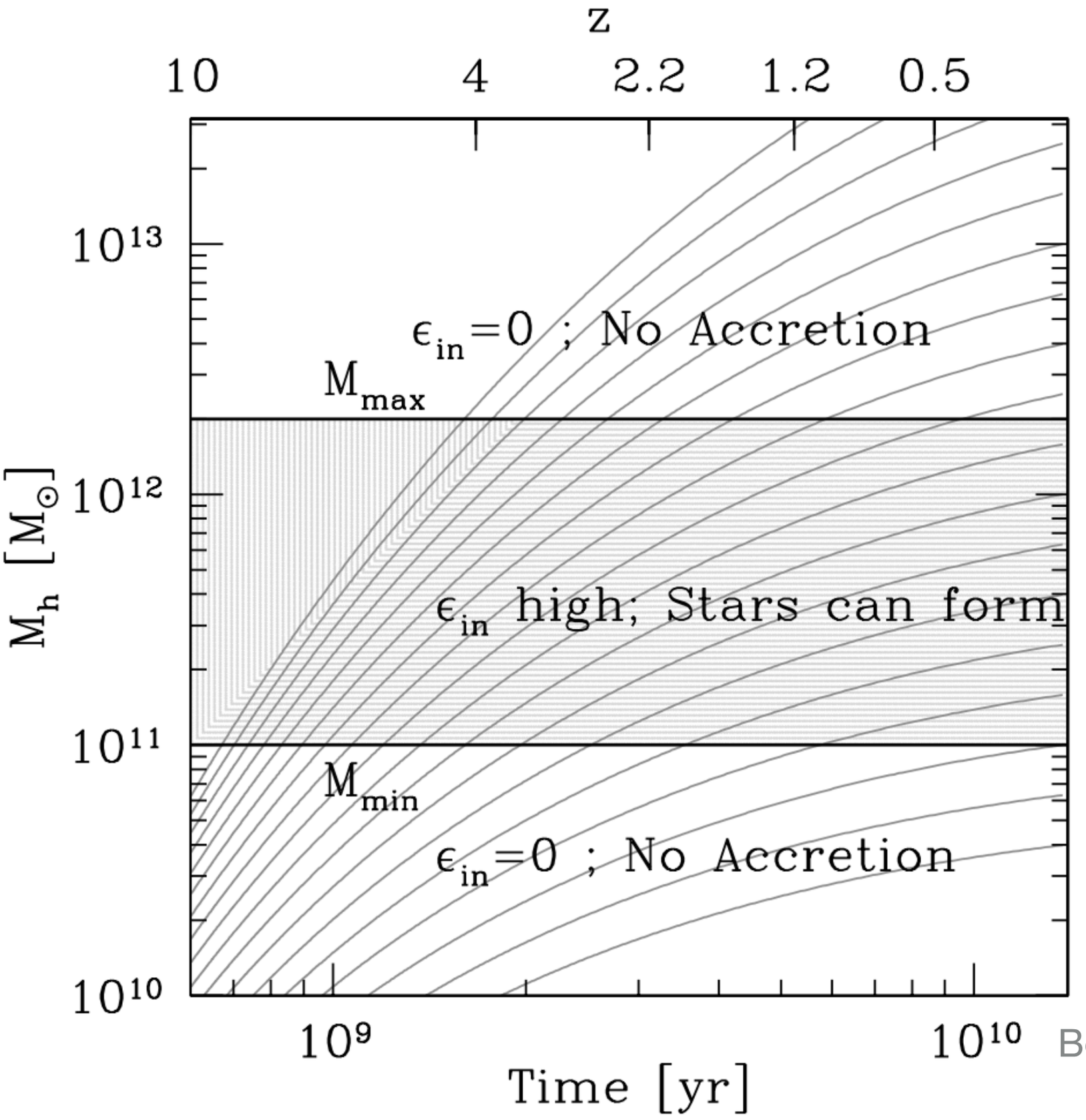

Accretion Rate ∝ Halo Growth Rate

$$\epsilon_{\rm cold} f_{\rm baryon} \frac{dM_{\rm halo}}{dt}$$

$$\frac{dM_{\rm halo}}{dt} \propto M_{\rm halo}^{1.1}(1+z)^{2.2}$$

Bouche+2010

The `Bathtub'' Model

(3) a star formation law, $\dot{M}_{\rm star} \propto M_{\rm gas}$

Change in Cold Gas Reservoir | **Accretion Rate ∝ Halo Growth Rate** | **Gas Consumption Rate ∝ Star Formation Rate**

$$\frac{dM_{\rm gas}}{dt} = \epsilon_{\rm cold} f_{\rm baryon} \frac{dM_{\rm halo}}{dt} - (1 - f_{\rm recycle} + f_{\rm outflow}) \frac{dM_{\rm star}}{dt}$$

$$\begin{cases} \dfrac{dM_{\rm halo}}{dt} \propto M_{\rm halo}^{1.1}(1+z)^{2.2} & \leftarrow \textbf{Halo Growth Rate from EPS} \\ \dfrac{dM_{\rm star}}{dt} = {\rm SFR} = \epsilon_{\rm SF} \dfrac{M_{\rm gas}}{\tau_{\rm dyn}} & \leftarrow \textbf{Star Formation Law} \end{cases}$$

cold gas accretion efficiency:

$$\begin{cases} \epsilon_{\rm cold} = 0.0 \text{ if } M_{\rm halo} < 10^{11} M_\odot \\ \epsilon_{\rm cold} = 0.7 \text{ if } 10^{11} < M_{\rm halo} < 10^{12.3} M_\odot \\ \epsilon_{\rm cold} = 0.0 \text{ if } M_{\rm halo} > 10^{12.3} M_\odot \end{cases}$$

recycle & feedback:

$$\begin{cases} f_{\rm recycle} = 0.5 \\ f_{\rm outflow} = 0.6 \end{cases}$$

Accretion-Driven Star Formation History

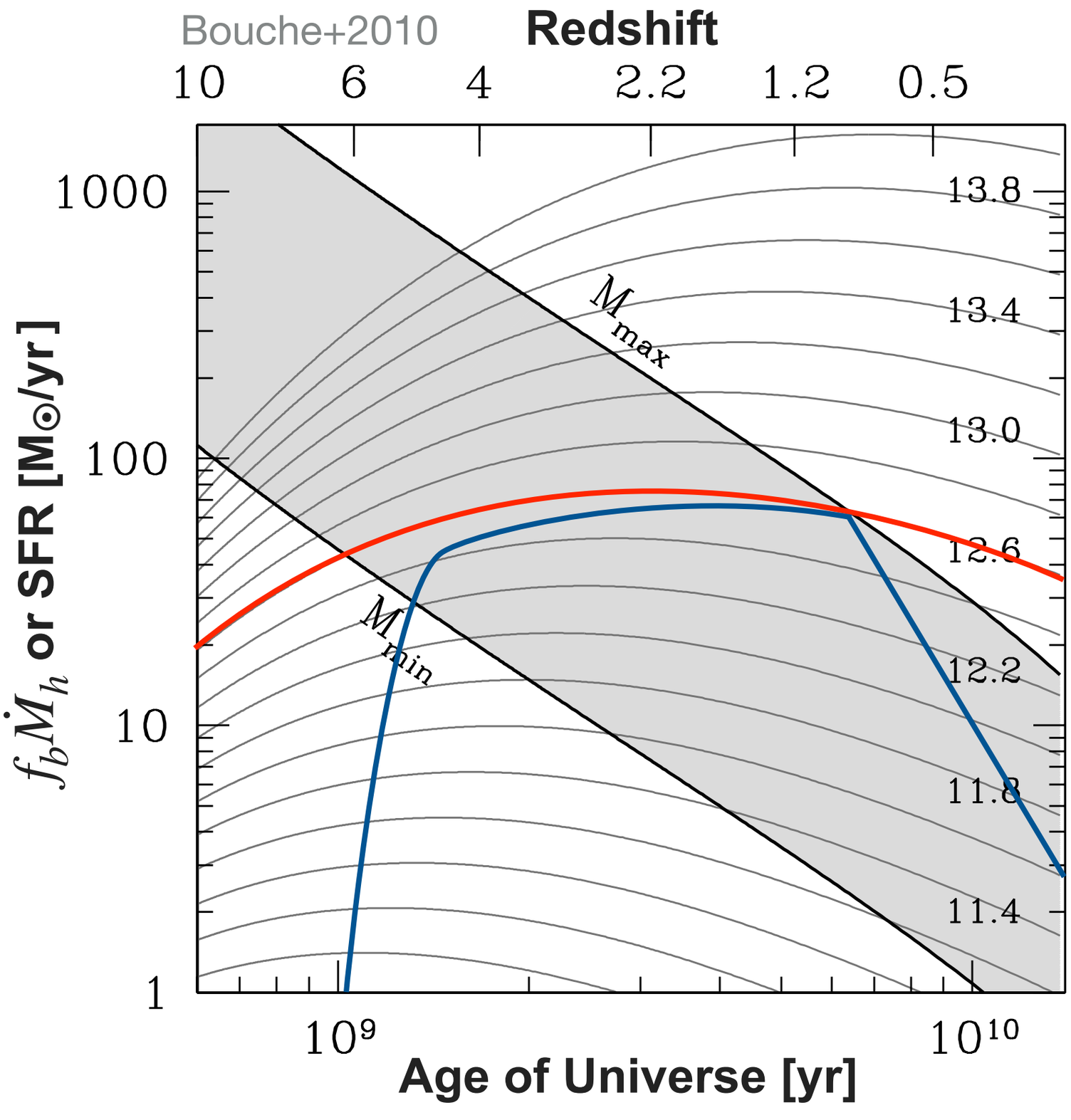

- **Grey region**: efficient cold gas accretion
  $10^{11} < M_{Halo} < 1.5\text{x}10^{12}\ M_\odot$
- **Gas accretion history** of a $10^{12.6}\ M_\odot$ halo (mass at $z = 0$)
- **Star formation history** from the continuity equation:

  1. Once the halo crosses the minimum mass (**$10^{11}\ M_\odot$**), the SFR rapidly rises to reach a steady state;
  2. As the halo mass reaches **$10^{12.3}\ M_\odot$**, cold gas accretion is choked and the SFR starts to decline with an *e*-folding time of **2-3 Gyr (=2 τ_{dyn}/e_{SF})**.

The simple “bathtub” model needs to explain key observational results

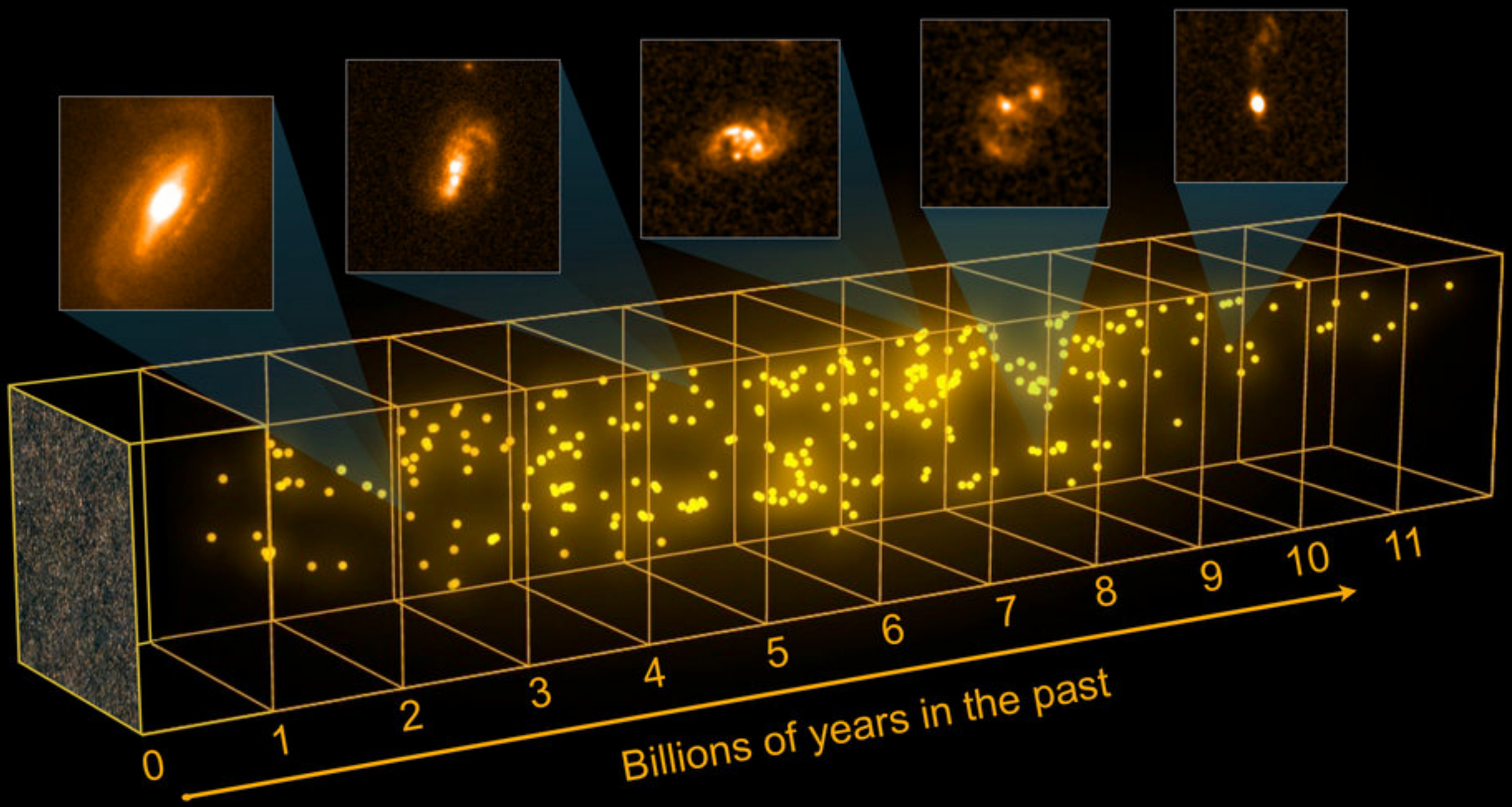

Stellar Mass Fraction Today
= Stellar Mass/Halo Mass

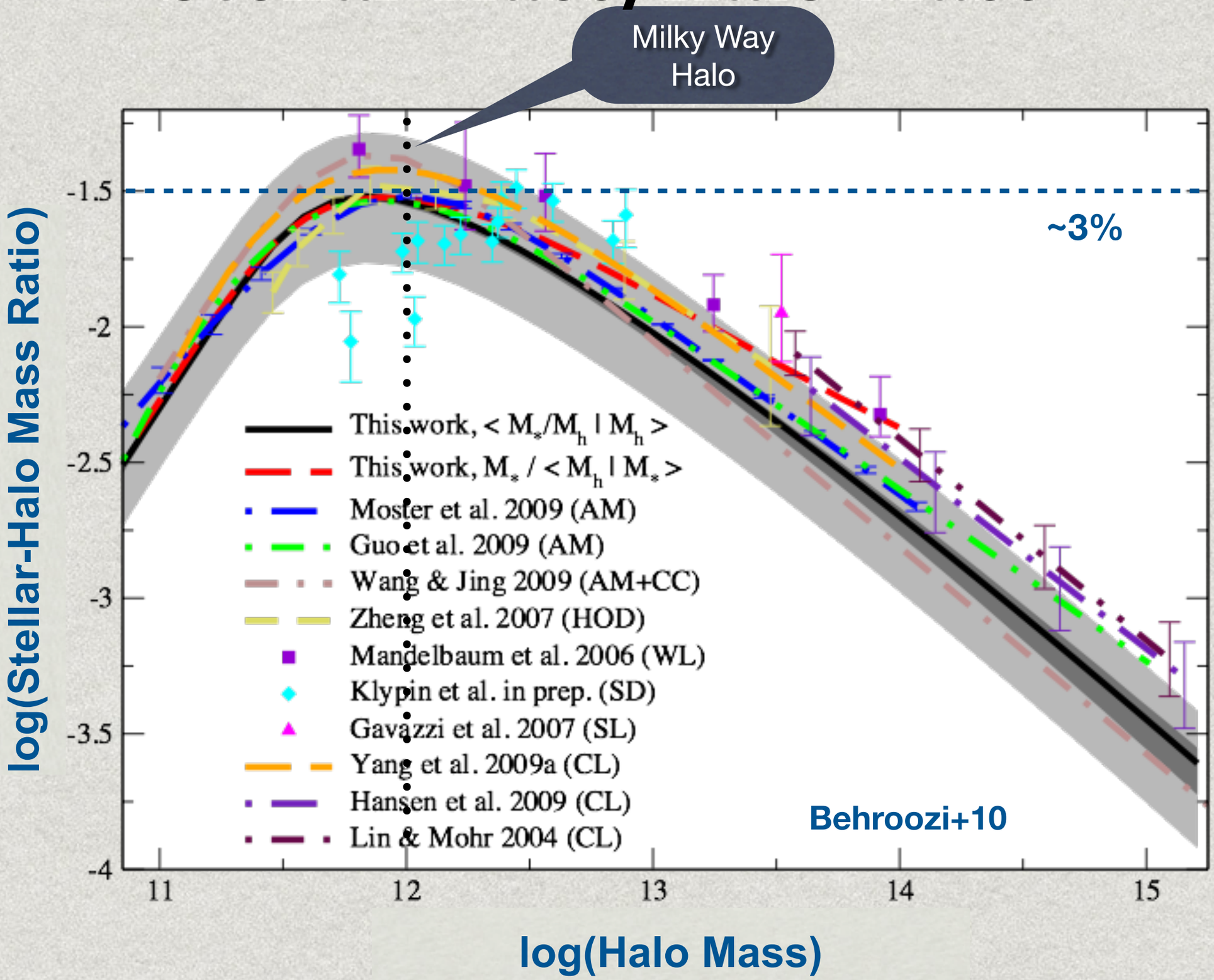

Problem: Stellar mass is a biased tracer of halo mass

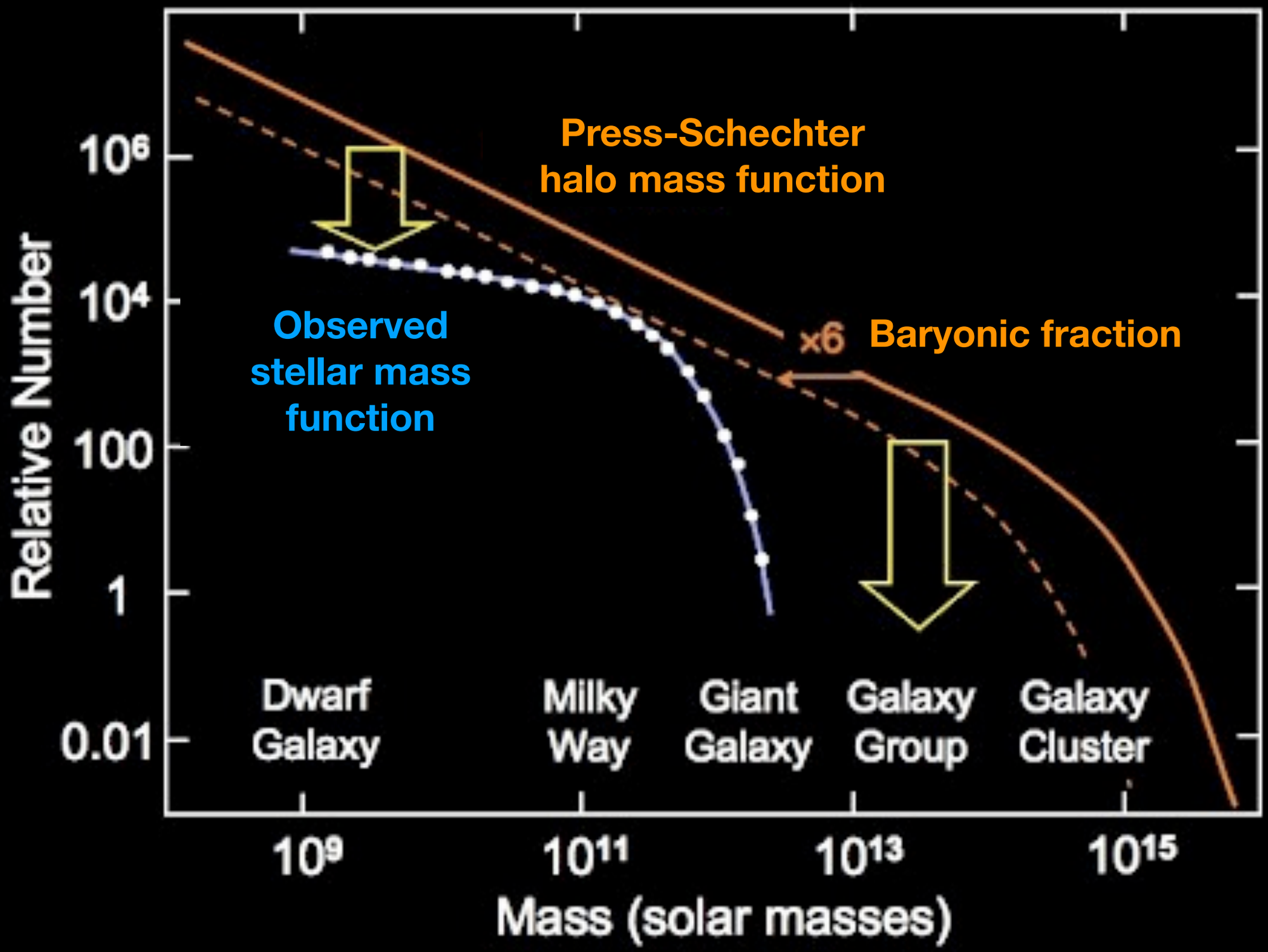

Cosmic Star Formation History

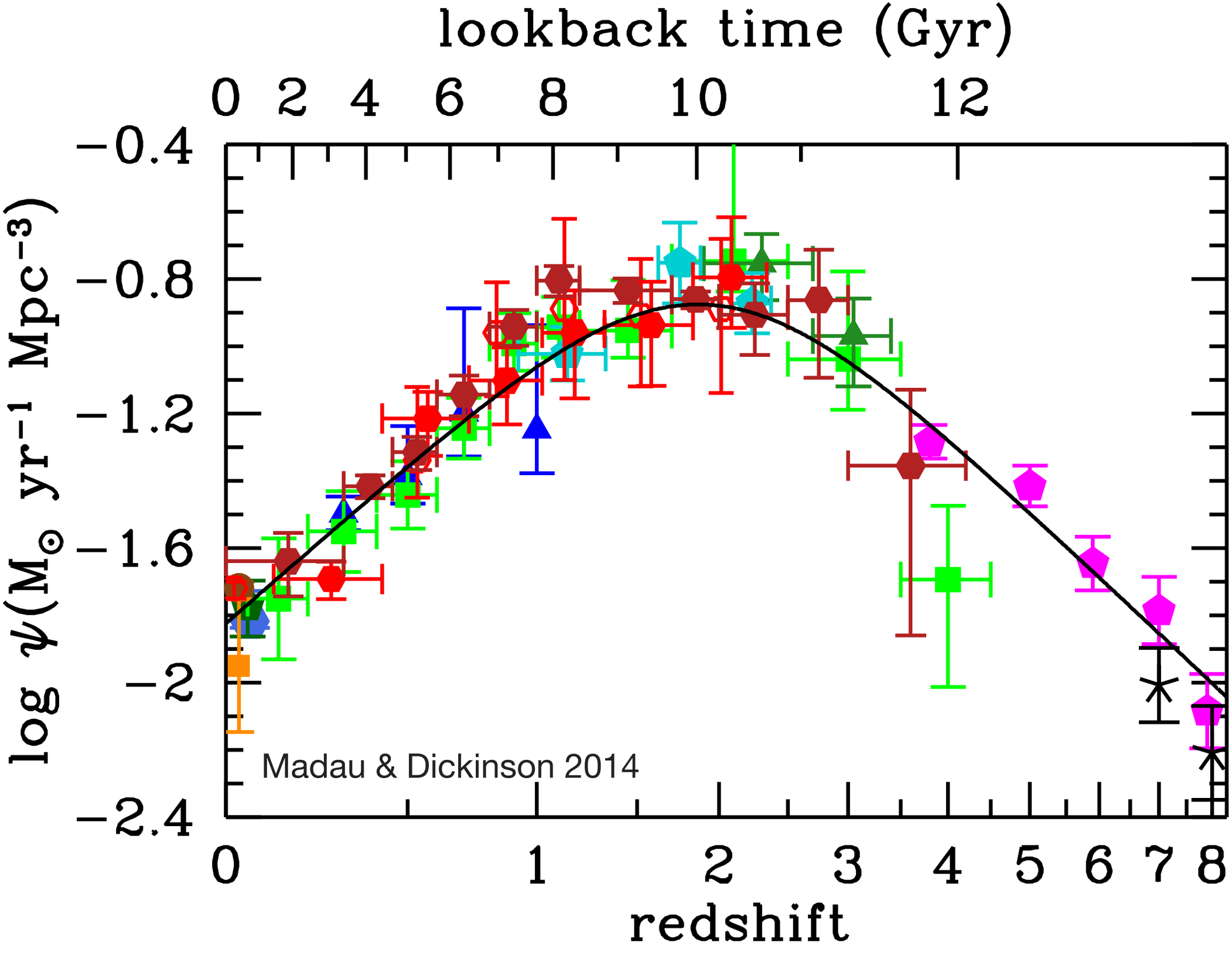

How to measure stellar mass and star formation rates in distant galaxies?

The Milky Way: A Mixture of Stellar Populations

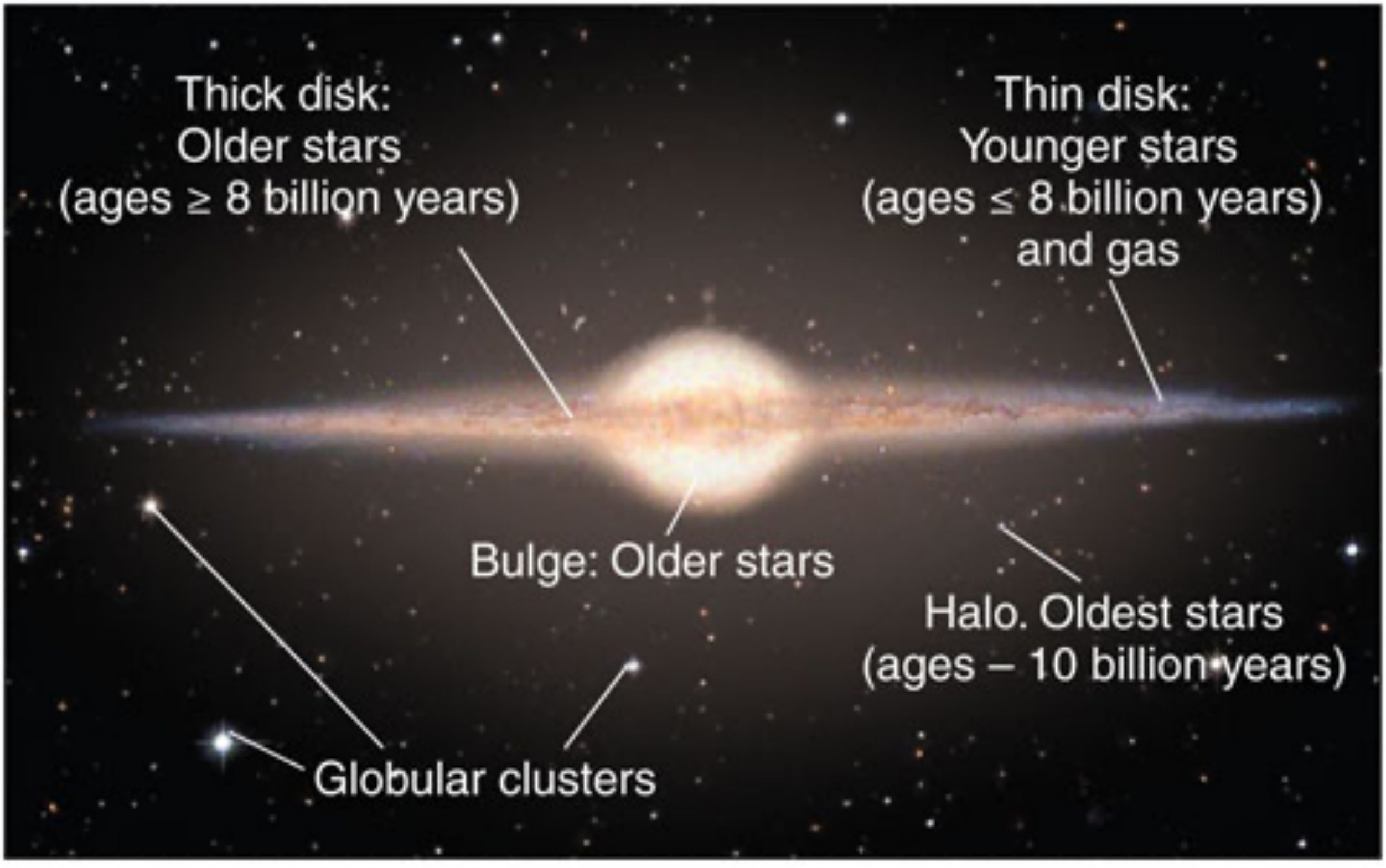

Non-resolved Populations

- Galaxies formed by several SSPs, sometimes we only know their integrated light spectra.
- Integrated light of a galaxy: colours, SED, spectra

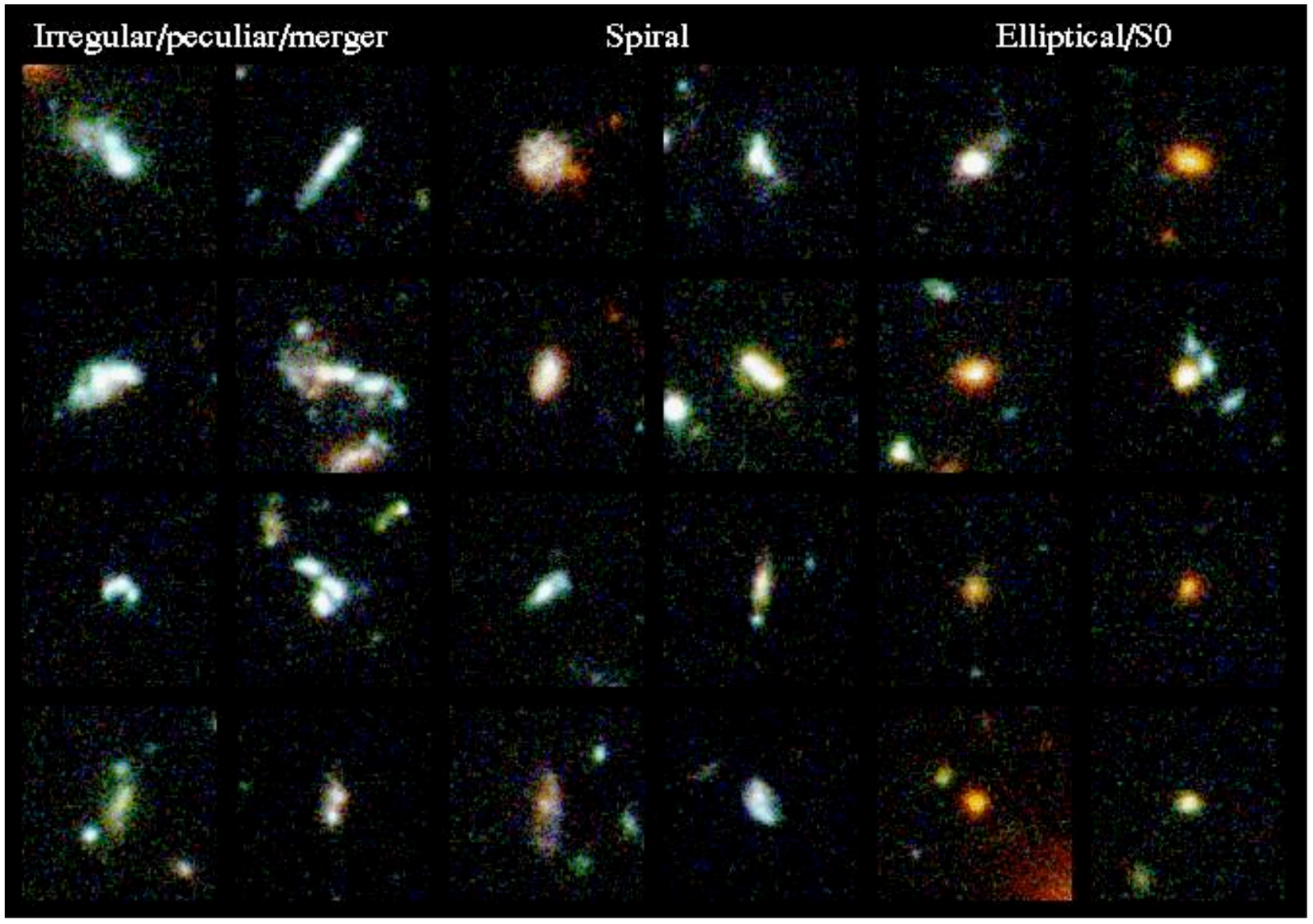

Evolution of Stellar Mass Function between 0 < z < 4

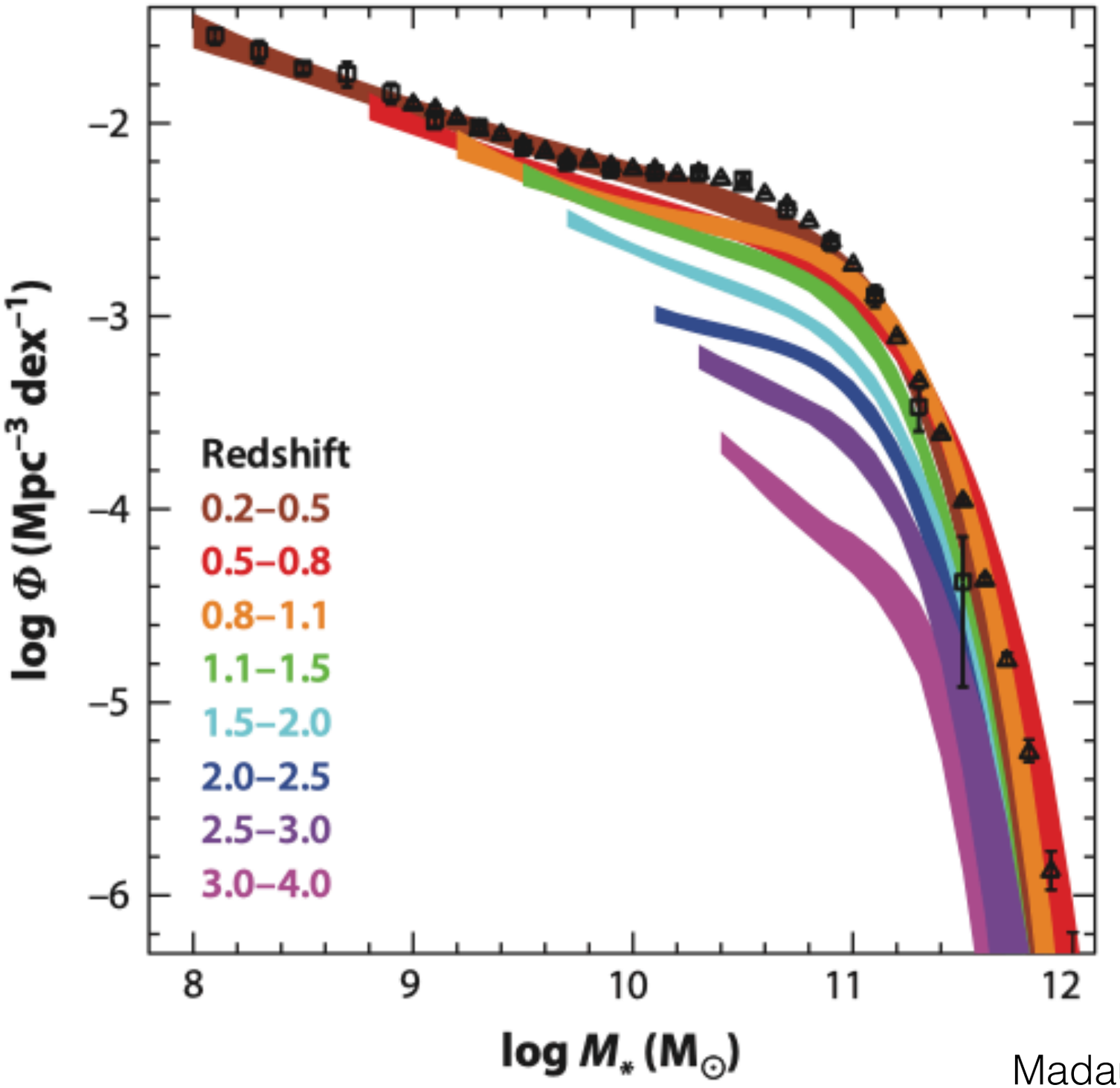

Madau & Dickinson 2014

Simple Stellar Population (SSP)

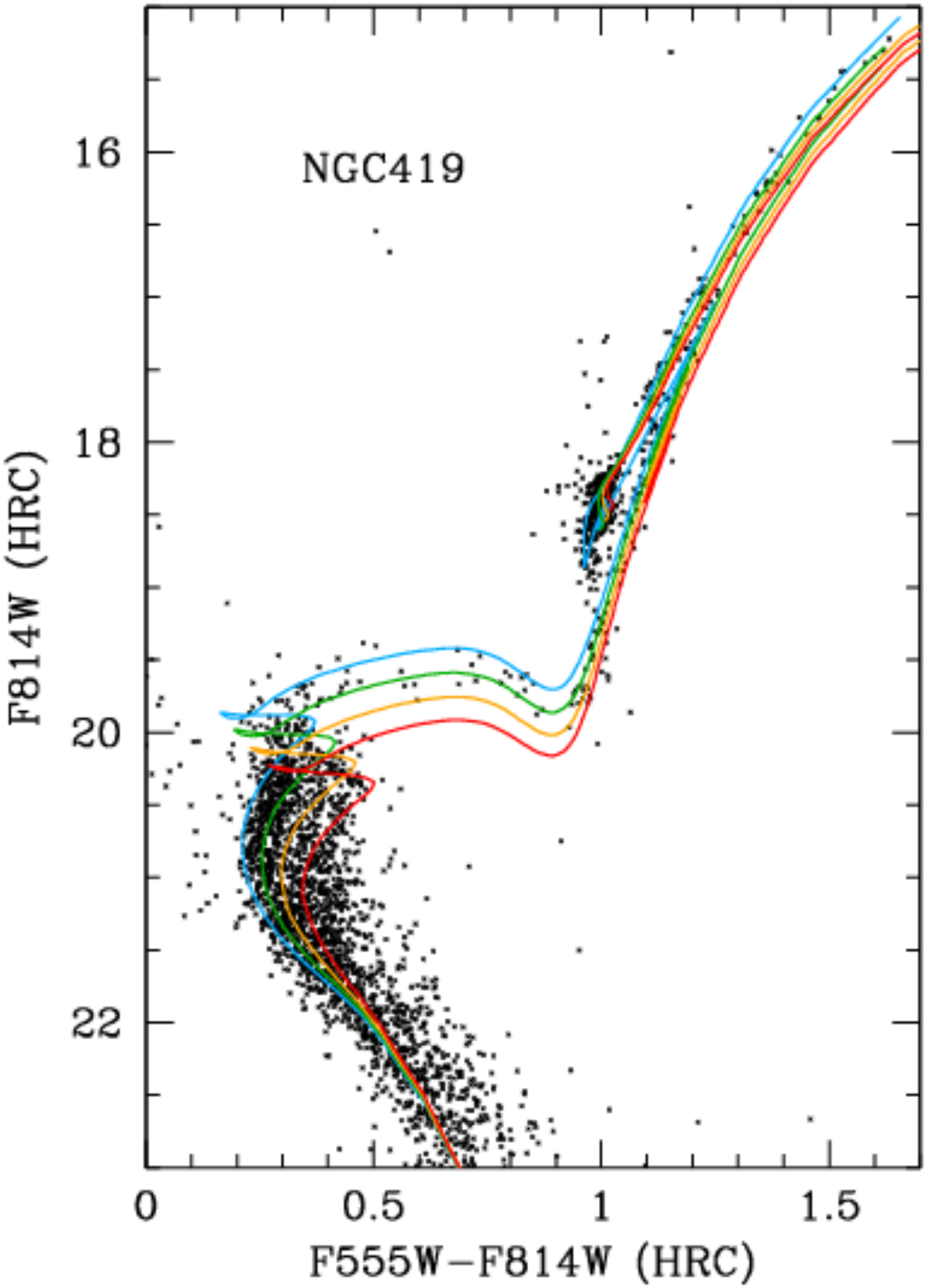

- Bressan+2012
- Th star cluster NGC 419
- The isochrones are for Z = 0.004, ages log(t/yr) = 9.15, 9.20, 9.25, 9.30

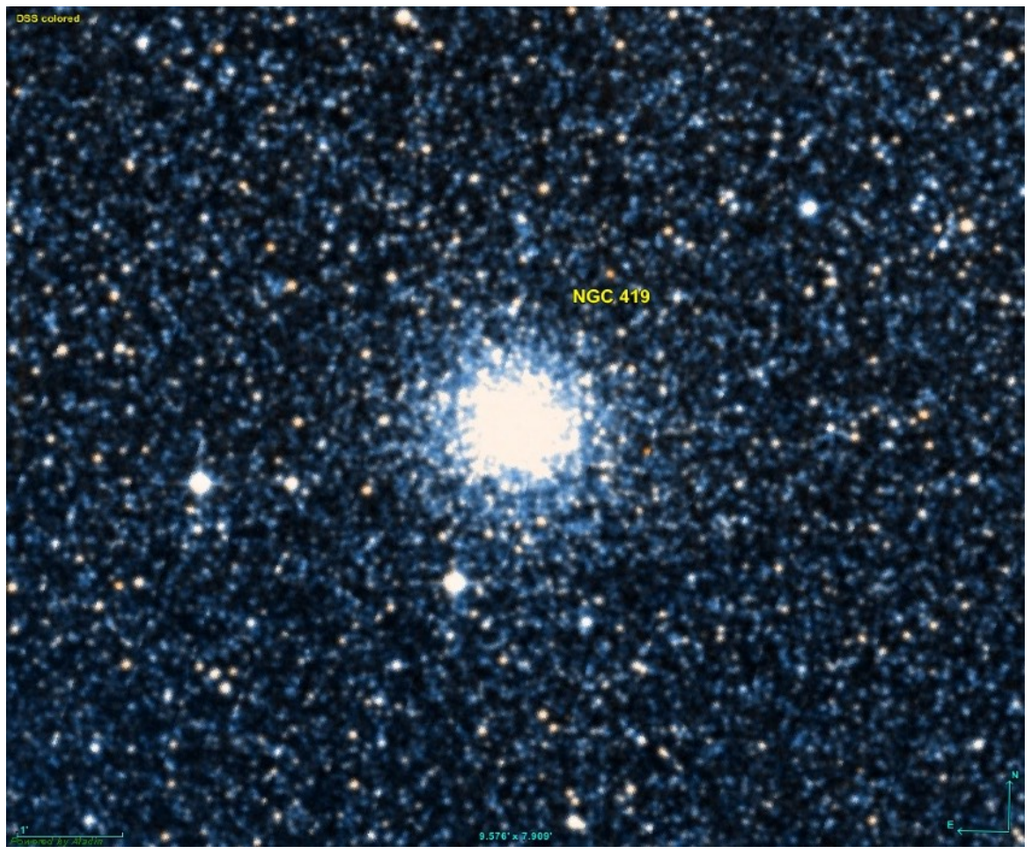

Isochrones of stellar populations vs. **evolution tracks** of individual stars

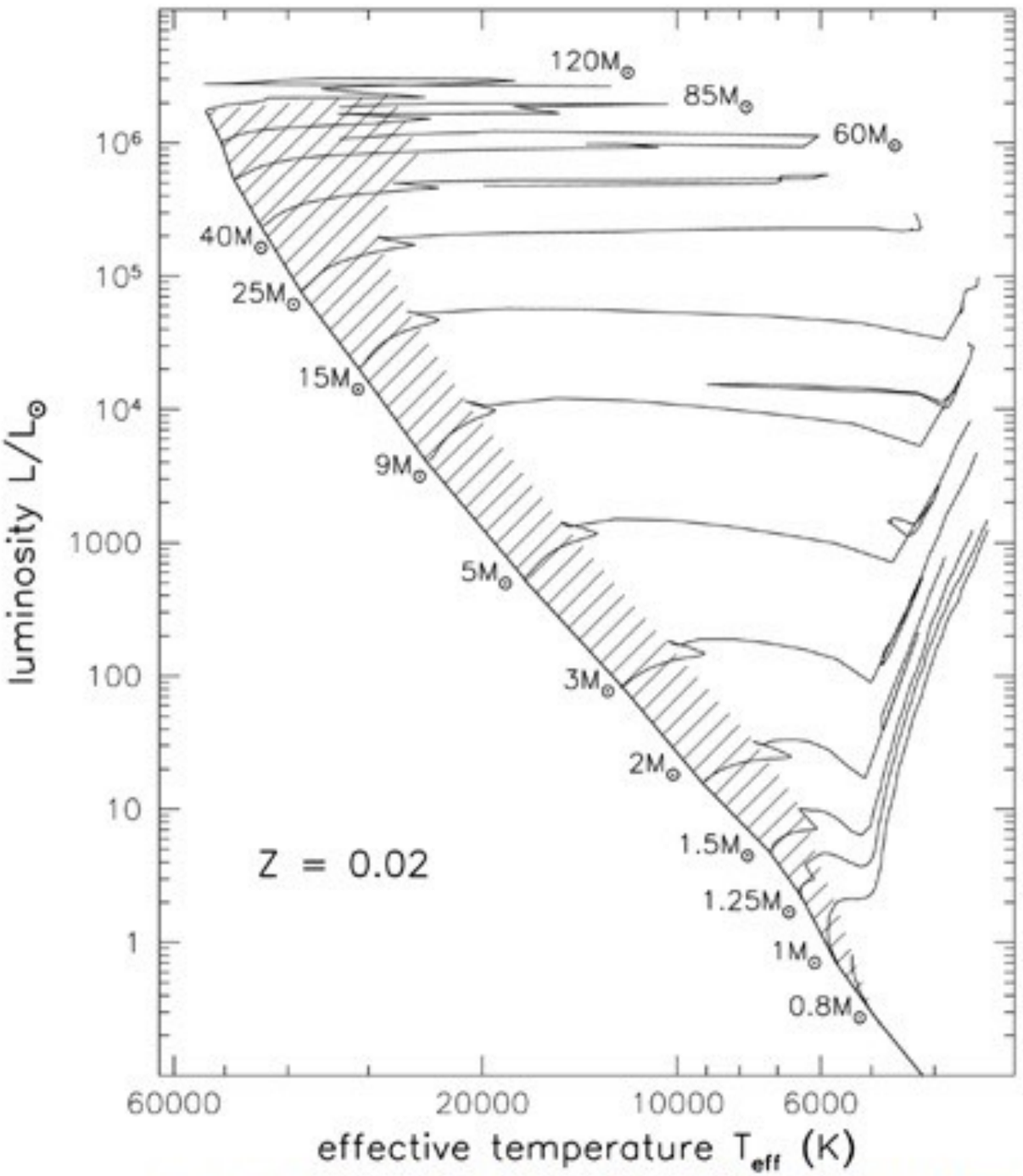

Fig 1.4 'Galaxies in the Universe' Sparke/Gallagher CUP 2007

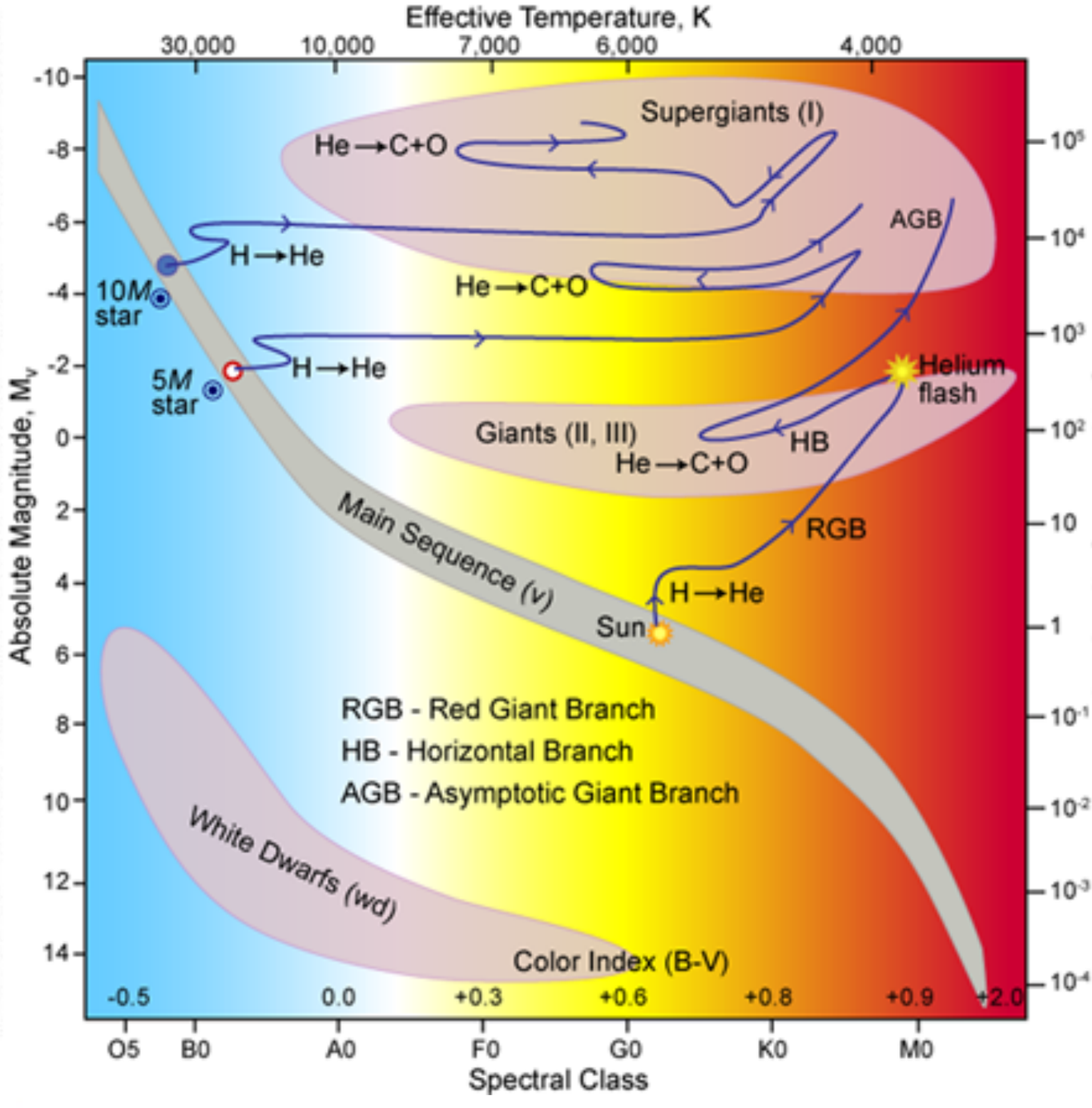

Spectra of Simple Stellar Populations (SSPs)

$$l_\lambda^{\mathrm{ssp}}(t, [\mathrm{M/H}]) = \int\int l_\lambda^*(L,T)\, p(L,T \mid t, [\mathrm{M/H}], \mathrm{IMF}, \mathrm{SEM})\, dL\, dT$$

simple means single age & metallicity

spectral library of individual stars:
$l_\lambda^*(L,T)$

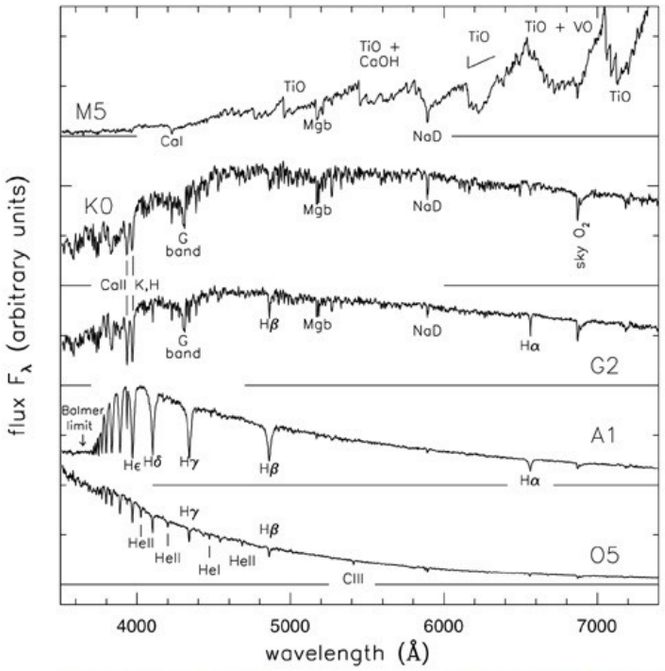

initial mass function (IMF):
$p(m) = p(L)\frac{dL}{dm}$

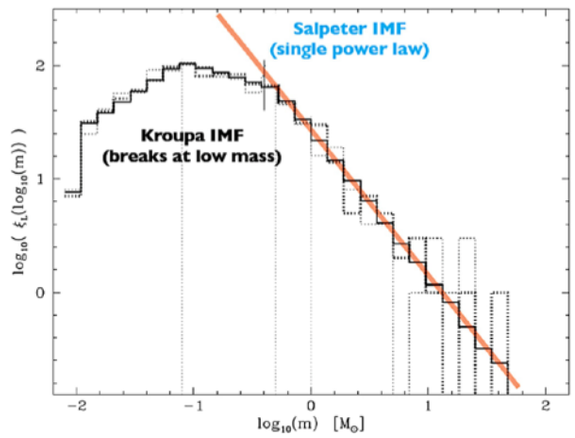

stellar evolution models (SEM)

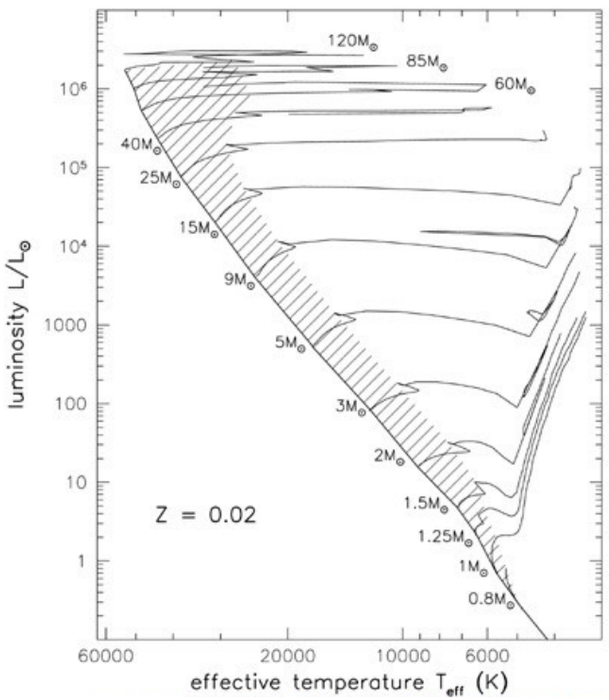

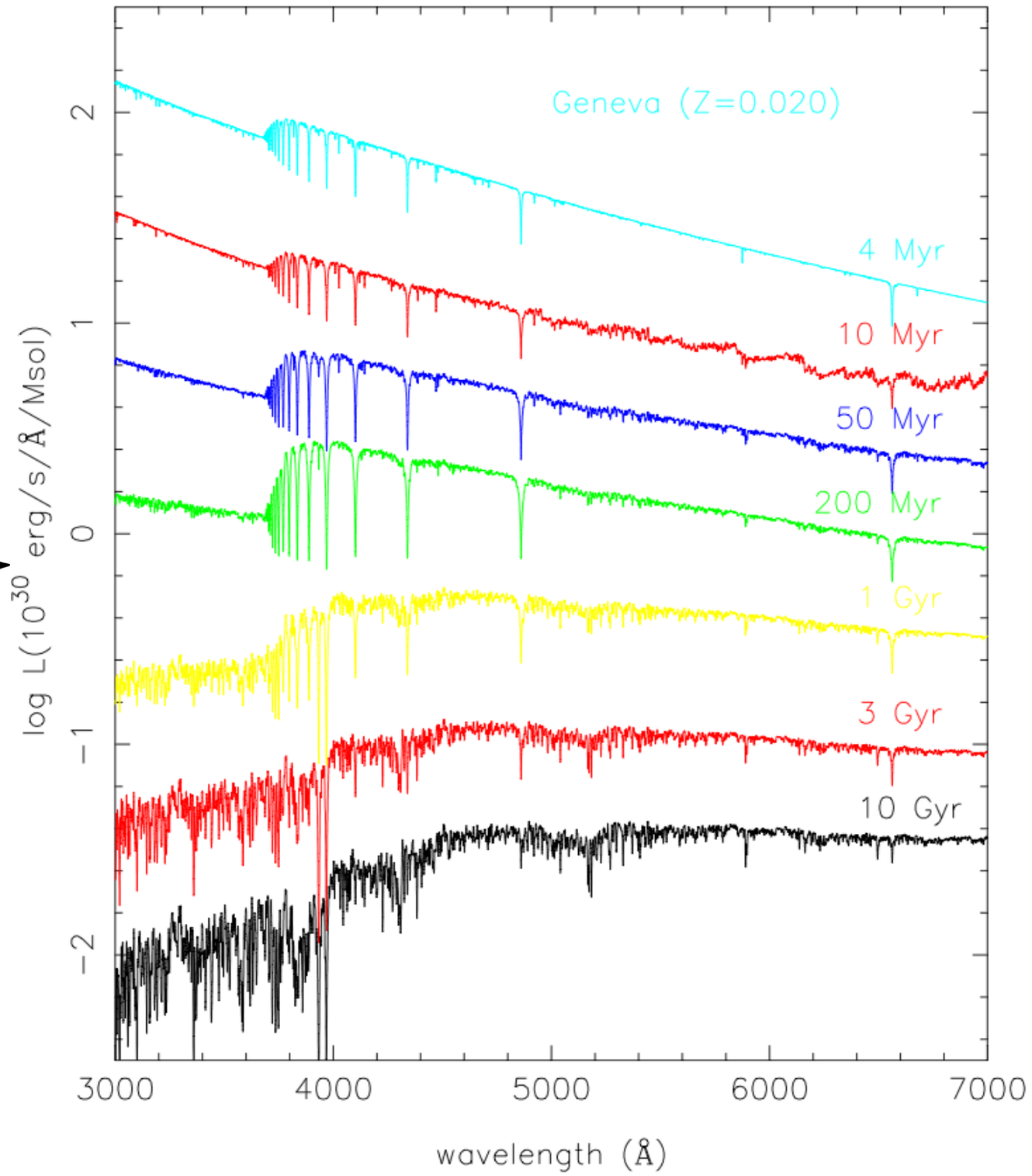

Complex Stellar Population (CSP)

SSP library: $l_\lambda(t, [\mathrm{M/H}])$

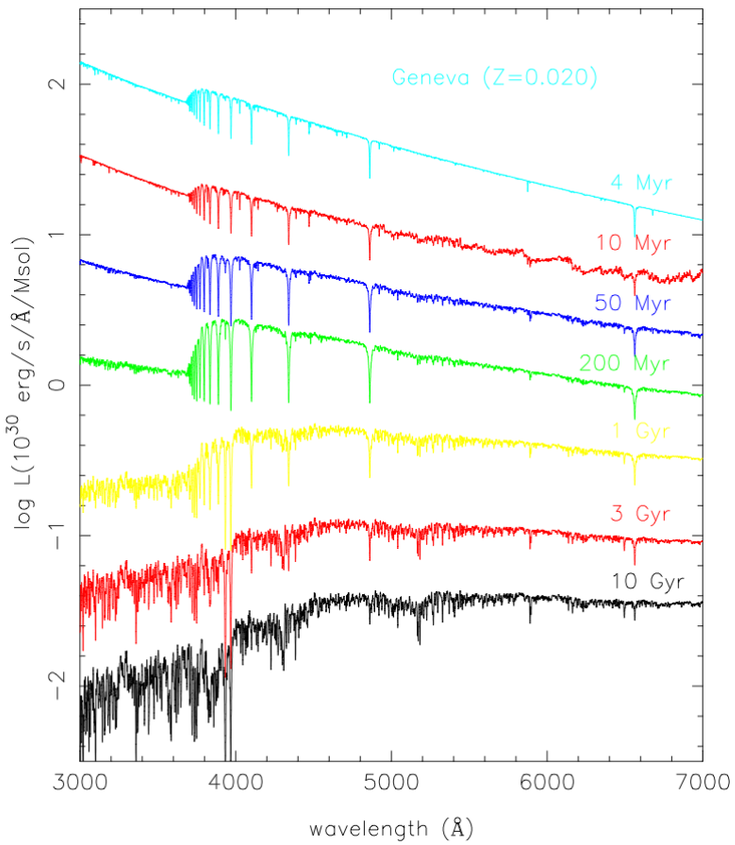

Weights of SSPs: $p(t)p([\mathrm{M/H}])$

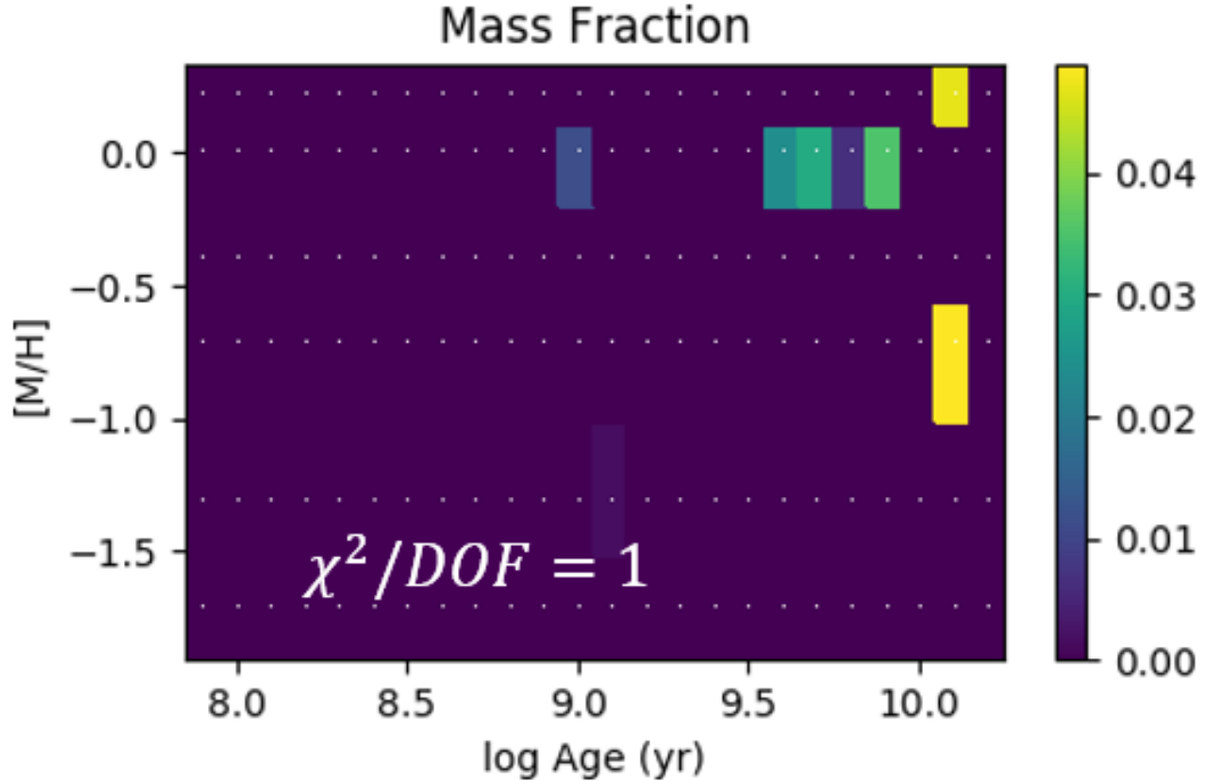

Complex Stellar Population (CSP): $$\int\int l_\lambda(t, [\mathrm{M/H}])p(t)p([\mathrm{M/H}])\,dt\,d[\mathrm{M/H}]$$

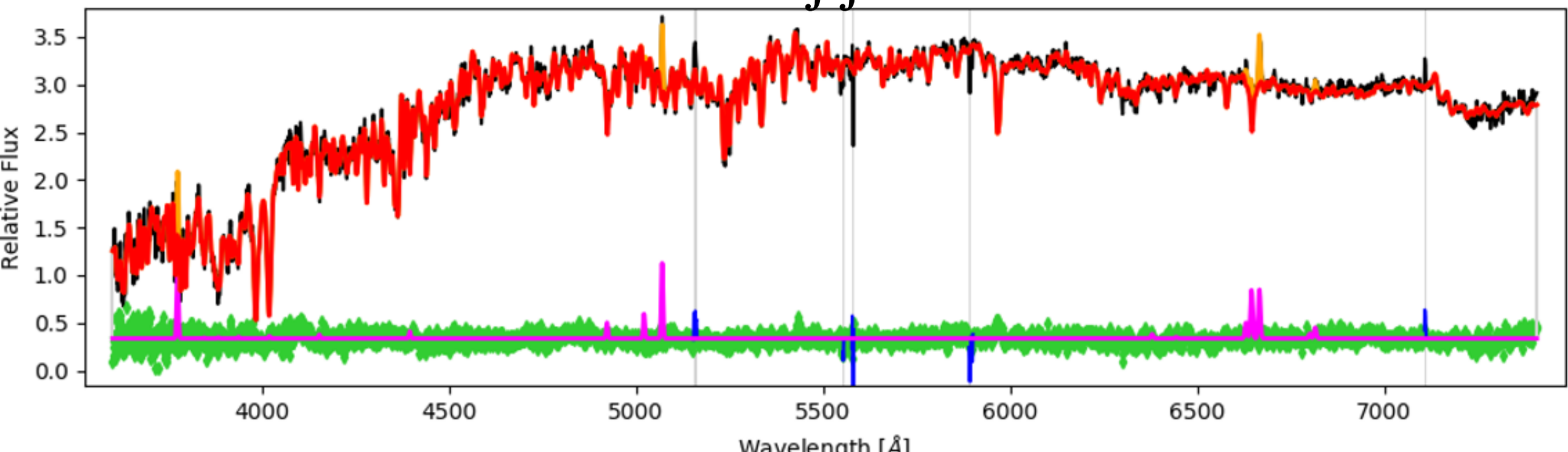

Spectra of Complex Stellar Population (CSP):

$$l_\lambda^{\mathrm{csp}} = \int\int l_\lambda^{\mathrm{ssp}}(t, [\mathrm{M/H}])p(t)p([\mathrm{M/H}])\,dt\,d[\mathrm{M/H}]$$

$$= \int\int \left(\int\int l_\lambda^{*}(L,T)p(L,T\,|\,t, [\mathrm{M/H}], \mathrm{IMF}, \mathrm{SEM})dL\,dT \right) p(t)p([\mathrm{M/H}])\,dt\,d[\mathrm{M/H}]$$

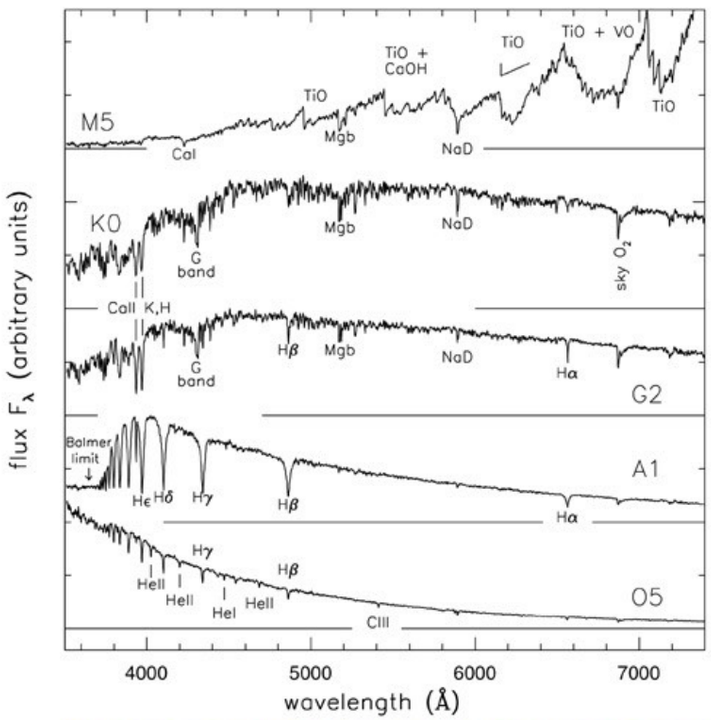

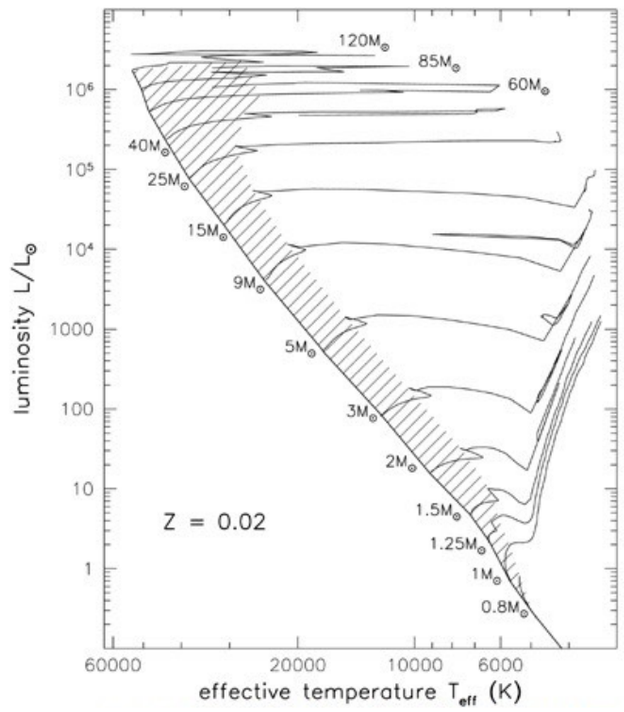

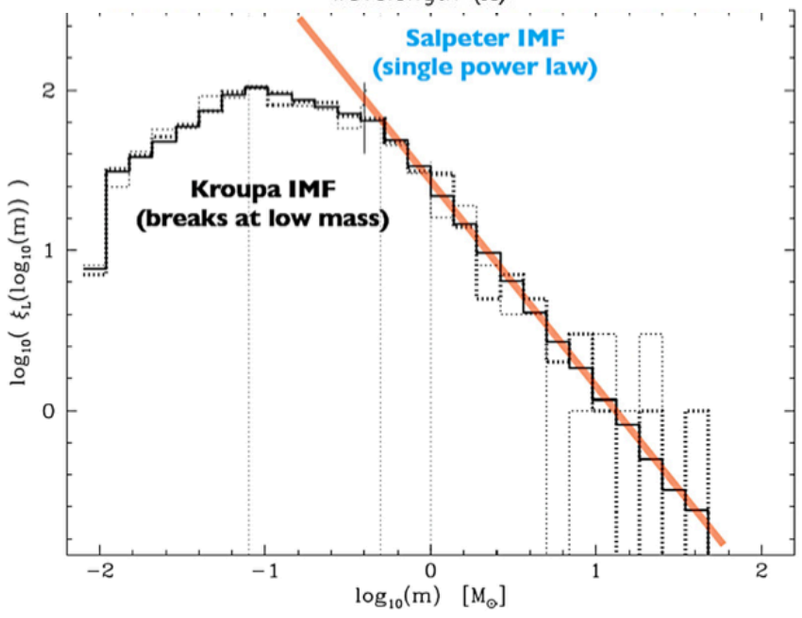

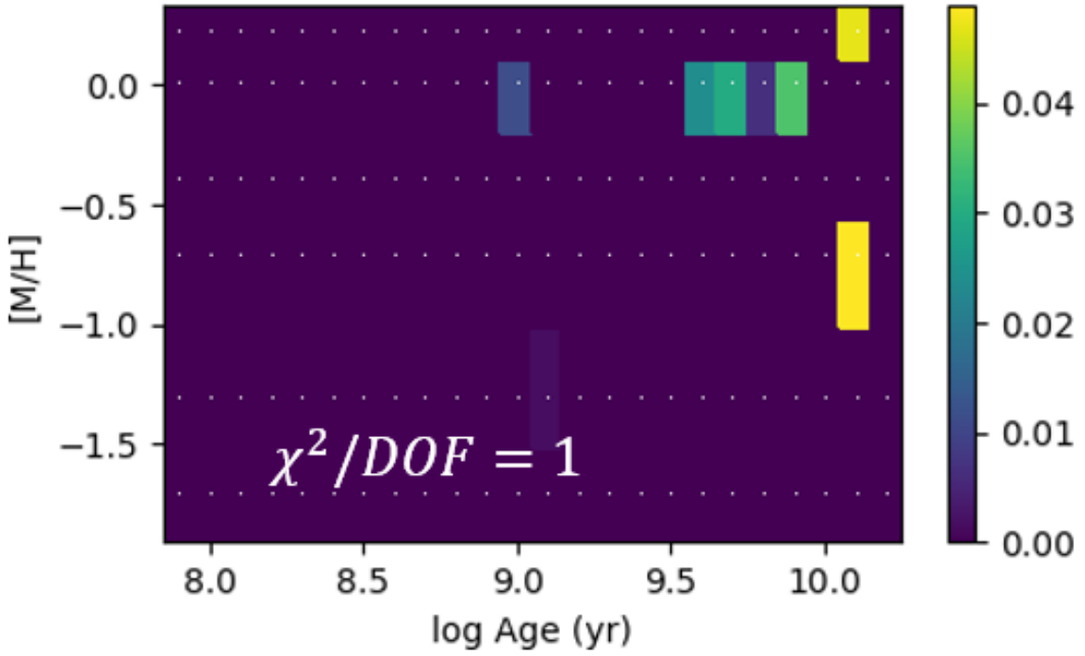

Stellar Mass from Spectral Fitting

Modeling an Observed Spectrum with Model CSP Spectra Requires Solving the Mass Weights: $M \cdot p(t) \cdot p([\mathrm{M/H}])$

$$l_\lambda^{\mathrm{csp}} = \int\int l_\lambda^{\mathrm{ssp}}(t, [\mathrm{M/H}]) p(t) p([\mathrm{M/H}])\, dt\, d[\mathrm{M/H}]$$

$$= \int\int \left(\int\int l_\lambda^{*}(L, T) p(L, T \mid t, [\mathrm{M/H}], \mathrm{IMF}, \mathrm{SEM}) dL\, dT \right) p(t) p([\mathrm{M/H}])\, dt\, d[\mathrm{M/H}]$$

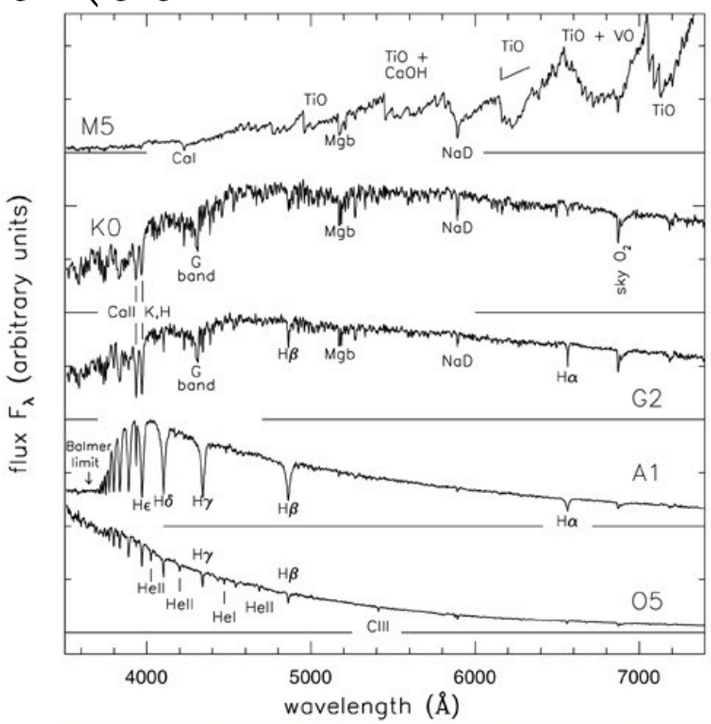

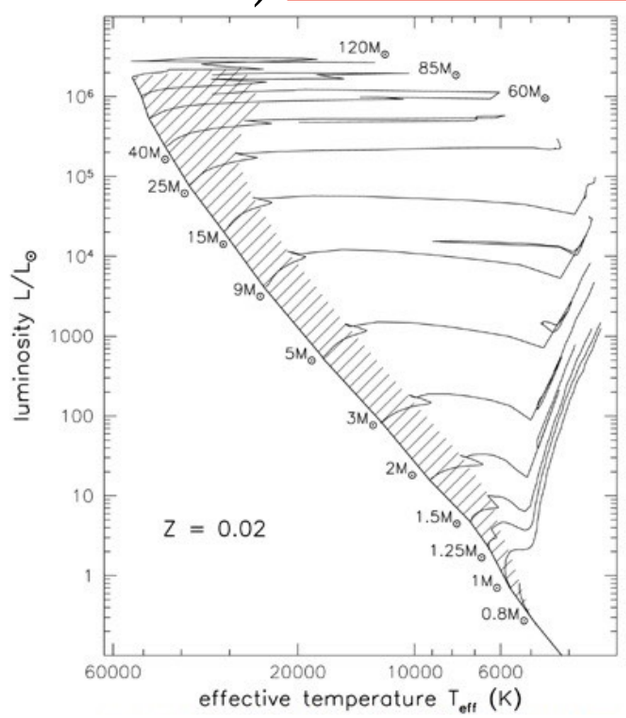

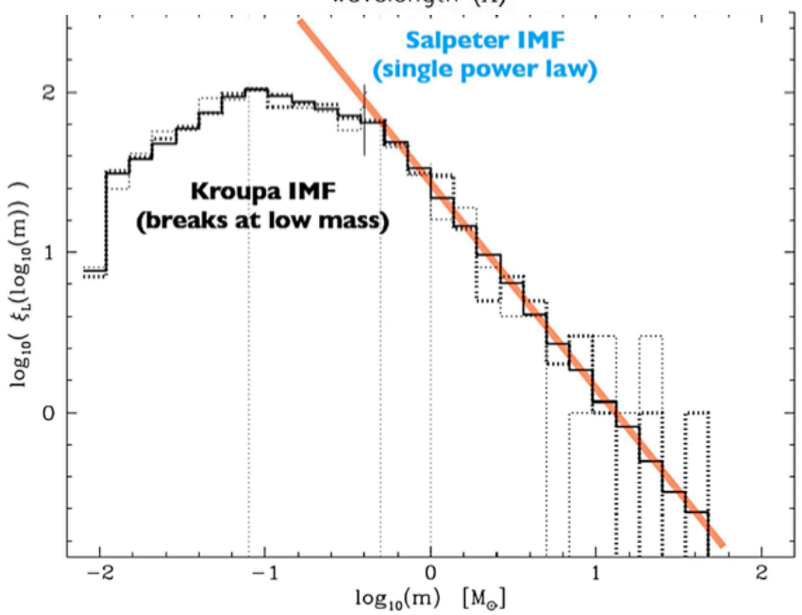

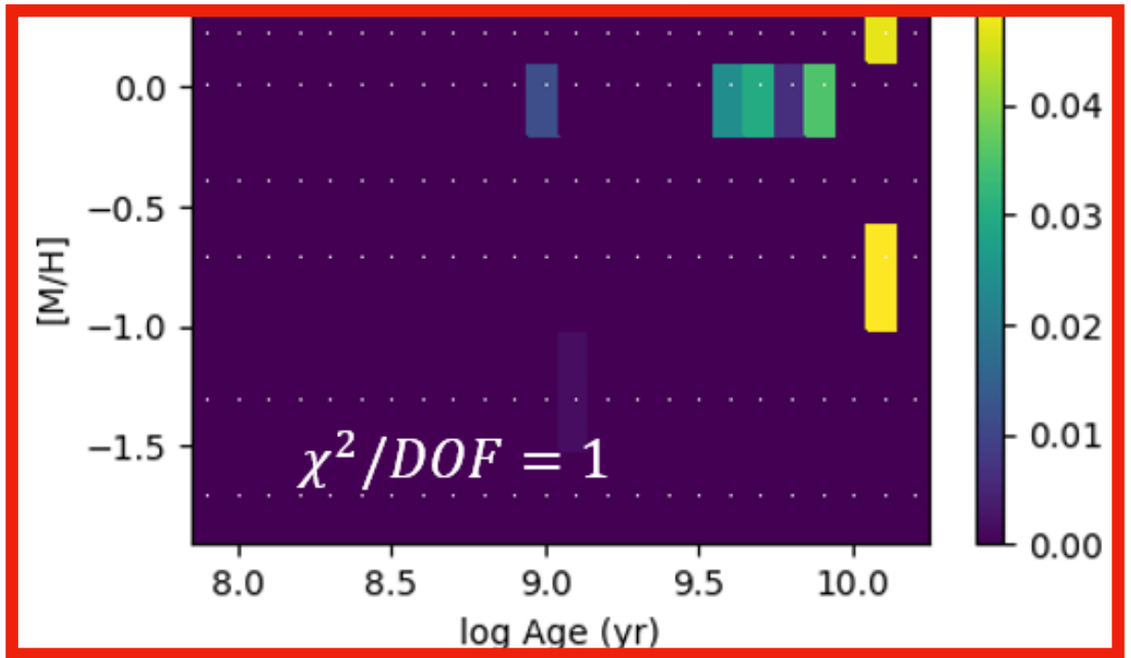

Solving for mass weights is a bounded-variables linear least squares problem (BVLS algorithm by Stark & Parker 1995)

$$\frac{M}{4\pi D_L^2} \sum l_\lambda^{\mathrm{ssp}}(t, [\mathrm{M/H}]) \times p(t, [\mathrm{M/H}]) \approx f_\lambda$$

$$\begin{bmatrix} 1 & 0 \\ 0 & 1 \\ 2 & 1 \end{bmatrix} \times \begin{bmatrix} x_1 \\ x_2 \end{bmatrix} \approx \begin{bmatrix} 1 \\ 3 \\ -2 \end{bmatrix}$$

Spectroscopic masses using SPS spectral models

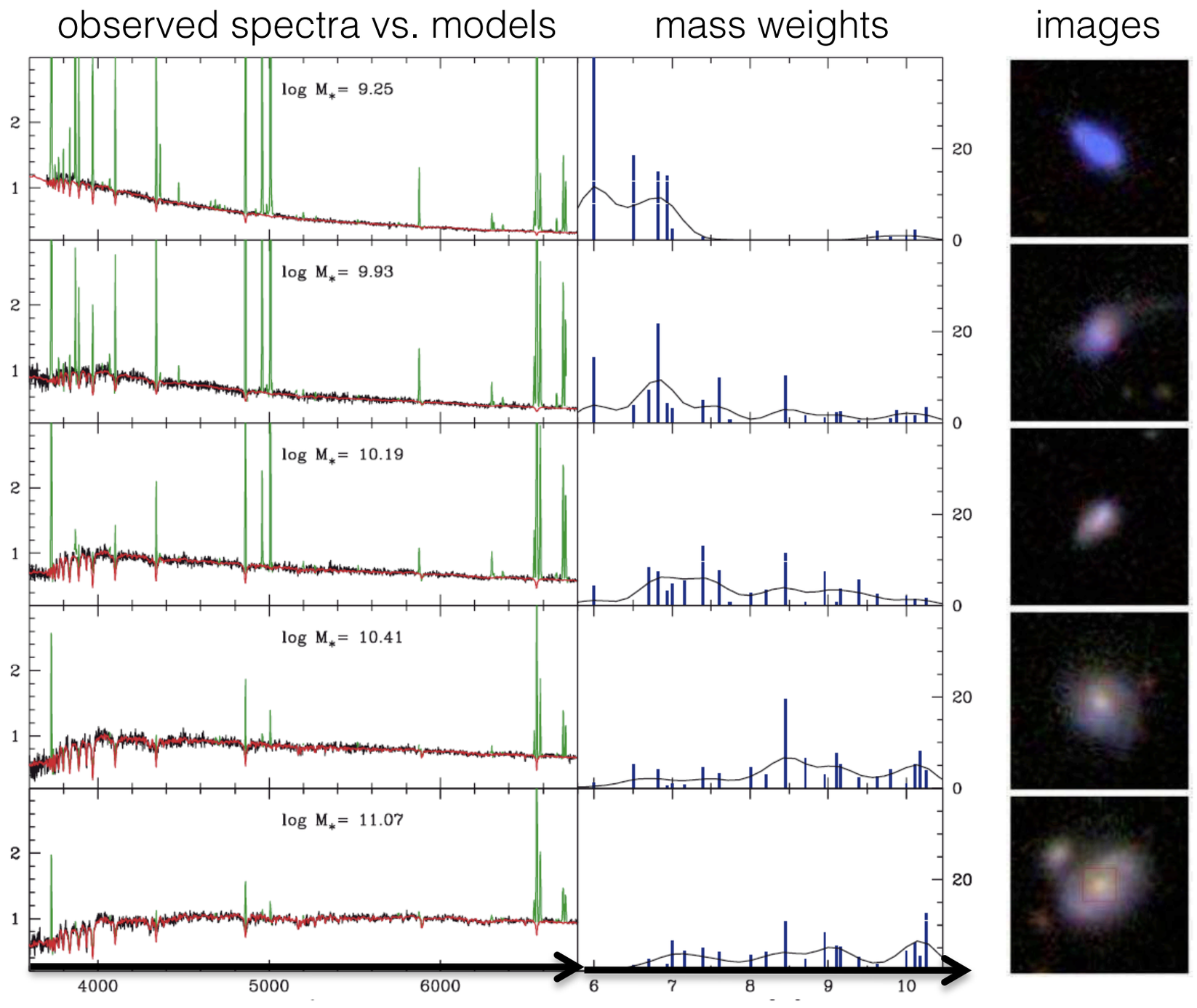

Asari, Cid Fernandes et al. 2007

Stellar Mass from Photometry

As a stellar population ages, it becomes redder and fainter

HR diagram of clusters covering a range of ages

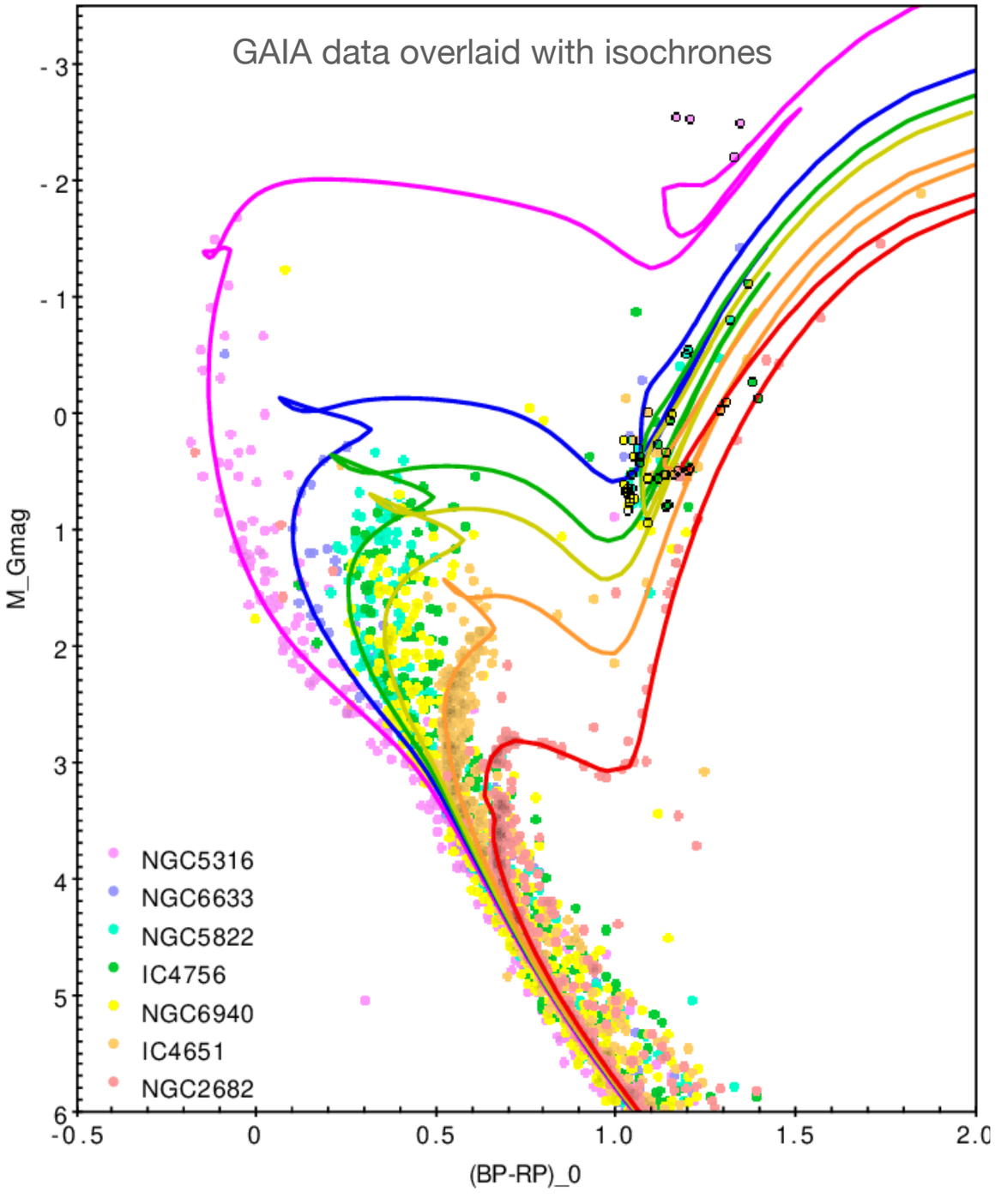

- Stellar population synthesis models follow the **isochrone evolution** of stellar populations and predict the **integrated color** and the **total luminosity** as a function of age.
- The **mass-to-light ratio (M/L)** increases because luminosity decreases faster than mass loss.

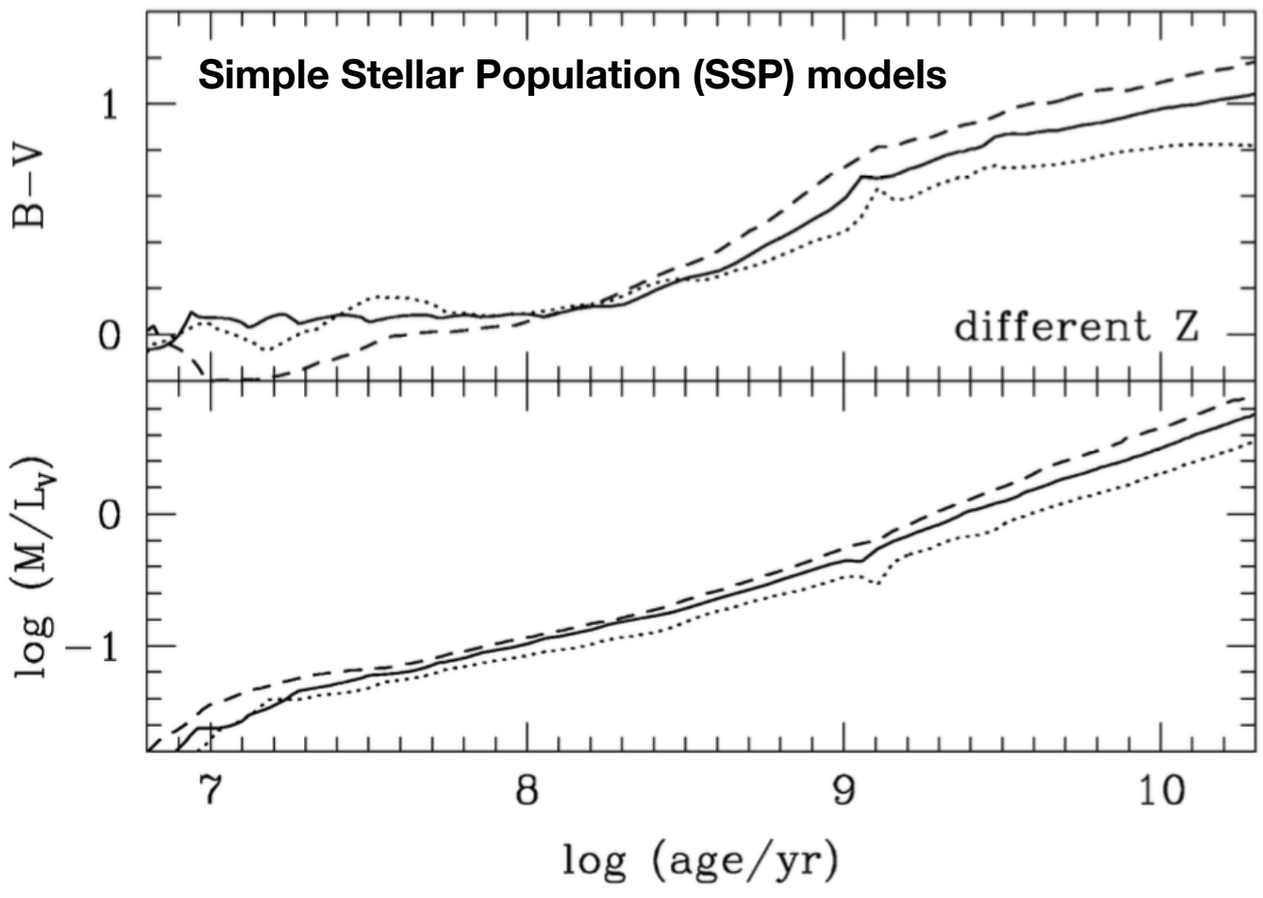

Photometric masses using mass-to-light ratio

$$\log \mathscr{M} = \log L_\lambda / L_{\lambda,\odot} + \log(\mathscr{M}/L_\lambda)$$
$$= 0.4(M_{\lambda,\odot} - m_\lambda + 25 + 5\log D_L) + \log(\mathscr{M}/L_\lambda)$$

* In practice, this approach is problematic because the mass-to-light ratio of a CSP depends on the **weights in age and metallicity**, just like the spectra of a CSP.
* When high S/N spectra are available, one can solve for $p(t) \cdot p([\mathrm{M/H}])$ with BVLS.
* When only photometry is available, the weights can not be solved, so they must be **prescribed** as if known a priori. e.g., the SSP models below assume δ functions.

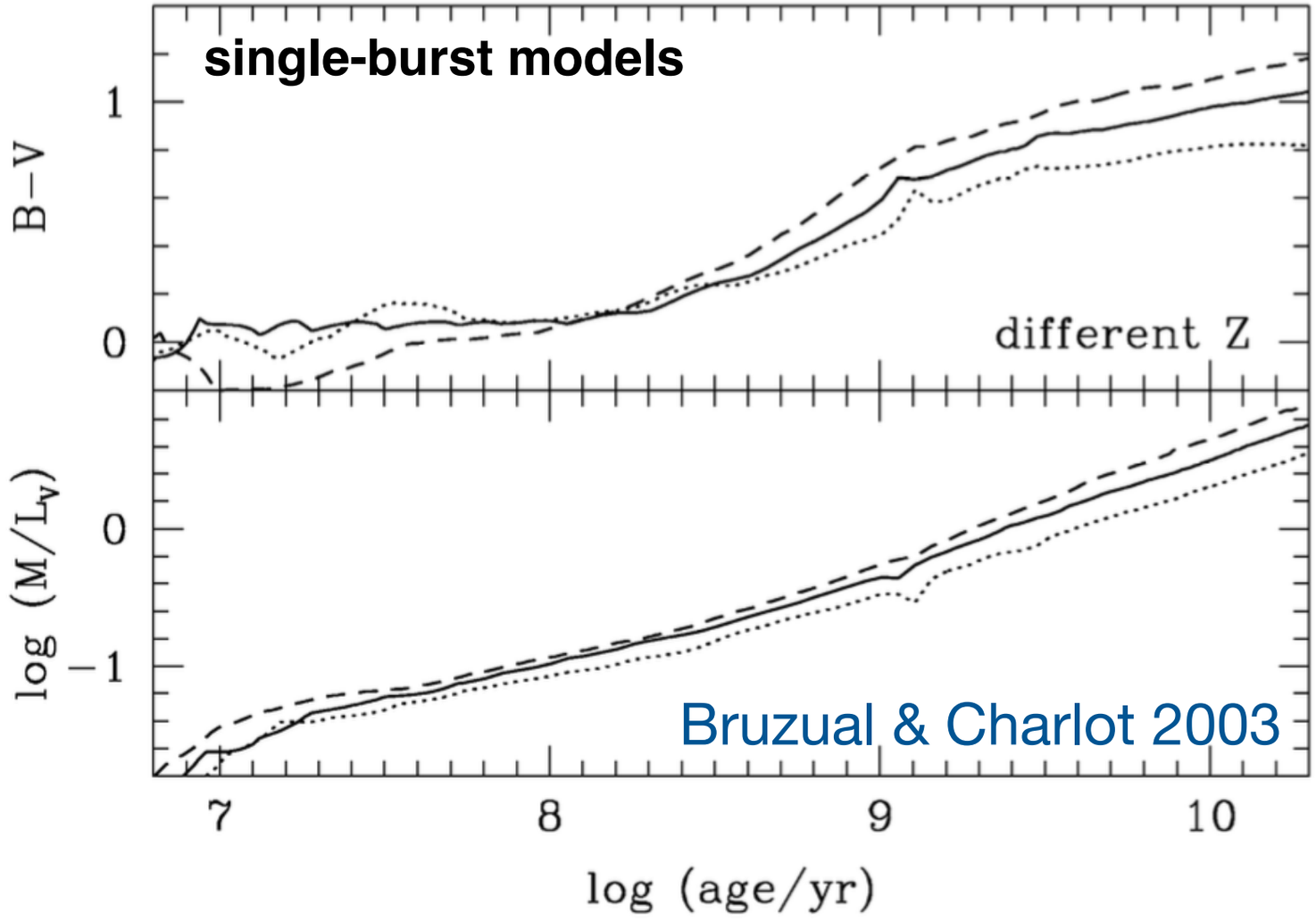

Spectral estimates of the mass-to-light ratio of quiescent and active (star-forming) galaxies

The masses are estimated from spectral fitting with CSP models, but the M/L can be applied on galaxies that have only photometry data and **photometric redshifts**

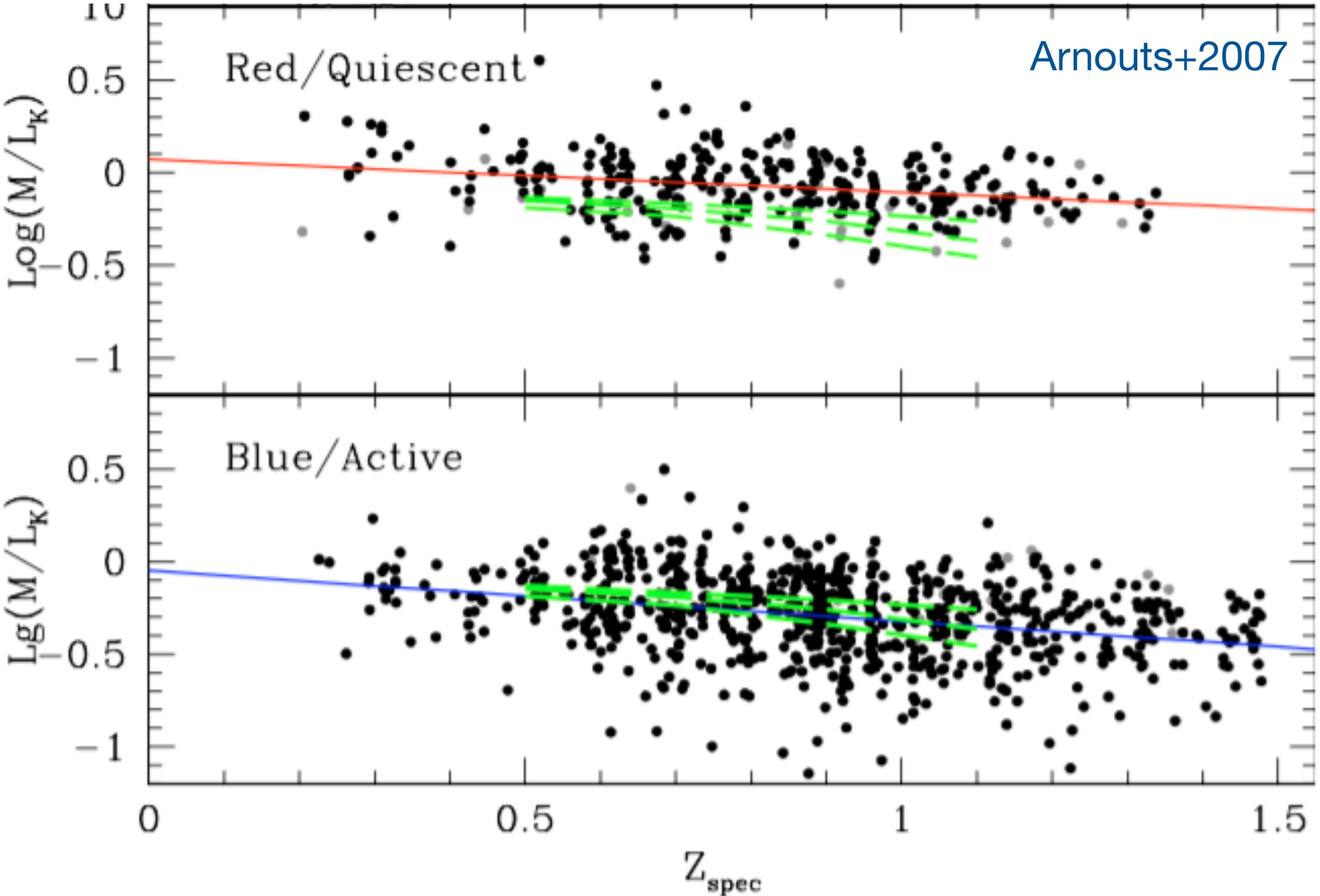

Photometric redshifts is critical, because spectroscopy of large samples of faint, distant galaxies is prohibitively expensive

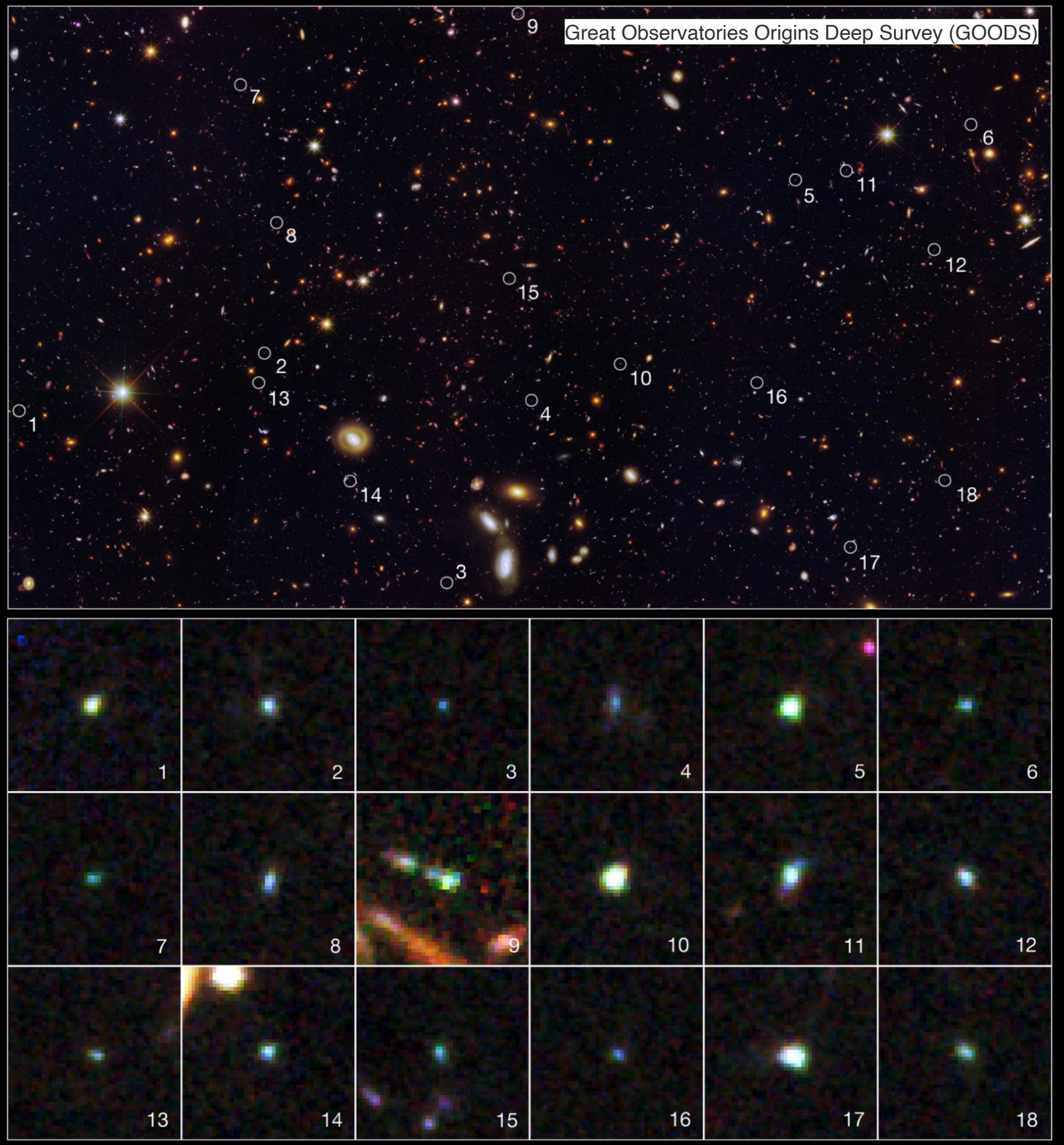

example z=1.5 galaxies

The Lyman Break:

Most Lyman continuum photons ($\lambda_{\rm rest} < 912\text{Å}$) are absorbed by either the ISM or the IGM

Steidel 98, 03
Ellis 98
Adelberger+04

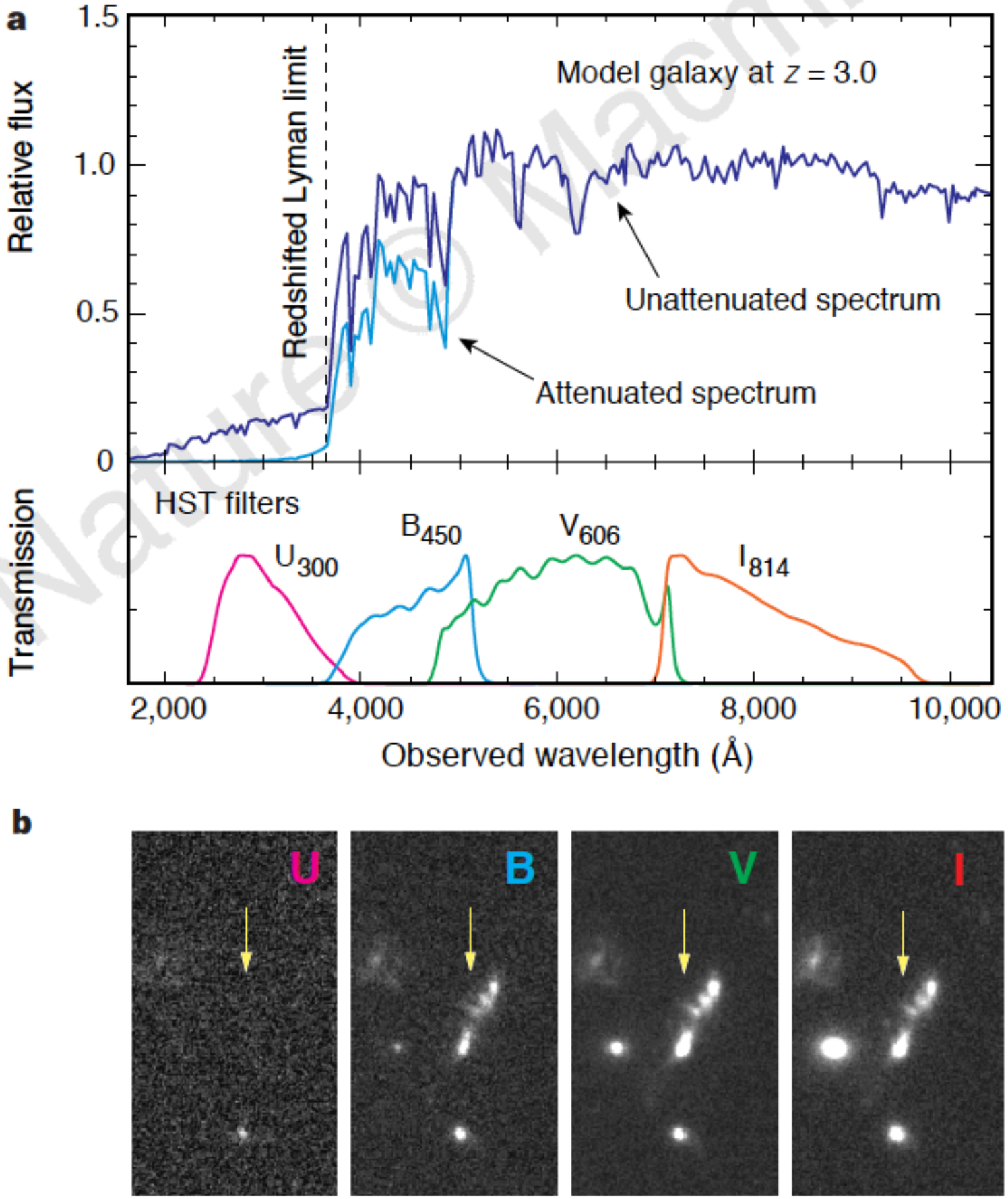

Separation of quiescent and active star-forming galaxies on the Color-Magnitude Diagram

HR Diagram of Stars vs. CM Diagram of Galaxies

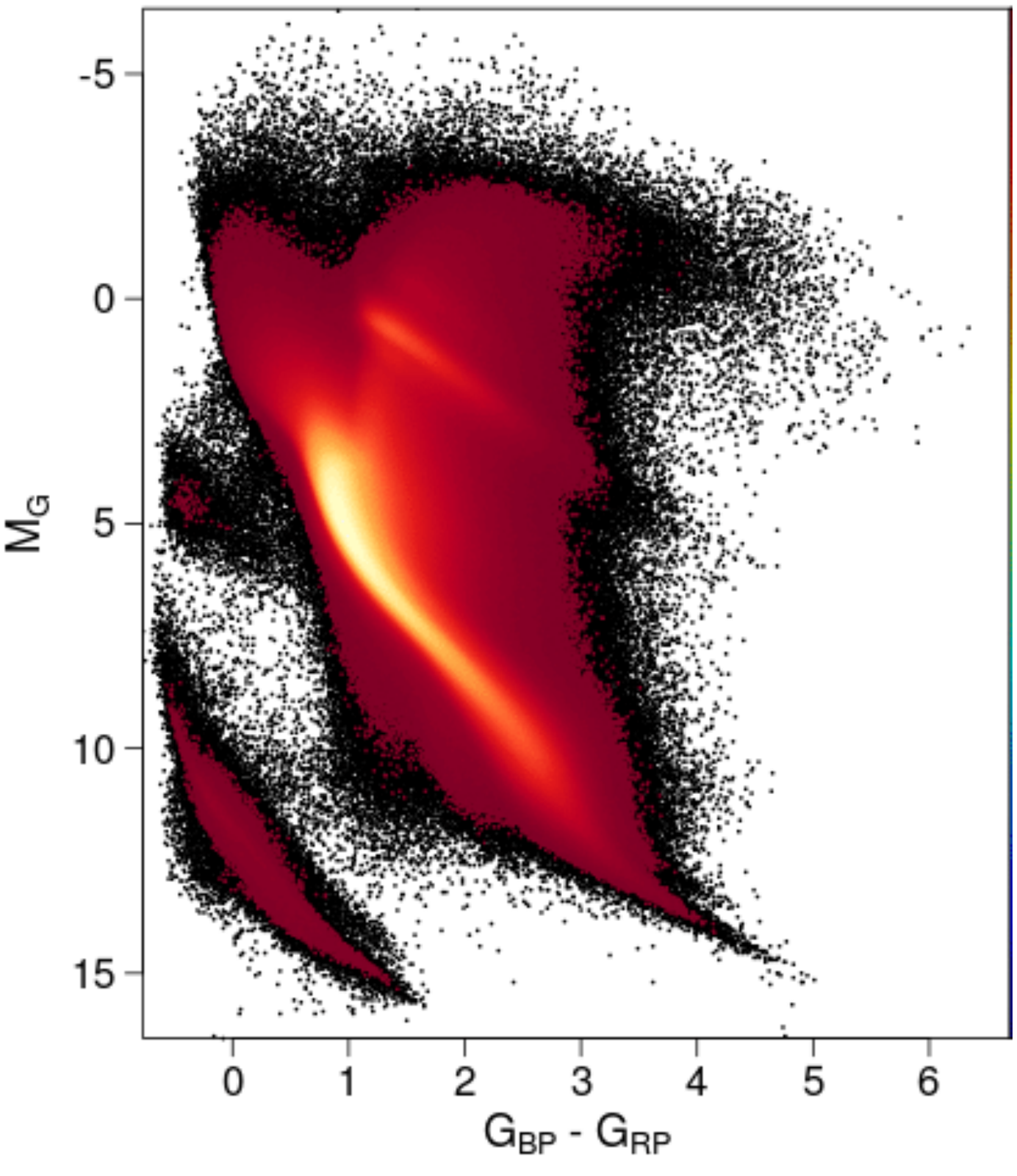

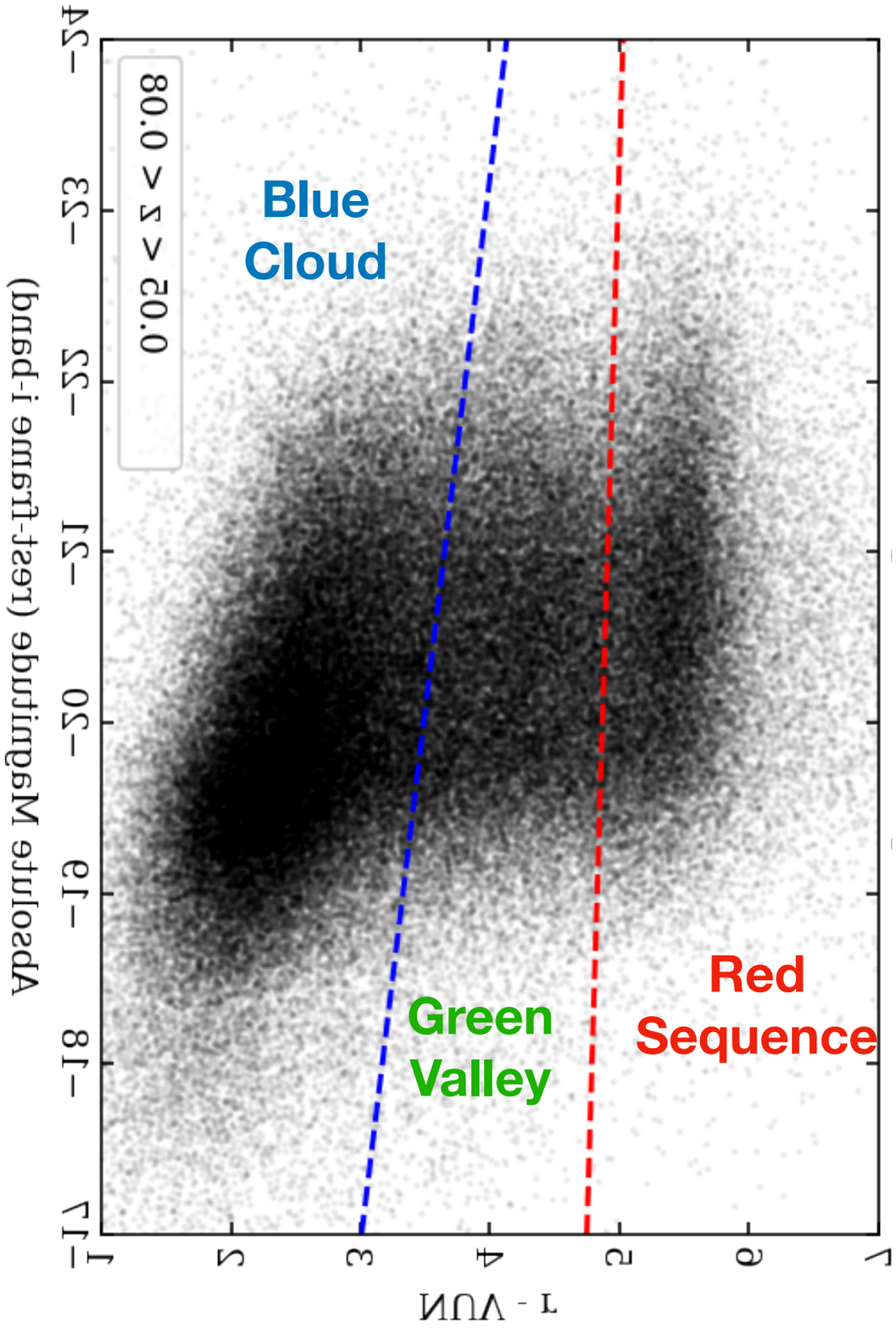

Color-Magnitude Diagram of Galaxies

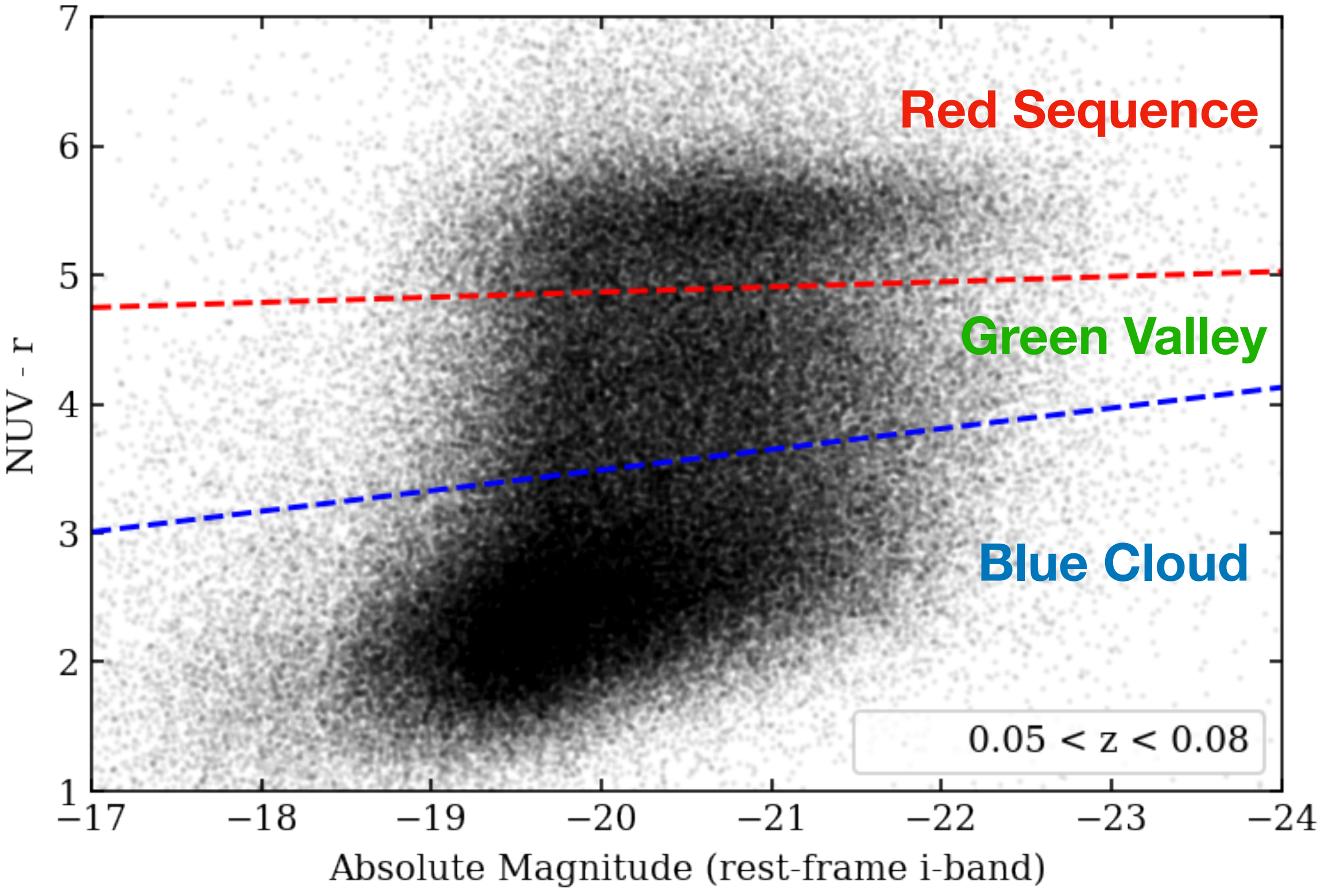

Color-Magnitude Diagram of Galaxies

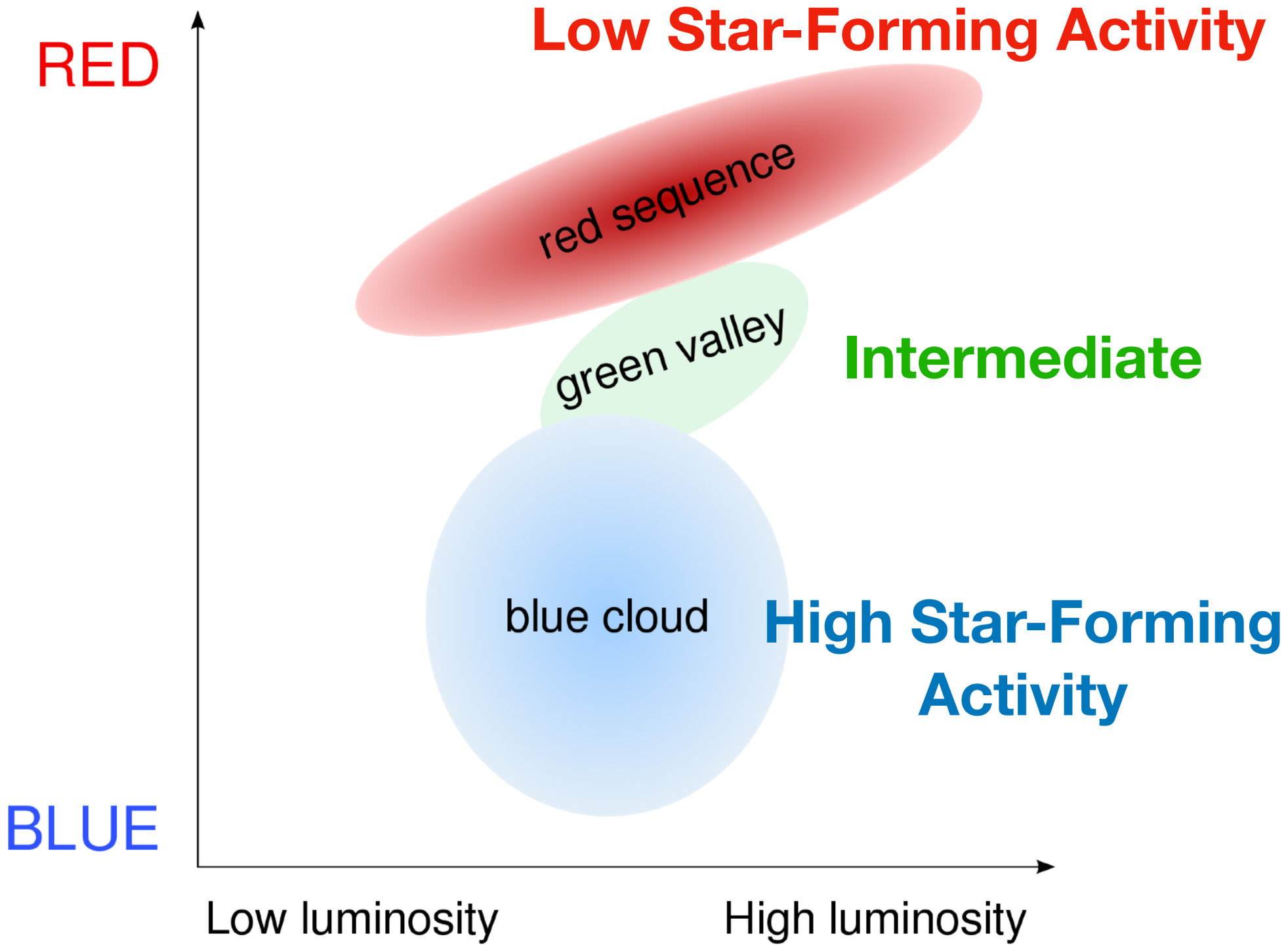

Integrated Color Naturally Separates Spirals and Ellipticals

Spectral estimates of the mass-to-light ratio of quiescent and active (star-forming) galaxies

The masses are estimated from spectral fitting with CSP models, but the M/L can be applied on galaxies that have only photometry data and **photometric redshifts**

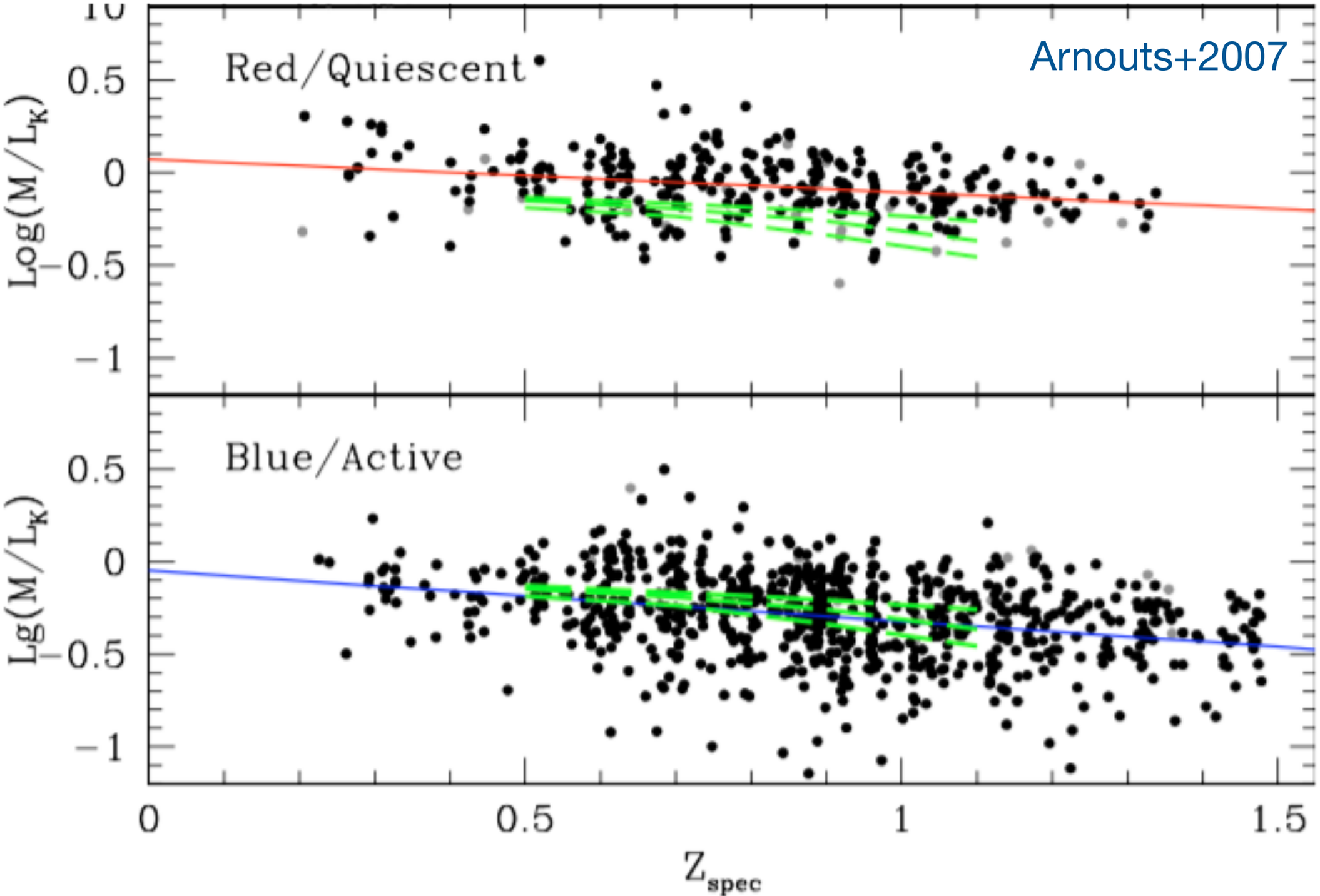

Star Formation Rates

Star Formation Rate using Mass Weights from CSP Modeling:

$$\mathrm{SFR} = \frac{M}{\tau} \int_{-3}^{1} \int_{0}^{\tau} p(t)p([\mathrm{M/H}])\, dtd[\mathrm{M/H}]$$

observed spectra vs. models

mass weights

images

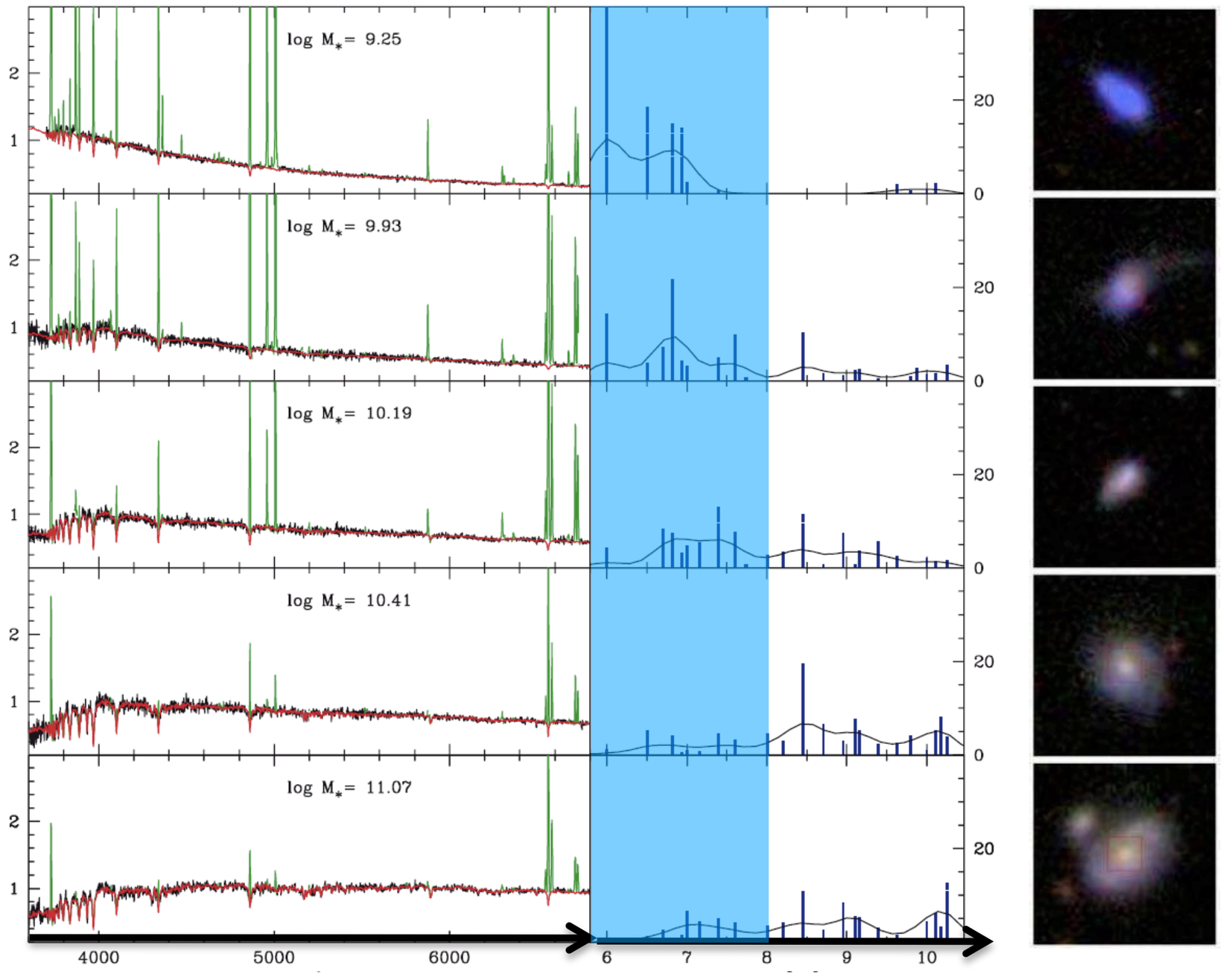

wavelength(Å)

log(age) (yr)

Asari, Cid Fernandes et al. 2007

To measure SFR, we may want to focus on **blue continuum** and **emission lines**

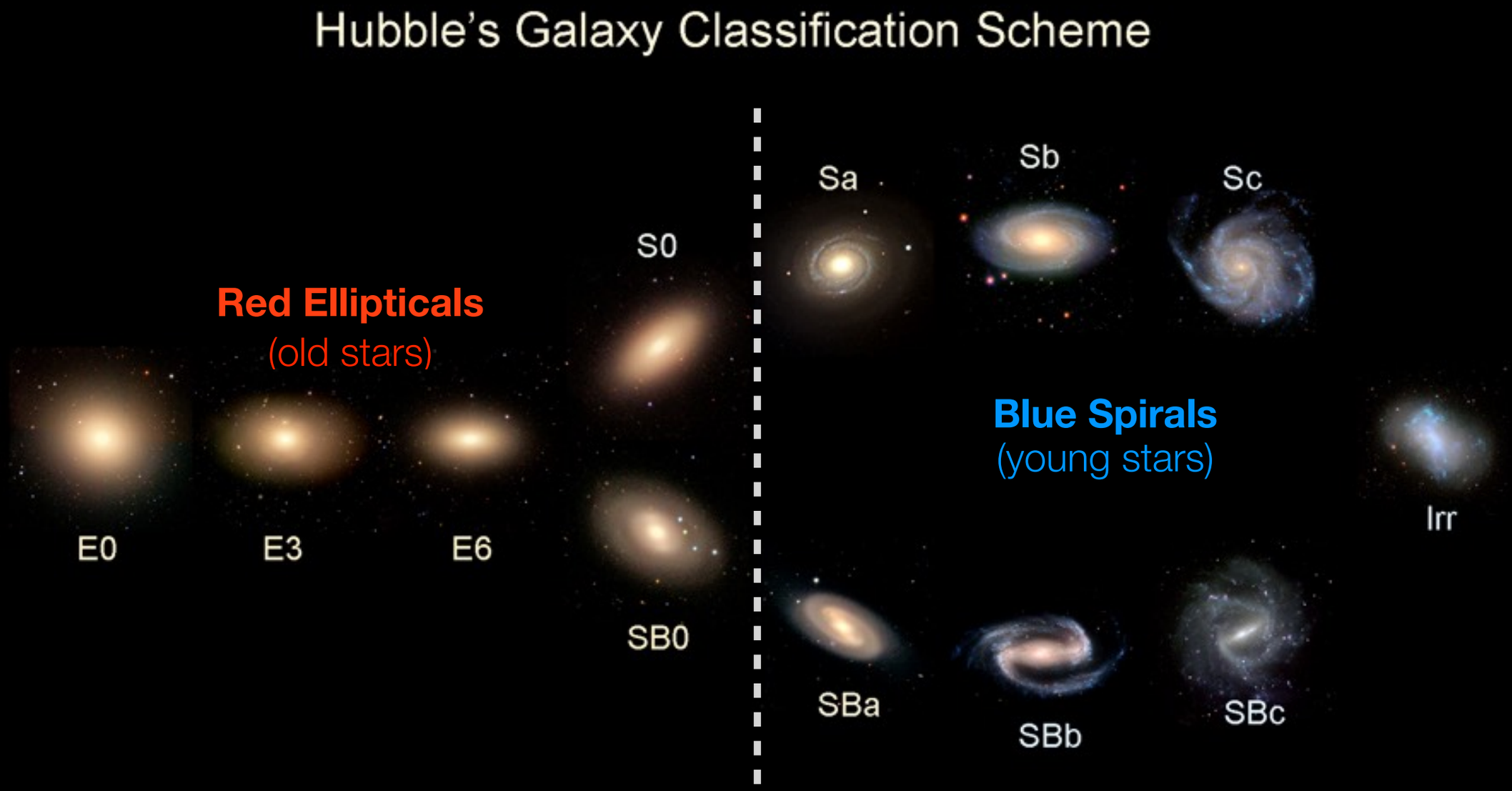

Single-Burst SFH: $b(t) = \delta(t - t_0)$

Luminosity declines as the stellar population ages

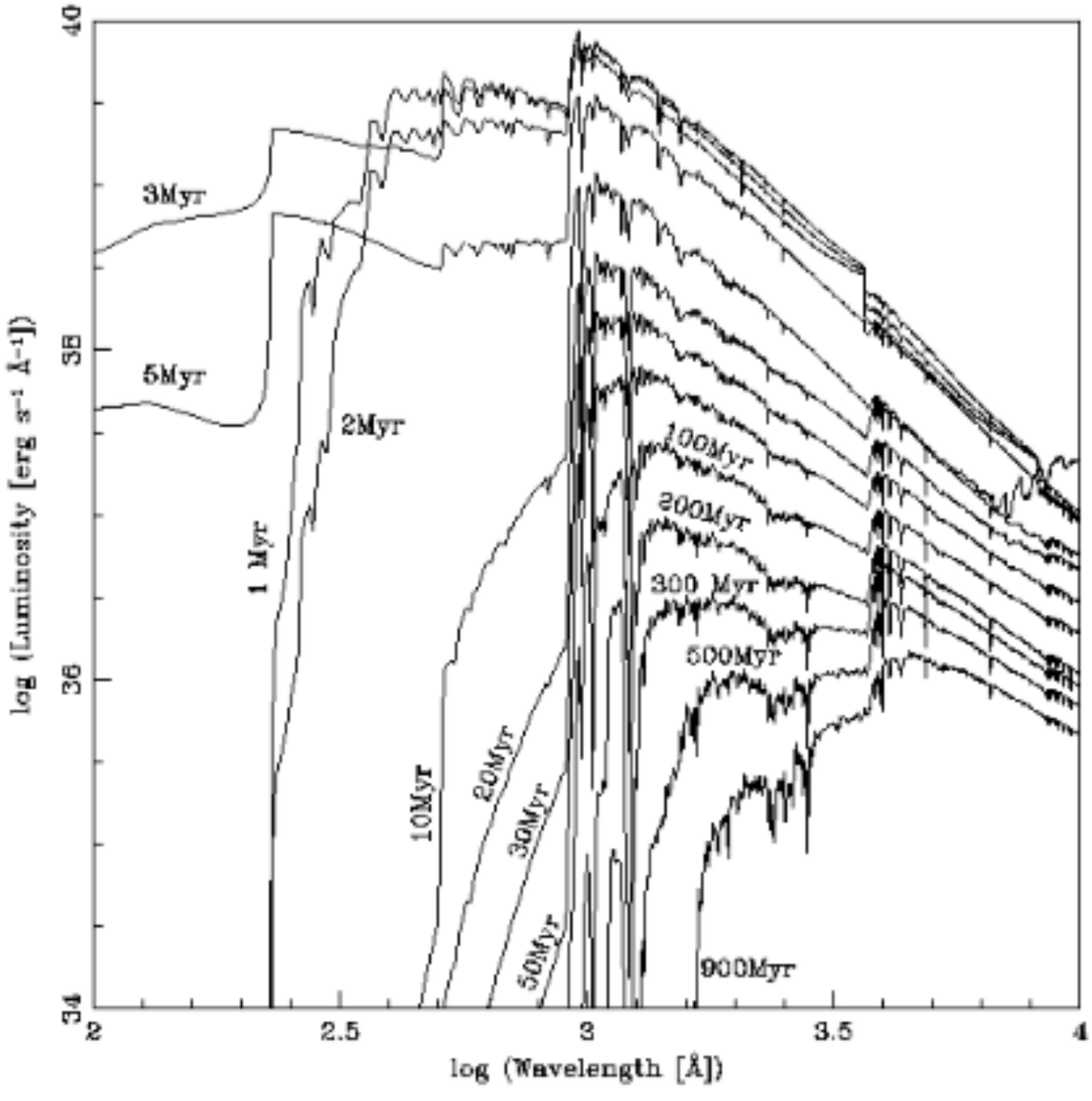

Leitherer+99: single-burst SF w/ ages of 1 Myr to 1 Gyr

Continuous, Constant SFH: $b(t) = 1$

Once the stellar types responsible for the photon contribution to a wavelength interval have reached **equilibrium (birth rate = death rate)**, the **luminosity** at the wavelength becomes **age independent**.

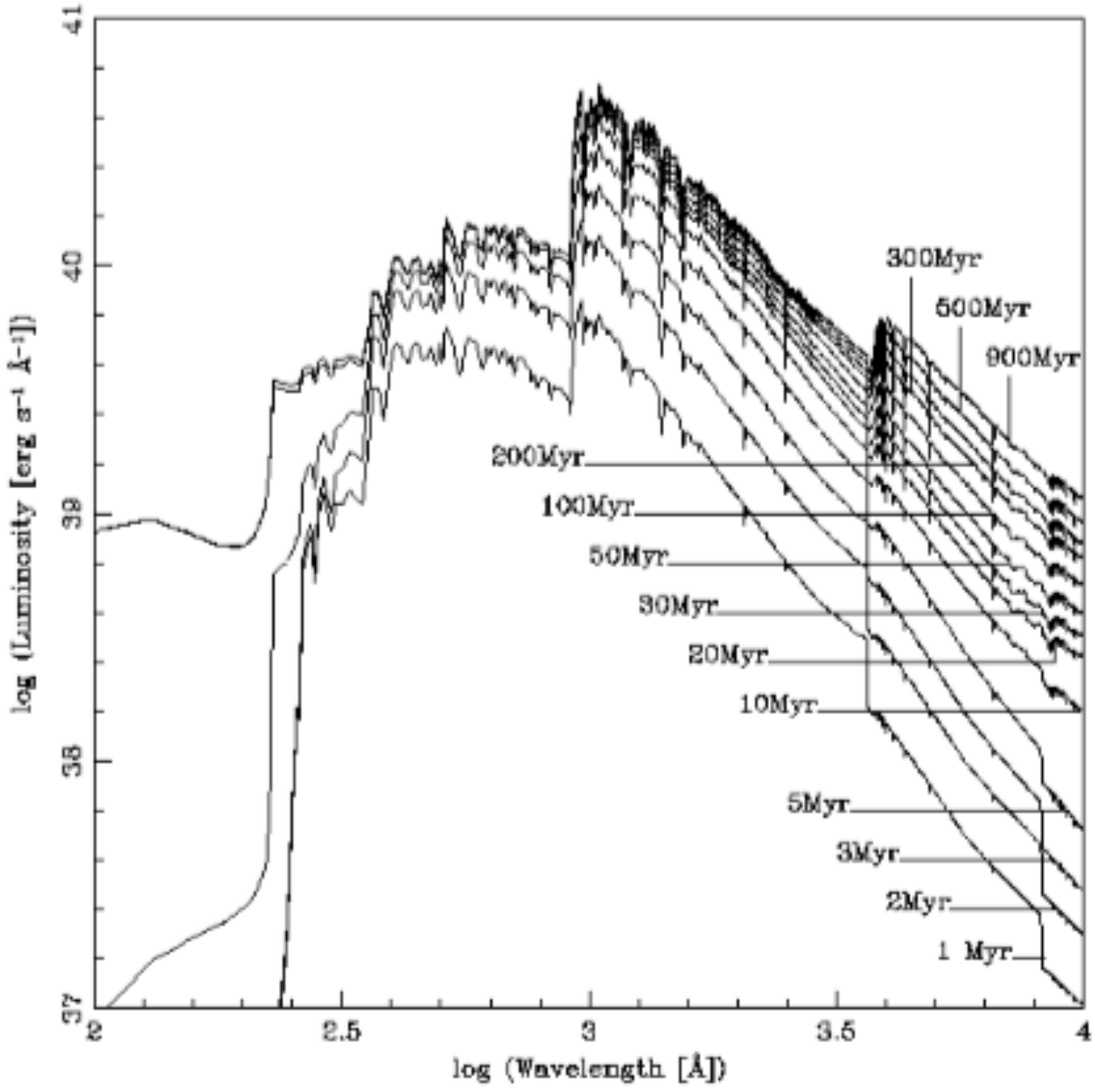

Leitherer+99: constant SF w/ durations of 1 Myr to 1 Gyr

Dust attenuated galaxies: use UV + IR luminosities

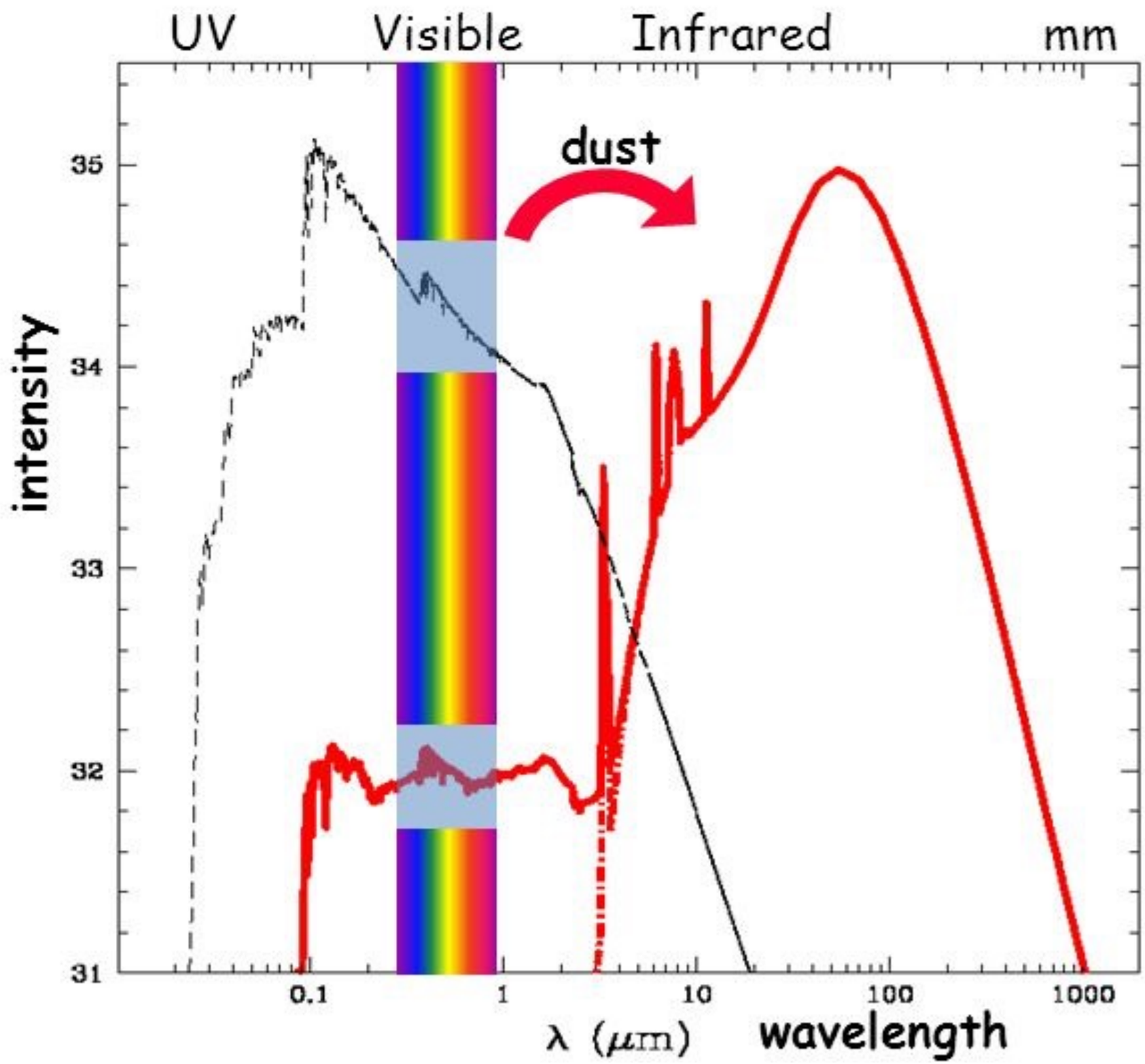

Commonly Used SFR estimators

Murphy+11: using the Kroupa IMF and Starburst99 SPS models

the following relation between the SFR and production rate of ionizing photons, $Q(H^0)$, at an age of ~100 Myr:

$$\left(\frac{\mathrm{SFR}}{M_\odot\,\mathrm{yr}^{-1}}\right) = 7.29\times10^{-54}\left[\frac{Q(H^0)}{\mathrm{s}^{-1}}\right]. \quad (1)$$

$$\begin{cases} \left(\frac{\mathrm{SFR_{H\alpha}}}{M_\odot\,\mathrm{yr}^{-1}}\right) = 5.37\times10^{-42}\left(\frac{L_{\mathrm{H\alpha}}}{\mathrm{erg\,s}^{-1}}\right). & (2) \\ \left(\frac{\mathrm{SFR_{FUV}}}{M_\odot\,\mathrm{yr}^{-1}}\right) = 4.42\times10^{-44}\left(\frac{L_{\mathrm{FUV}}}{\mathrm{erg\,s}^{-1}}\right). & (3) \\ \left(\frac{\mathrm{SFR_{IR}}}{M_\odot\,\mathrm{yr}^{-1}}\right) = 3.88\times10^{-44}\left(\frac{L_{\mathrm{IR}}}{\mathrm{erg\,s}^{-1}}\right). & (4) \end{cases}$$

Commonly used SFR estimators

(Murphy+11)

SPS Models

derive corresponding calibrations using Starburst99 (Leitherer et al. 1999) for a common IMF. We choose a Kroupa (Kroupa 2001) IMF, having a slope of −1.3 for stellar masses between 0.1–0.5 $M_\odot$ and −2.3 for stellar masses ranging between 0.5 and 100 $M_\odot$.

Luminosity of Recombination Lines

Assuming a solar metallicity and continuous star formation (i.e., a fixed SFR), Starburst99 stellar population models yield the following relation between the SFR and production rate of ionizing photons, $Q(H^0)$, at an age of ∼100 Myr:

$$\left(\frac{\mathrm{SFR}}{M_\odot\,\mathrm{yr}^{-1}}\right) = 7.29\times10^{-54}\left[\frac{Q(H^0)}{\mathrm{s}^{-1}}\right]. \quad (1)$$

The ionizing photon rate can of course be expressed as an (extinction corrected) H recombination line flux, such that for Case B recombination, and assuming an electron temperature $T_e = 10^4$ K, the Hα recombination line strength is related to the SFR by

$$\left(\frac{\mathrm{SFR}_{\mathrm{H}\alpha}}{M_\odot\,\mathrm{yr}^{-1}}\right) = 5.37\times10^{-42}\left(\frac{L_{\mathrm{H}\alpha}}{\mathrm{erg\,s}^{-1}}\right). \quad (2)$$

UV+IR Continuum Luminosities

The integrated UV spectrum is dominated by young stars, making it a sensitive probe of recent (∼10–100 Myr; Kennicutt 1998; Calzetti et al. 2005; Salim et al. 2007) star formation activity. We convolve the output Starburst99 spectrum with the *GALEX* FUV transmission curve to obtain the following conversion between SFR and FUV luminosity,

$$\left(\frac{\mathrm{SFR}_{\mathrm{FUV}}}{M_\odot\,\mathrm{yr}^{-1}}\right) = 4.42\times10^{-44}\left(\frac{L_{\mathrm{FUV}}}{\mathrm{erg\,s}^{-1}}\right). \quad (3)$$

To derive a calibration for the total infrared (IR; 8–1000 μm), we make the assumption that the entire Balmer continuum is absorbed and re-radiated by dust and that the dust emission is optically thin. Integrating the output Starburst99 spectrum over this wavelength range (i.e., 912 Å < λ < 3646 Å) results in the following (predicted) relation between the IR emission and current SFR:

$$\left(\frac{\mathrm{SFR}_{\mathrm{IR}}}{M_\odot\,\mathrm{yr}^{-1}}\right) = 3.88\times10^{-44}\left(\frac{L_{\mathrm{IR}}}{\mathrm{erg\,s}^{-1}}\right). \quad (4)$$

$$\mathrm{SFR}_{\mathrm{tot}} = \mathrm{SFR}_{\mathrm{FUV}} + \mathrm{SFR}_{\mathrm{IR}}. \quad (8)$$

Using the above calibrations, this relation can be expressed as a linear combination of the UV and total IR emission such that

$$\left(\frac{\mathrm{SFR}_{\mathrm{tot}}}{M_\odot\,\mathrm{yr}^{-1}}\right) = 4.42\times10^{-44}\left(\frac{L_{\mathrm{FUV}} + 0.88L_{\mathrm{IR}}}{\mathrm{erg\,s}^{-1}}\right). \quad (9)$$

UV and IR Luminosity Functions and Cosmic Star Formation History

Evolution of UV Luminosity Function

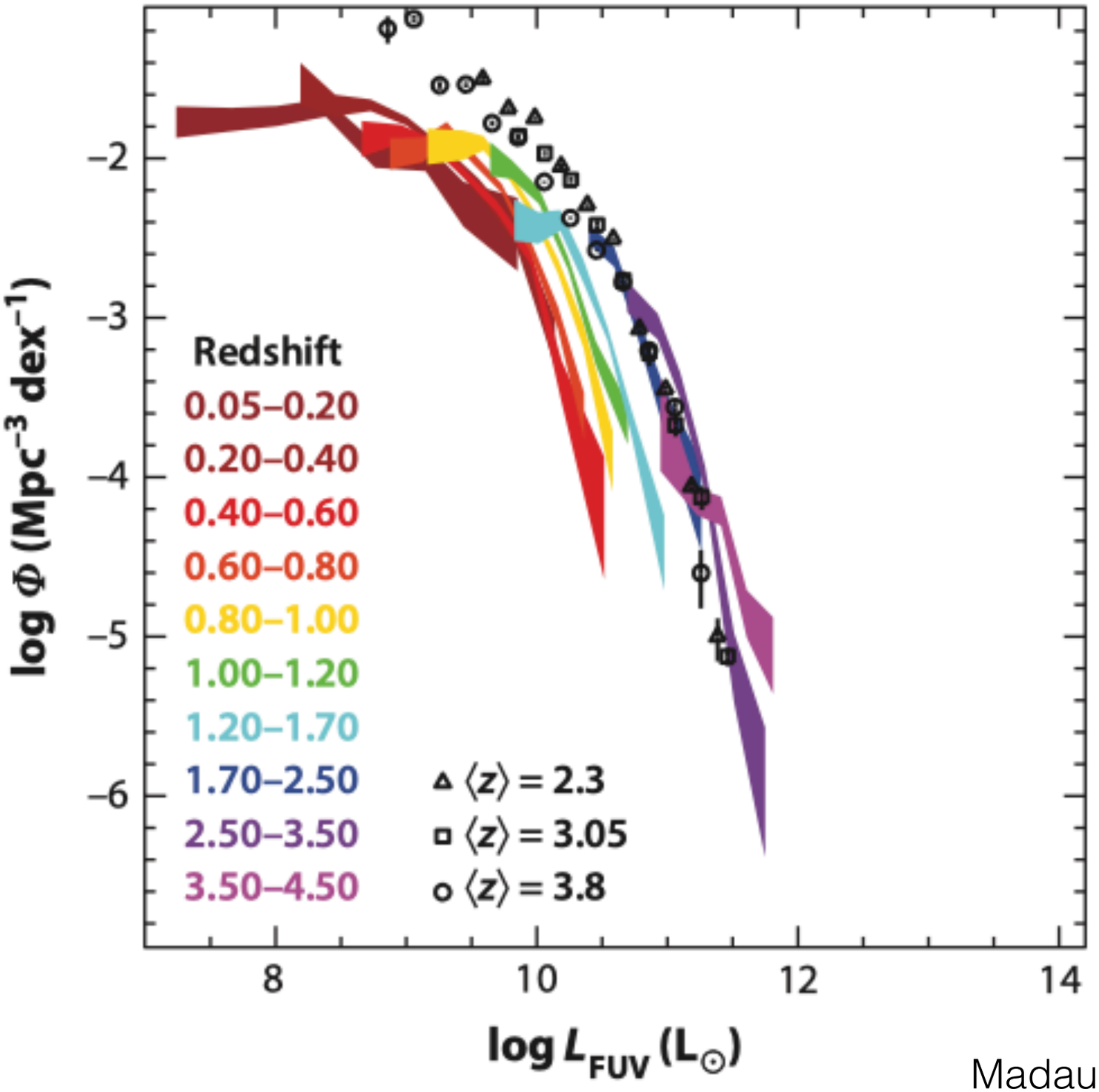

Madau & Dickinson 2014

Evolution of Far-IR Luminosity Function

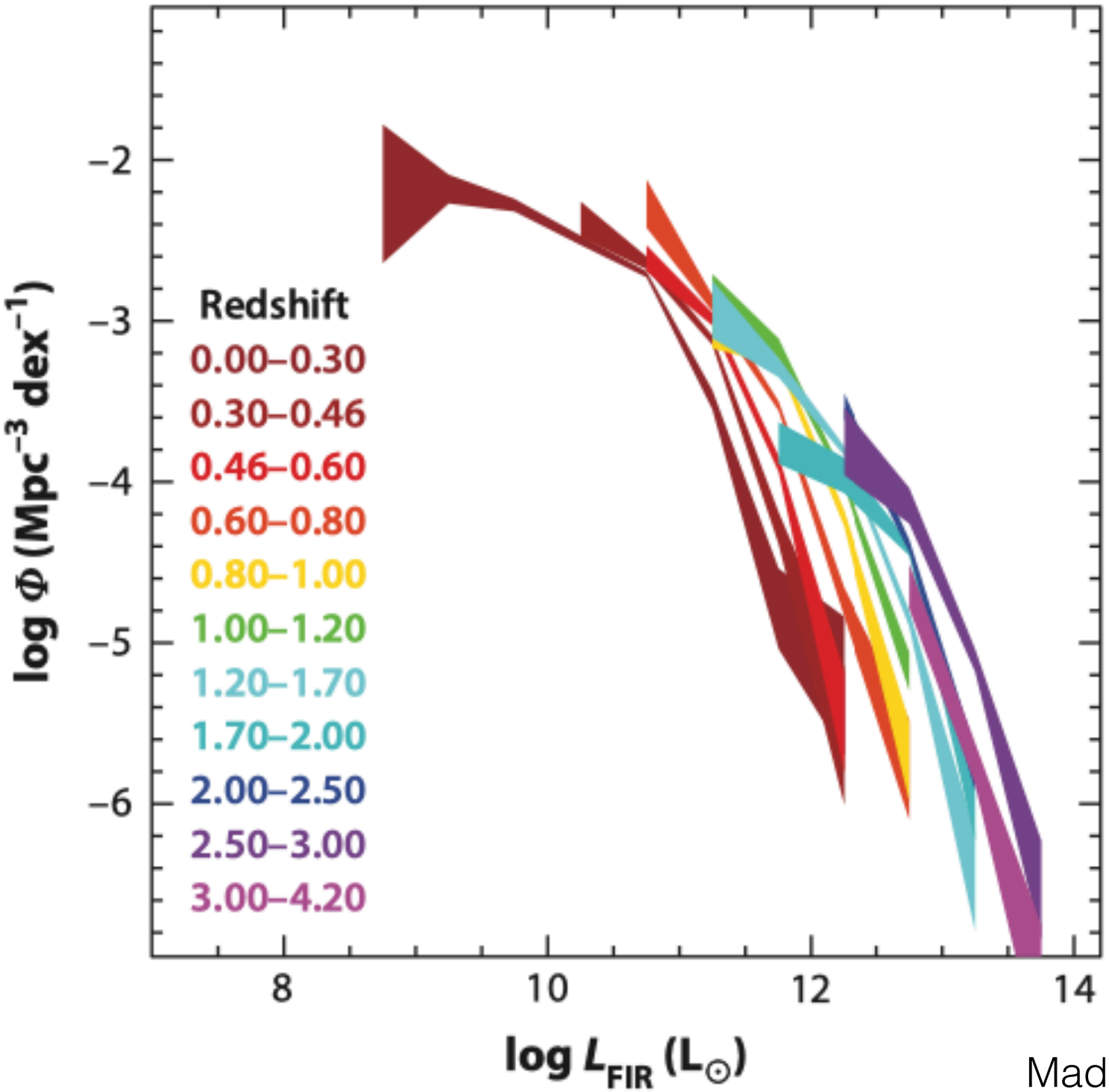

Madau & Dickinson 2014

Integrated UV+FIR LFs -> Cosmic SF History

$$\psi(z) = 0.015 \frac{(1+z)^{2.7}}{1+[(1+z)/2.9]^{5.6}}\ \mathrm{M}_\odot\ \mathrm{year}^{-1}\ \mathrm{Mpc}^{-3}. \qquad (15)$$

solid line is a fit to the data points

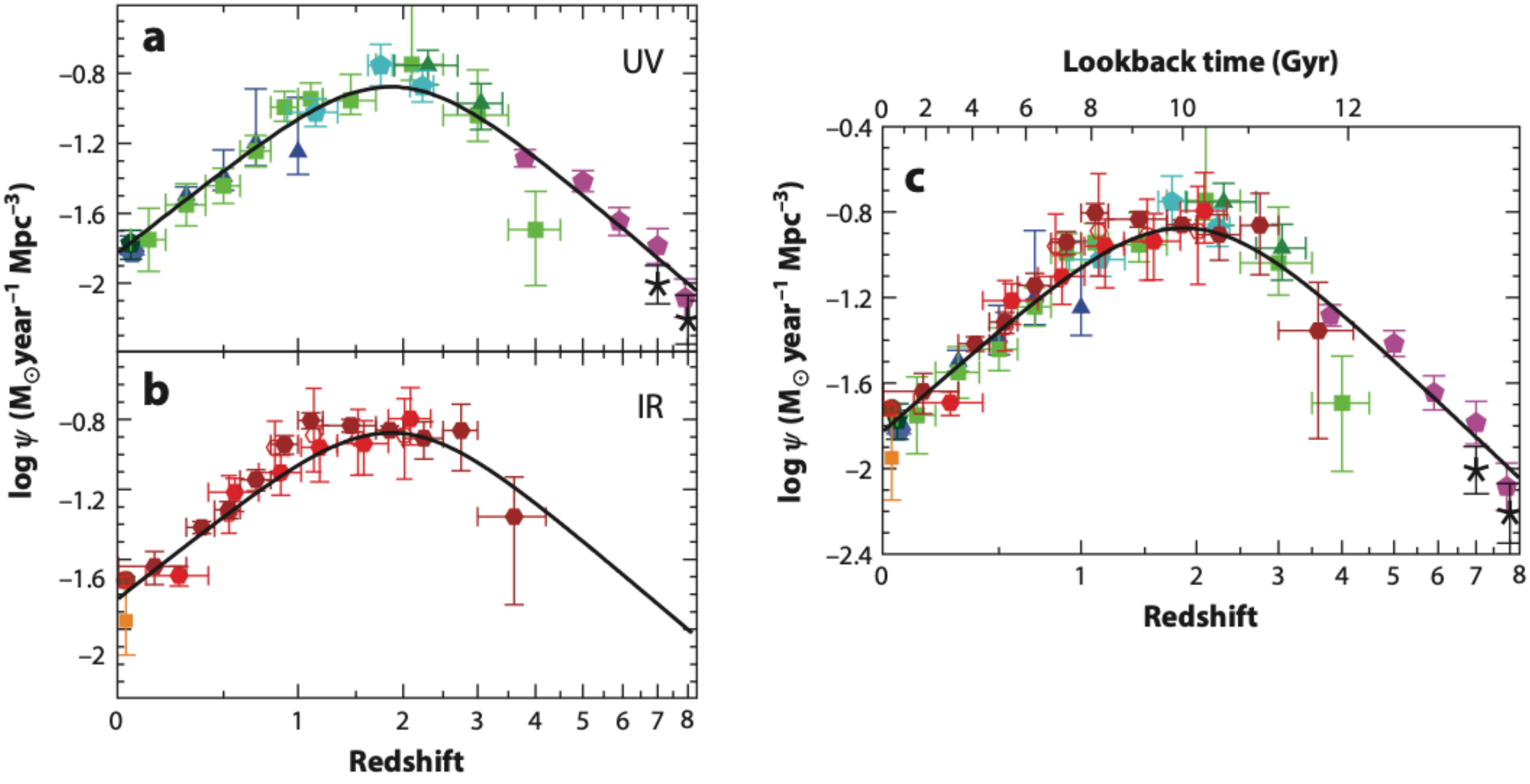

Sanity Check:

are stellar mass functions consistent with cosmic SF history?

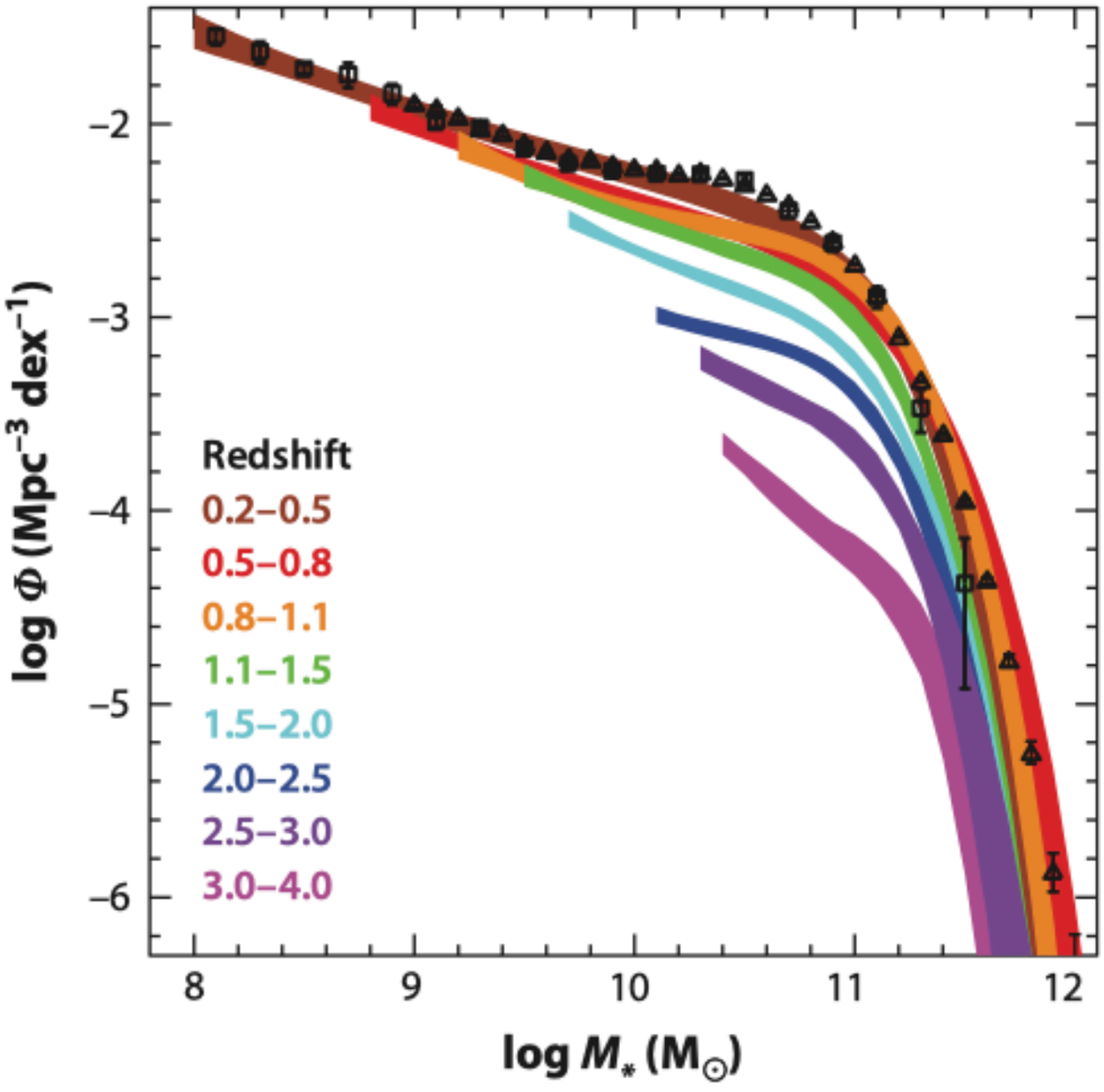

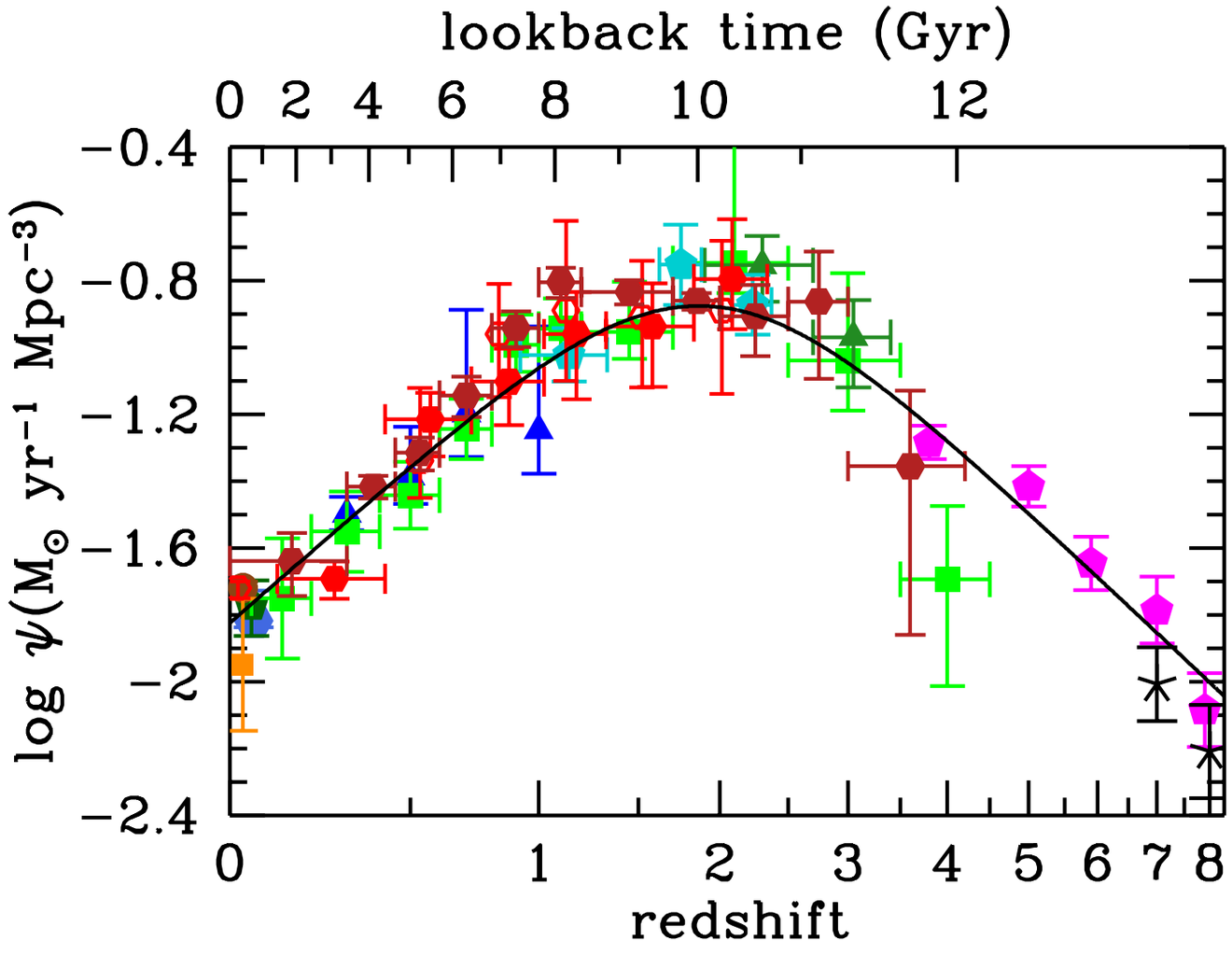

Madau & Dickinson 2014

Integrated MF vs. Integrated SFH

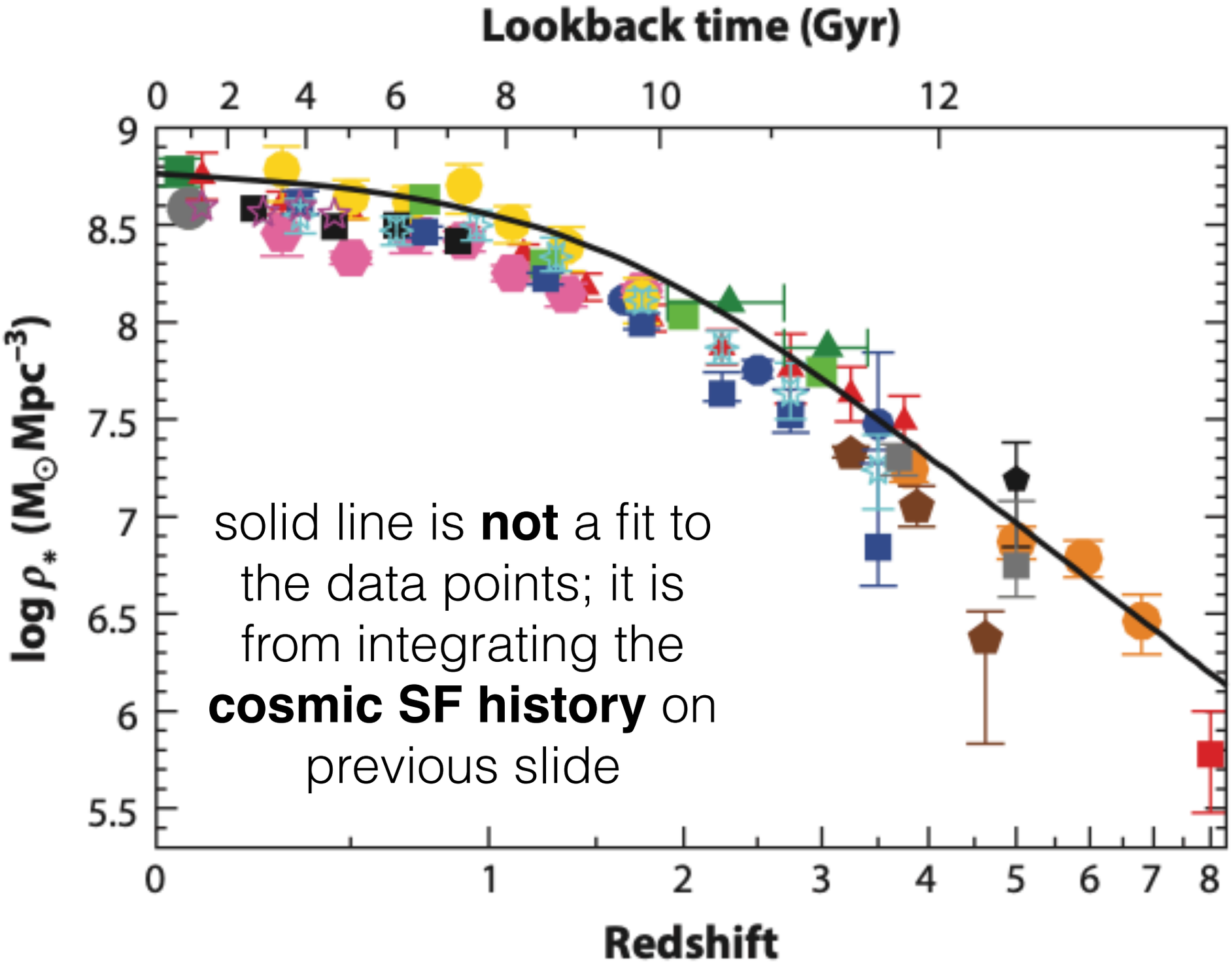

solid line is **not** a fit to the data points; it is from integrating the **cosmic SF history** on previous slide

Bathtub Model Predictions Compared to Observations

The ``Bathtub'' Model: Accretion-Driven Star Formation

a continuity equation coupled with
a halo growth history and a star formation law

Change in Cold Gas Reservoir | **Accretion Rate** $\propto$ **Halo Growth Rate** | **Gas Consumption Rate** $\propto$ **Star Formation Rate**

$$\int \frac{dM_{\rm gas}}{dt} = \epsilon_{\rm cold} f_{\rm baryon} \frac{dM_{\rm halo}}{dt} - (1 - f_{\rm recycle} + f_{\rm outflow}) \frac{dM_{\rm star}}{dt}$$

$$\begin{cases} \dfrac{dM_{\rm halo}}{dt} \propto M_{\rm halo}^{1.1}(1+z)^{2.2} & \leftarrow \textbf{Halo Growth Rate from EPS} \\ \dfrac{dM_{\rm star}}{dt} = {\rm SFR} = \epsilon_{\rm SF} \dfrac{M_{\rm gas}}{\tau_{\rm dyn}} & \leftarrow \textbf{Kennicutt-Schmidt Relation} \end{cases}$$

cold gas accretion efficiency:

$$\begin{cases} \epsilon_{\rm cold} = 0.0 \text{ if } M_{\rm halo} < 10^{11} M_\odot \\ \epsilon_{\rm cold} = 0.7 \text{ if } 10^{11} < M_{\rm halo} < 10^{12.3} M_\odot \\ \epsilon_{\rm cold} = 0.0 \text{ if } M_{\rm halo} > 10^{12.3} M_\odot \end{cases}$$

recycle & feedback:

$$\begin{cases} f_{\rm recycle} = 0.5 \\ f_{\rm outflow} = 0.6 \end{cases}$$

Observed Stellar Mass Fraction Today

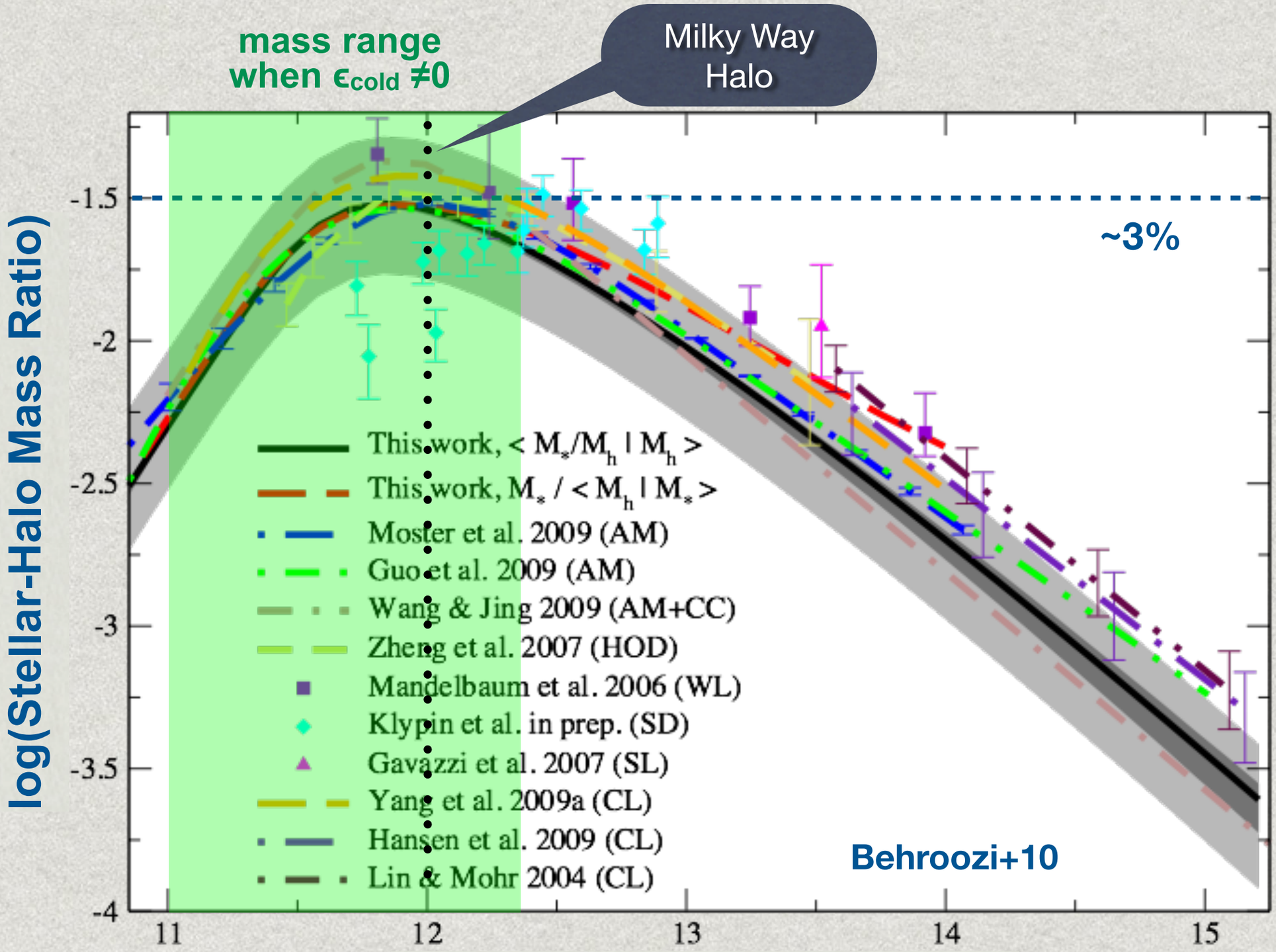

Stellar mass fraction

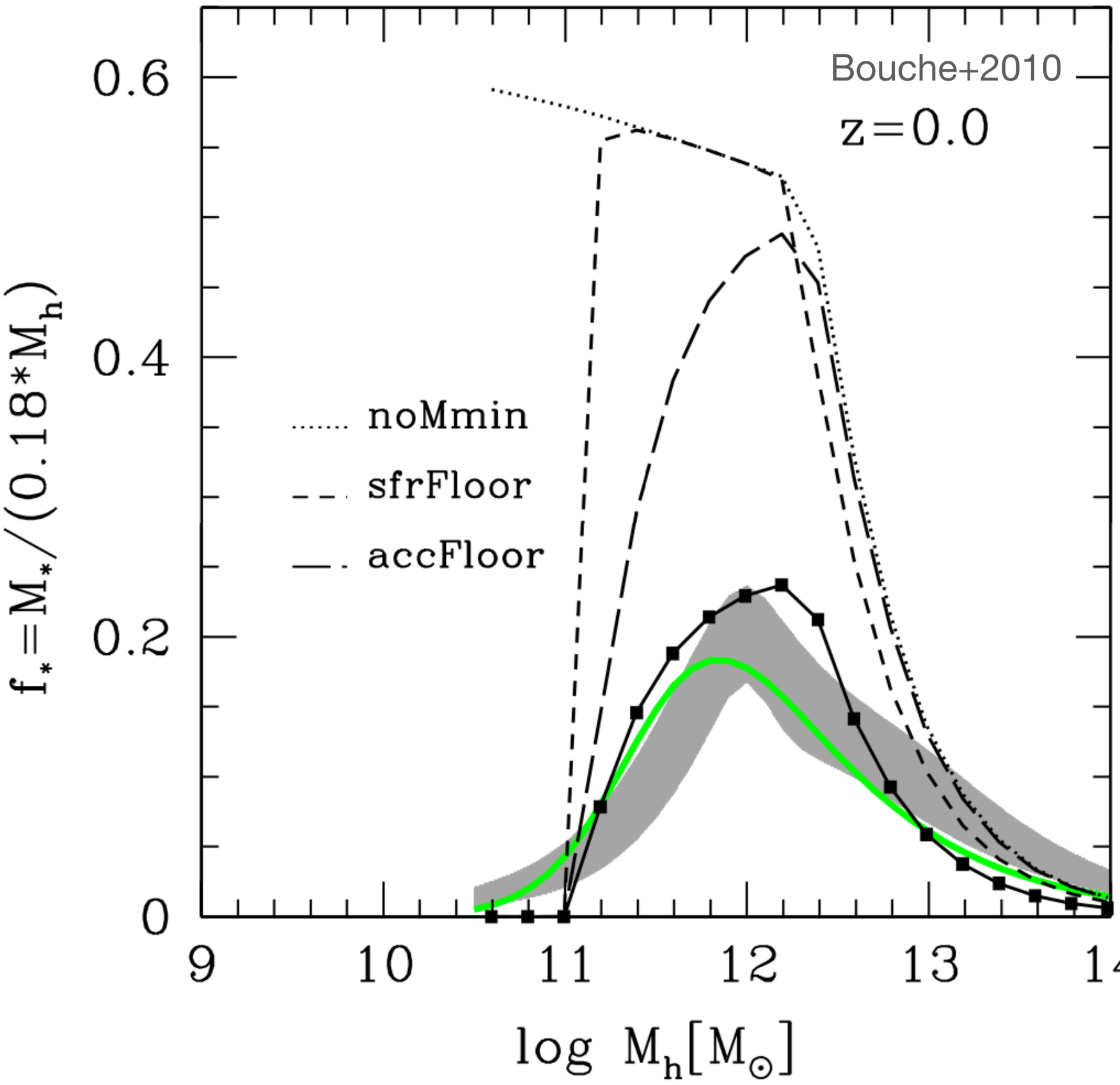

The z = 0 stellar fractions from Moster et al. (2010) and Guo et al. (2010) are shown as the shaded area and thick line, respectively.

Cosmic Star Formation History

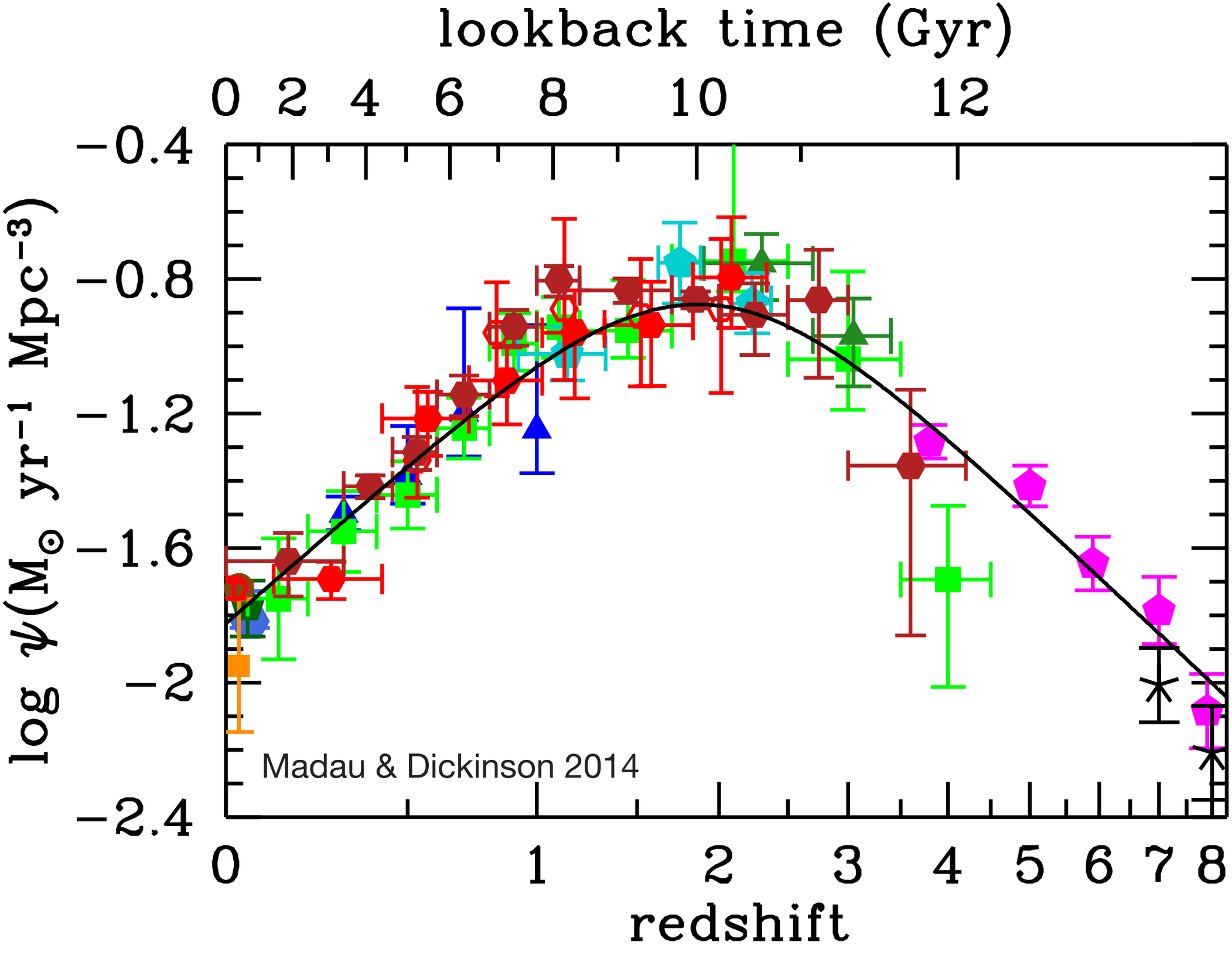

Stellar mass fraction

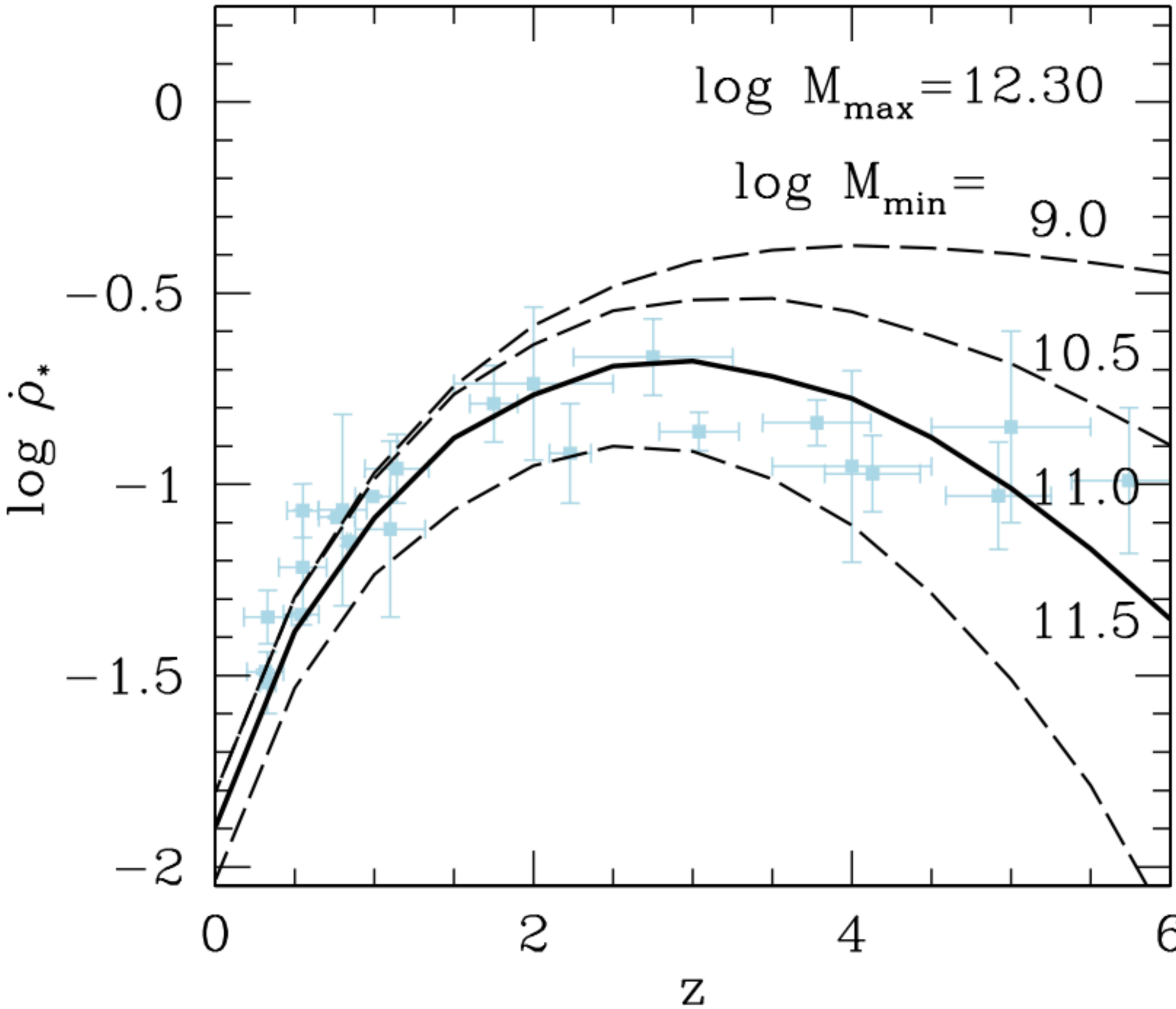

Bouche+2010

Unresolved Issue #1: Bimodal color distribution

Color Bimodality: Galaxies are either blue or red

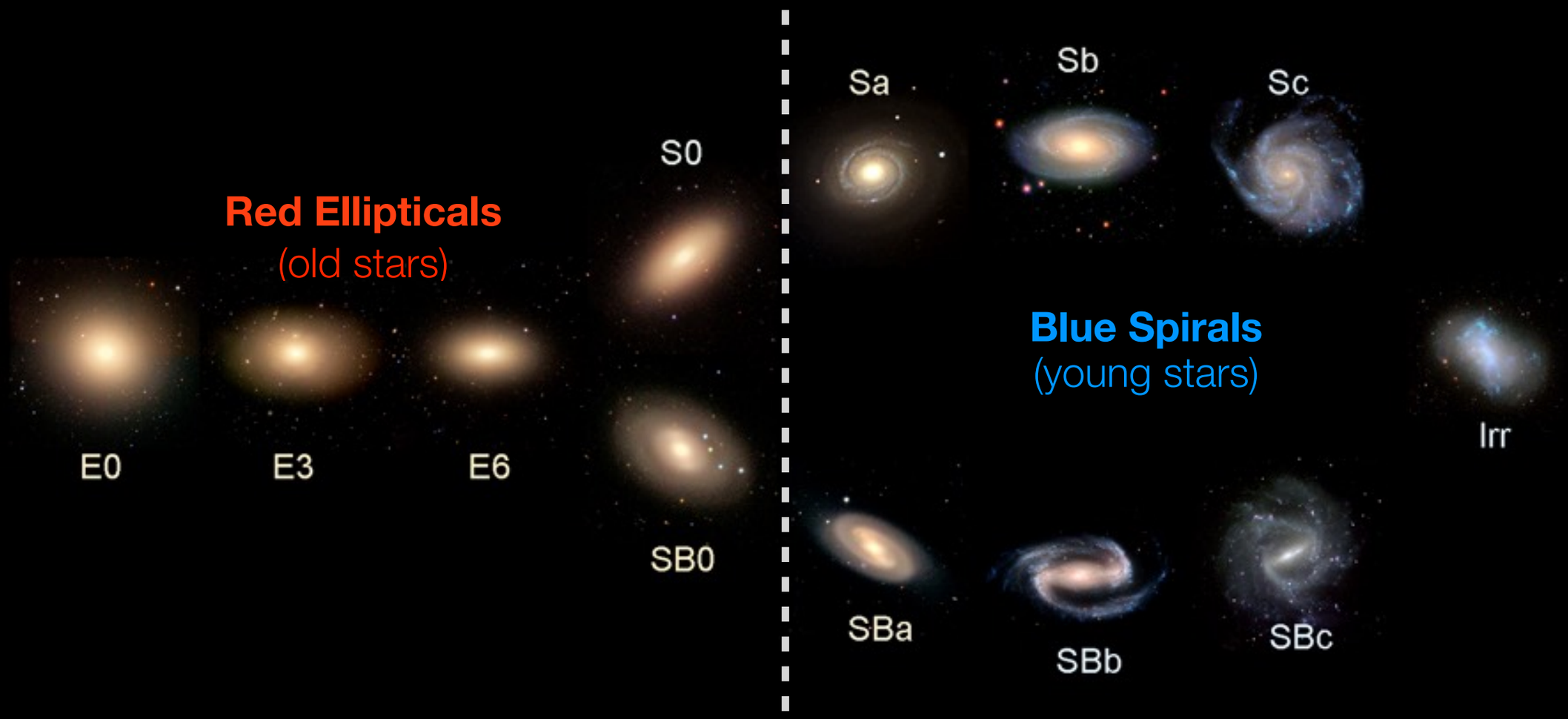

Galaxies in the Current universe

Color Bimodality

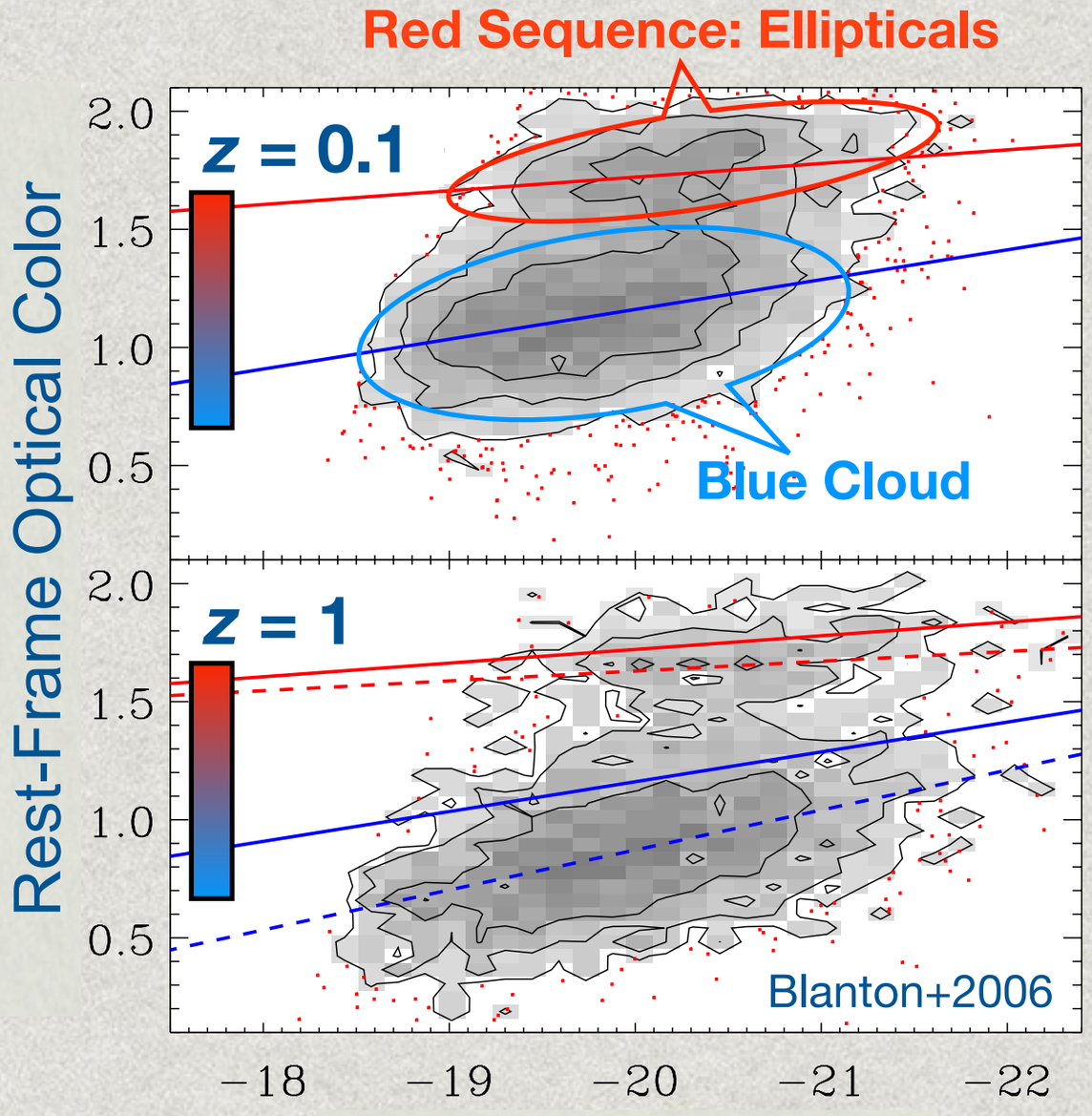

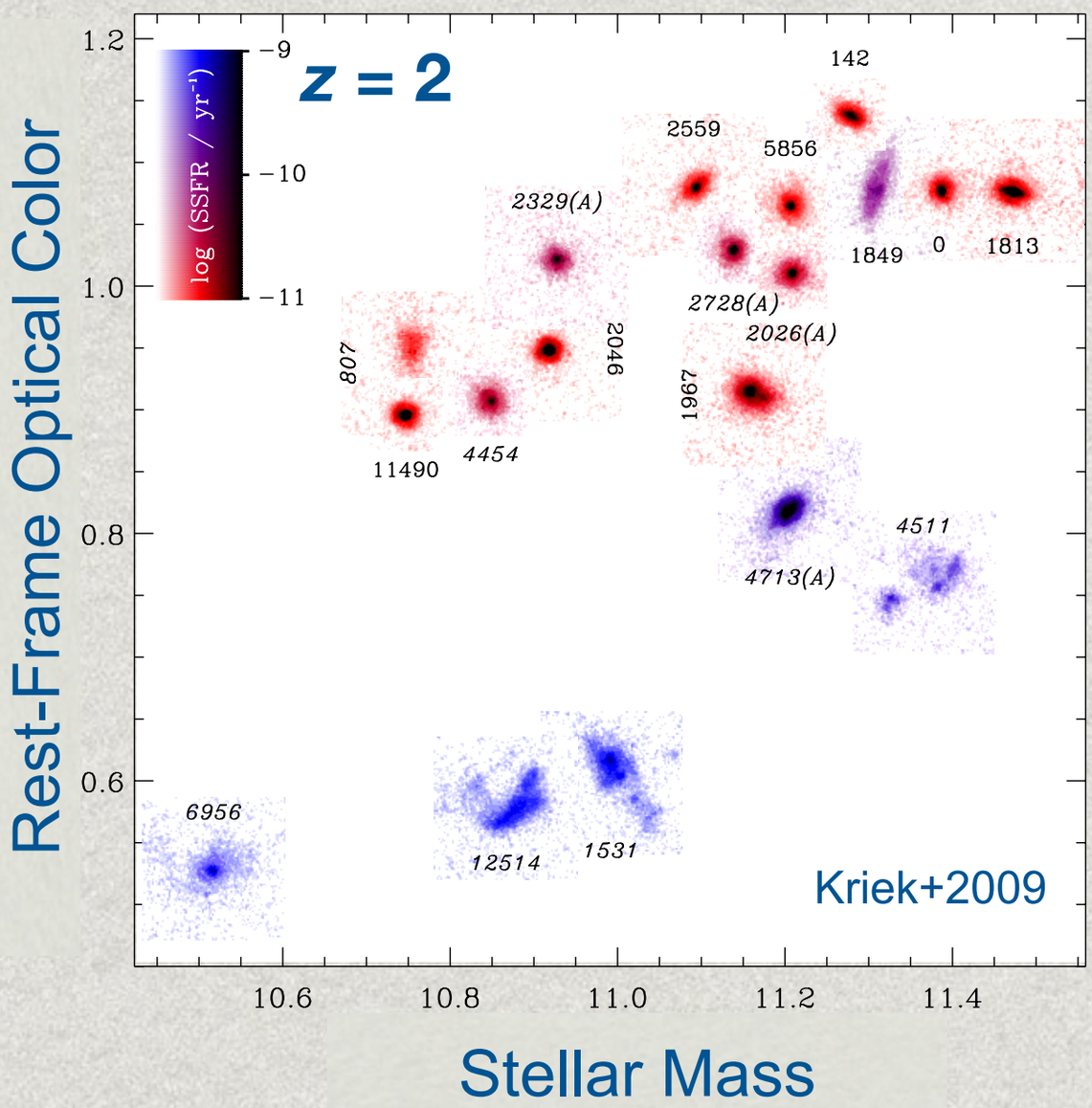

The early & rapid build-up of the red sequence

the evolution of the total comoving stellar mass density of quiescent galaxies

- **Early Completion**: Most of the stellar mass in the red sequence is already in place by $z = 1$
- **Rapid Build-Up**: Stellar mass density increased more than 20x in just 2.5 Gyr ($1 < z < 2$).

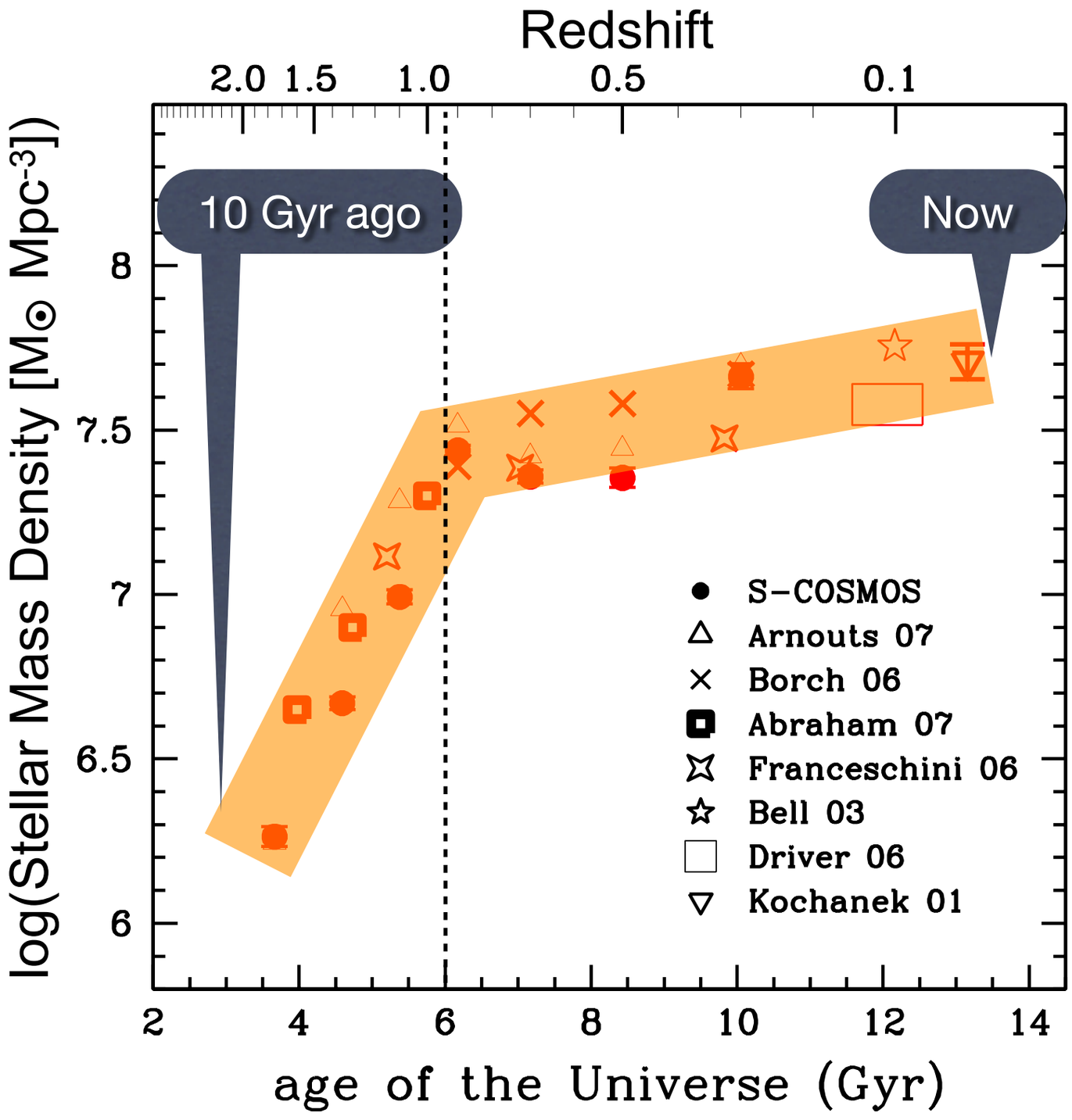

Ilbert+2010

Color bimodality at high-redshift requires rapid quenching

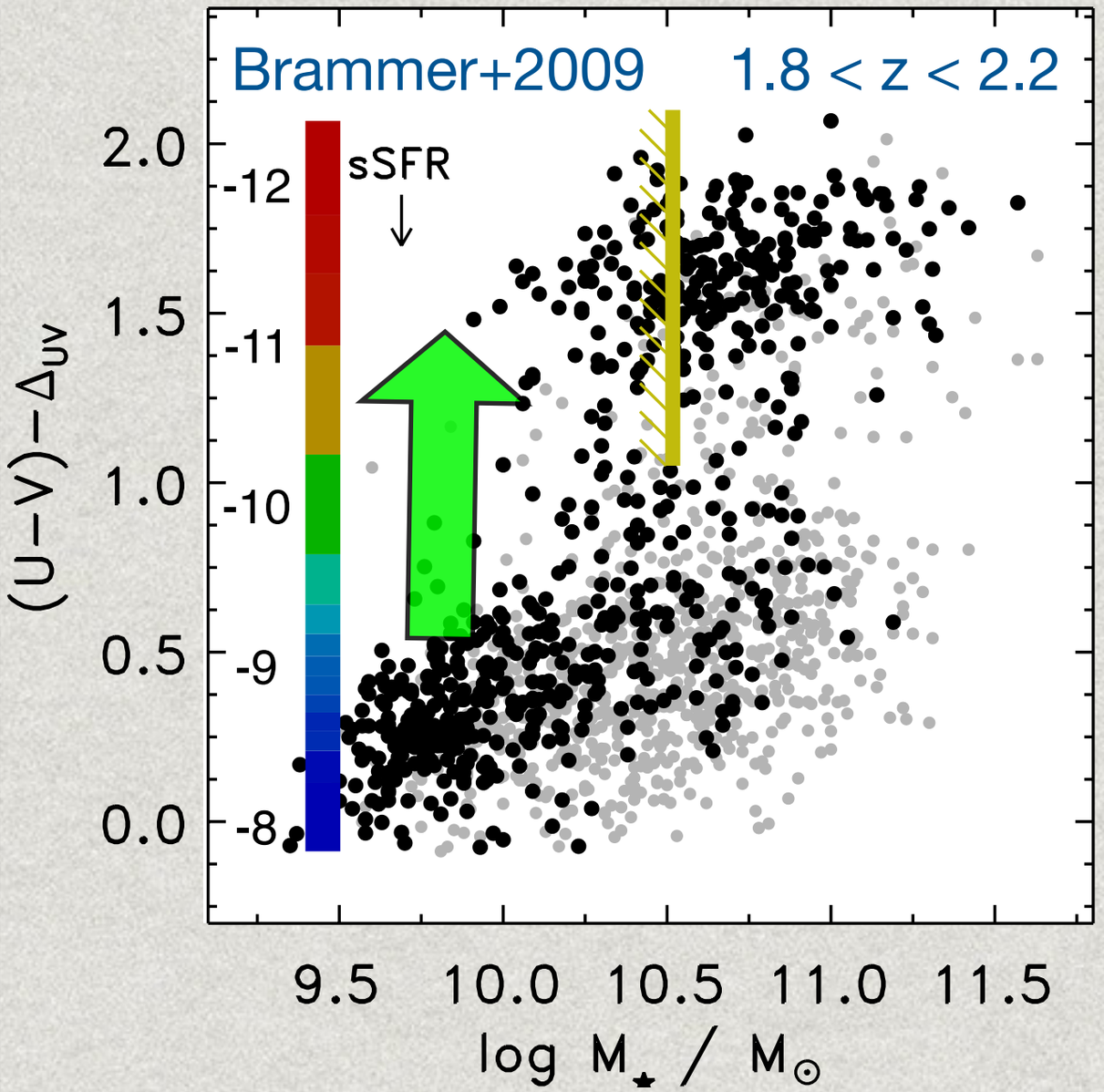

The lack of galaxies between blue cloud and red sequence requires very rapid transition:

* It takes ~5 e-folding time to cross the green valley (**e^5 = 150**)
* red-sequence e-folding timescale of 1 Gyr indicates an SFR e-folding time **<0.2 Gyr** (consistent w/ Goncalves+2012)

This is 10x shorter than the gas exhaustion time (~**2 Gyr**)!

$$\tau = \frac{\tau_{\rm dyn}}{\epsilon_{\rm SF}(1 - f_{\rm recycle} + f_{\rm outflow})}$$

When cold gas accretion stops: drain the tub

SFR exponentially declines with an e-folding time of 2 Gyr

$$\begin{cases} \dfrac{dM_{\rm gas}}{dt} = \cancel{\epsilon_{\rm cold} f_{\rm baryon} \dfrac{dM_{\rm halo}}{dt}} - (1 - f_{\rm recycle} + f_{\rm outflow}){\rm SFR} \\ {\rm SFR} = \epsilon_{\rm SF} \dfrac{M_{\rm gas}}{\tau_{\rm dyn}} \end{cases}$$

← **KS Star Formation Law**

when $\epsilon_{\rm cold} = 0$ we have :

$$\frac{d{\rm SFR}}{dt} = -\frac{\epsilon_{\rm SF}(1 - f_{\rm recycle} + f_{\rm outflow})}{\tau_{\rm dyn}}{\rm SFR}$$

Solving this equation, we get an exponentially declining SFR :

$${\rm SFR} \propto \exp(-\frac{t}{\tau}) \text{ and } \tau = \frac{\tau_{\rm dyn}}{\epsilon_{\rm SF}(1 - f_{\rm recycle} + f_{\rm outflow})} \simeq 2 \text{ Gyr}$$

How to quench star formation? (i.e. reduce the e-folding time by 10x)

$$\mathrm{SFR} \propto \exp(-\frac{t}{\tau}) \text{ and } \tau = \frac{\tau_{\mathrm{dyn}}}{\epsilon_{\mathrm{SF}}(1 - f_{\mathrm{recycle}} + f_{\mathrm{outflow}})} \simeq 2 \text{ Gyr}$$

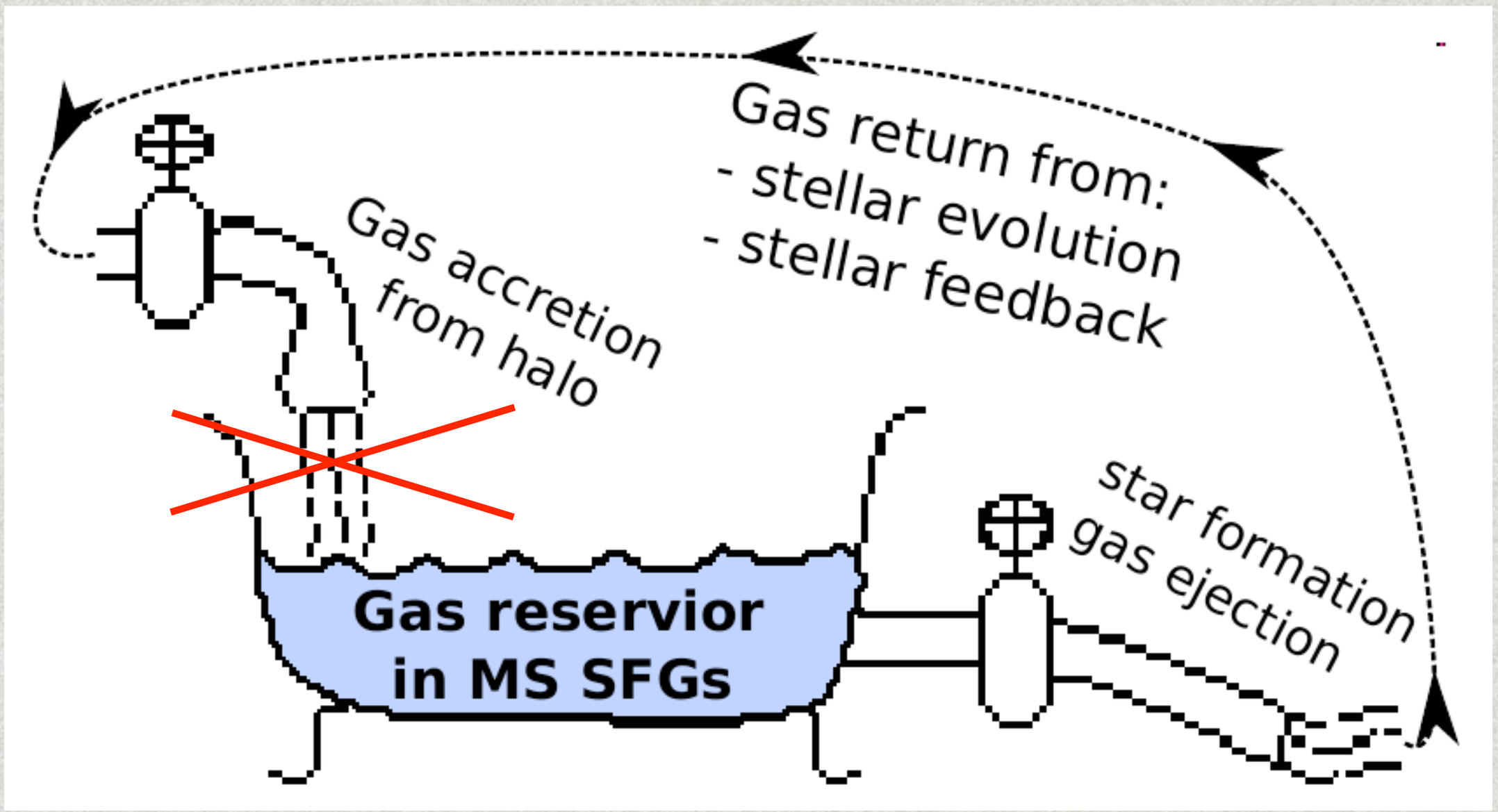

Unresolved Issue #2: Starbursts at high-redshift

Submm-Bright Galaxies (SMGs) at z ~ 2.5

- SMG definition:
  S(850um) > 2-3 mJy
- Bright in submm,
  but extremely faint
  in optical
- Median properties:
  <z> ~ 2.5
  $\langle L_{IR} \rangle \sim 5 \times 10^{12}\ L_\odot$
  $\langle SFR \rangle \sim 500\ M_\odot/yr$
- Strong clustering strength:
  $M_{halo} \sim 10^{13}\ M_\odot$
  similar to z ~2 QSOs

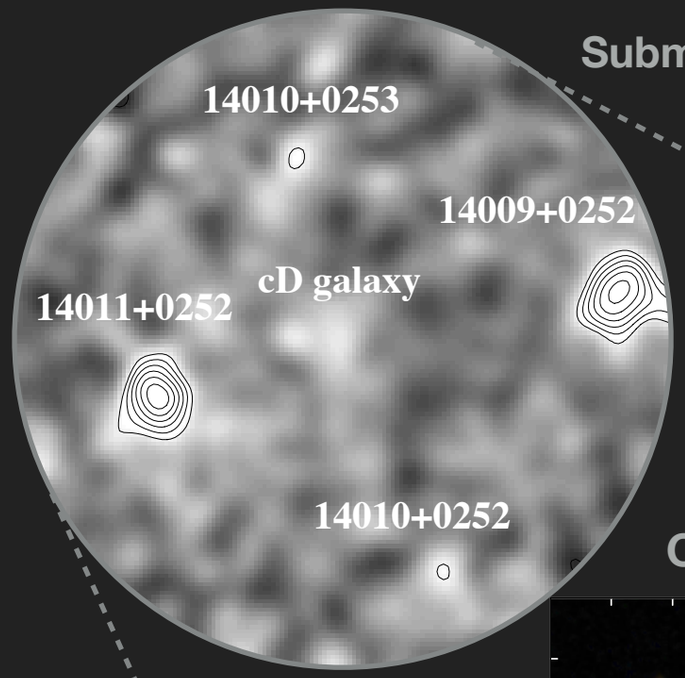

Ivison+00
Barger+98
Smail+98
Eales+99

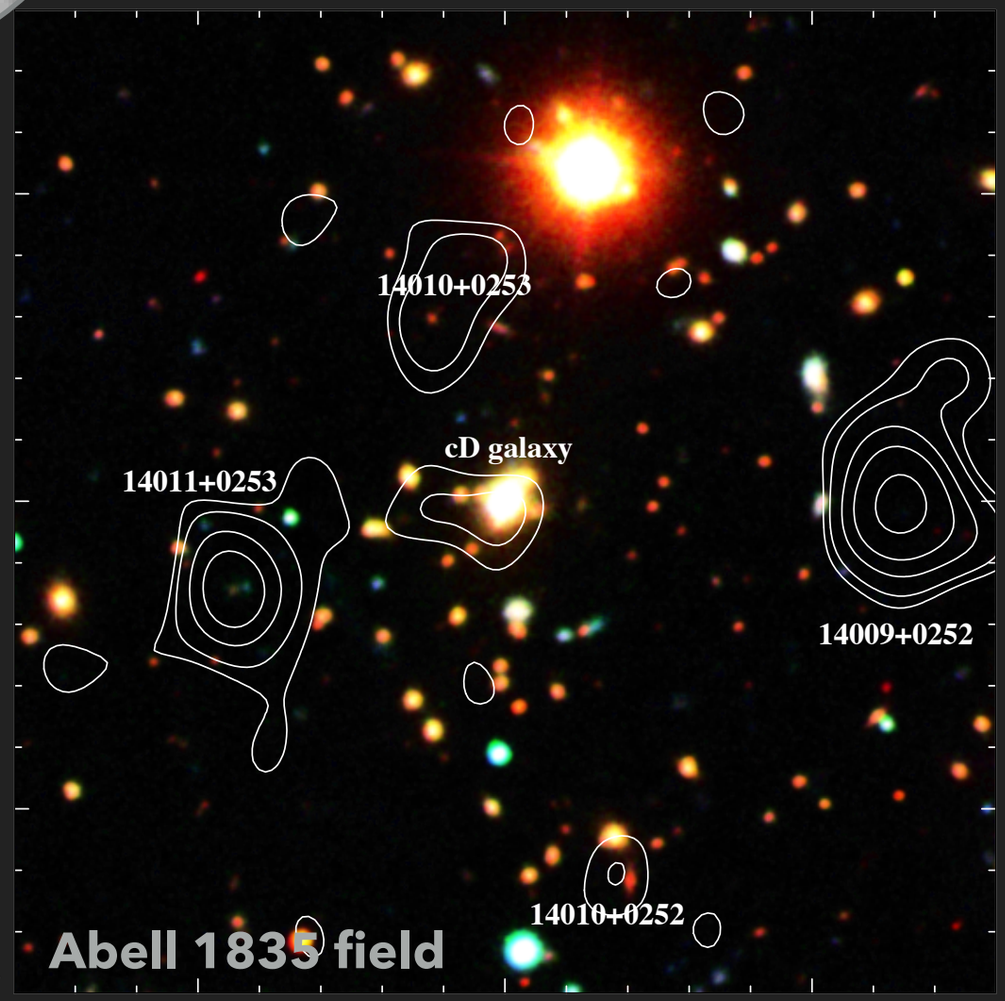

Intense Starburst Galaxies at z ~ 2

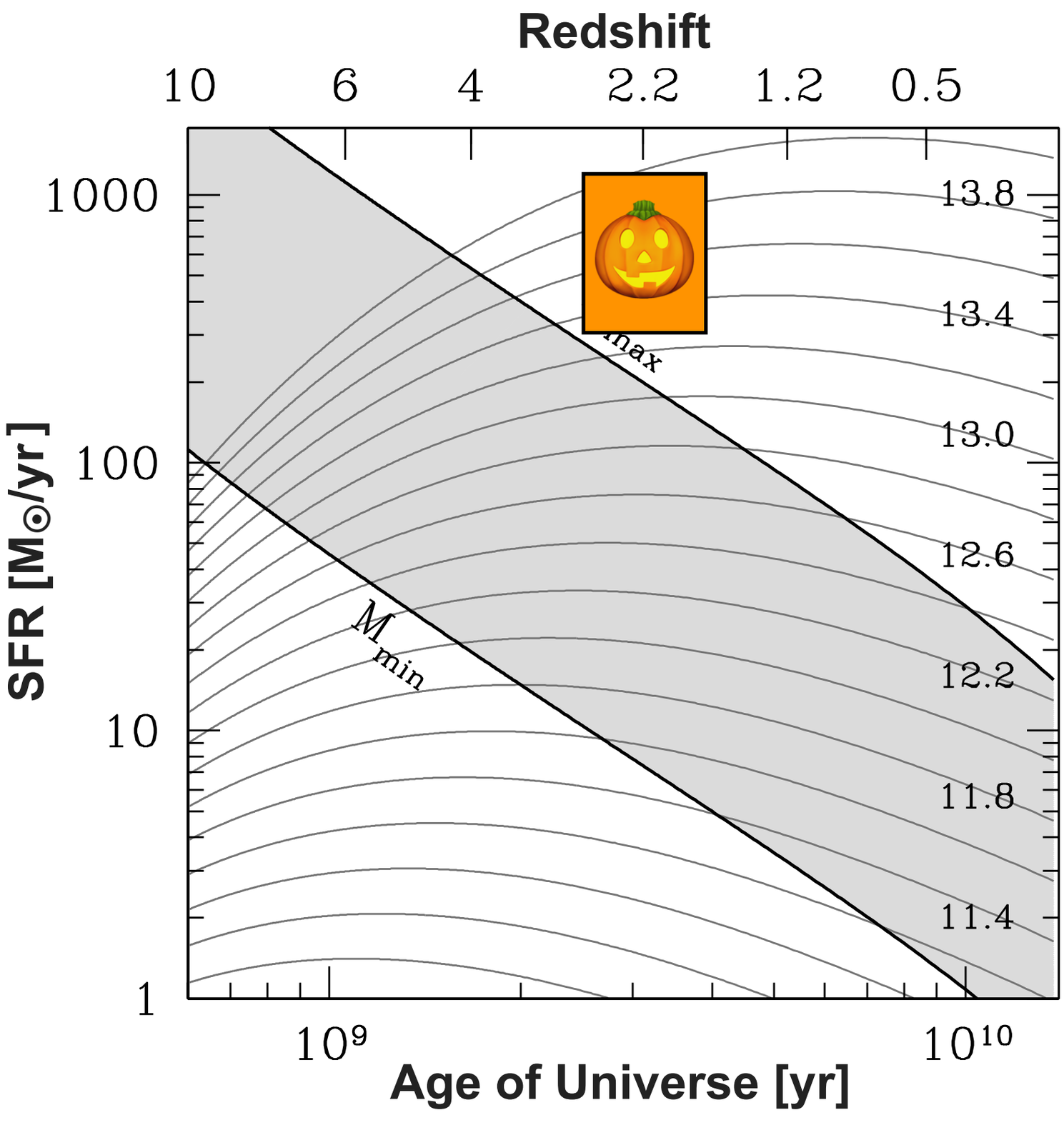

- **Green region:** star formation tracks of all halos less than 10^{14} $M_\odot$ at $z = 0$.
- **Orange: The SFRs of these galaxies appear too high for any halos at their epoch.**

Misaligned stellar and ISM emission

typical offsets: a few kpc (0.5" = 4 kpc @ z = 2.5)

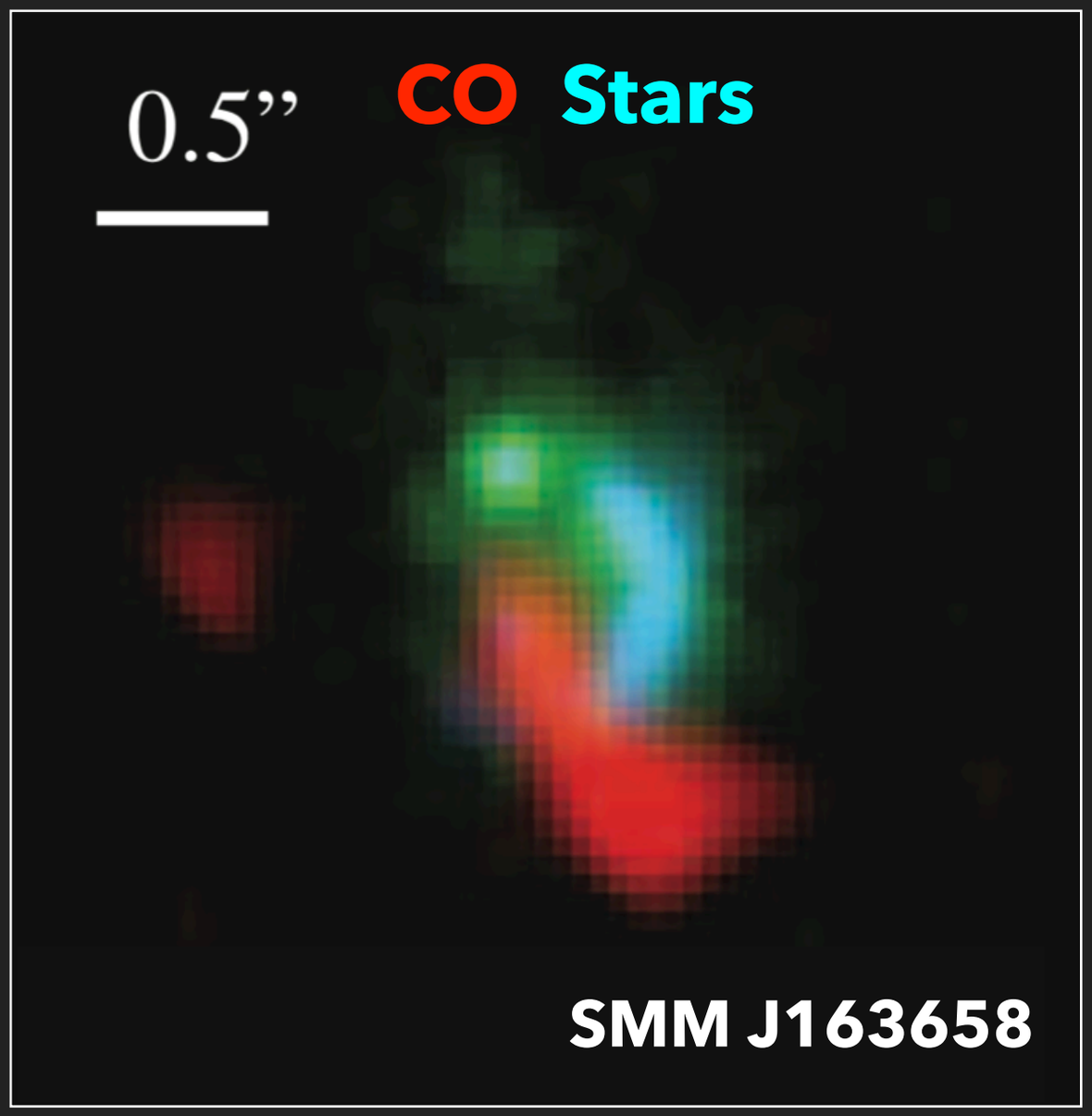

Tacconi+2008

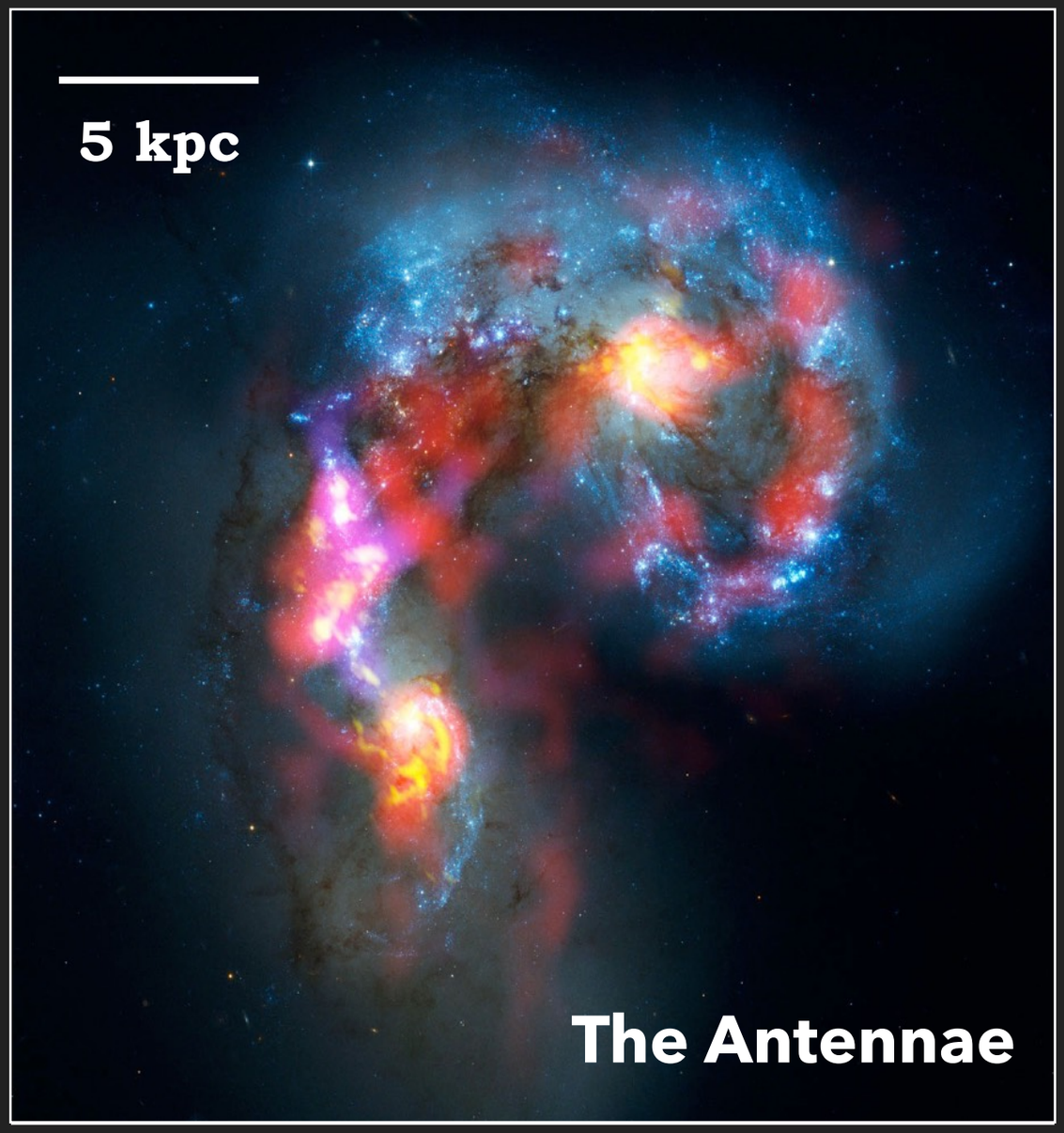

Calistro Rivera+2018

A clumpy, rotating gas disk in an SMG

GN20, CO J=2-1 @ z = 4.05, VLA observations

$M_{dyn} = 5x10^{11}\ M_{sun}$, disk diameter ~ 14 kpc

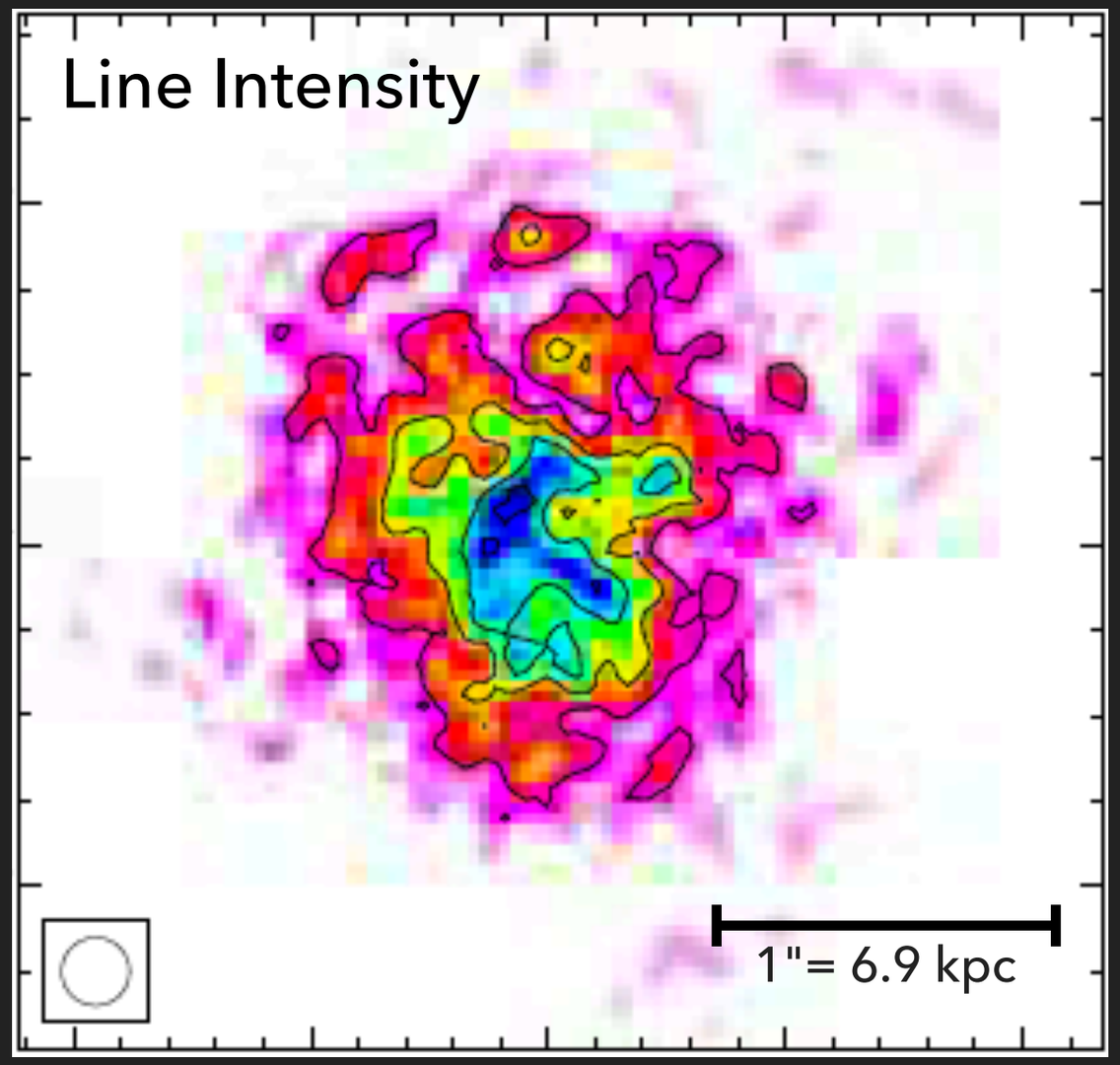

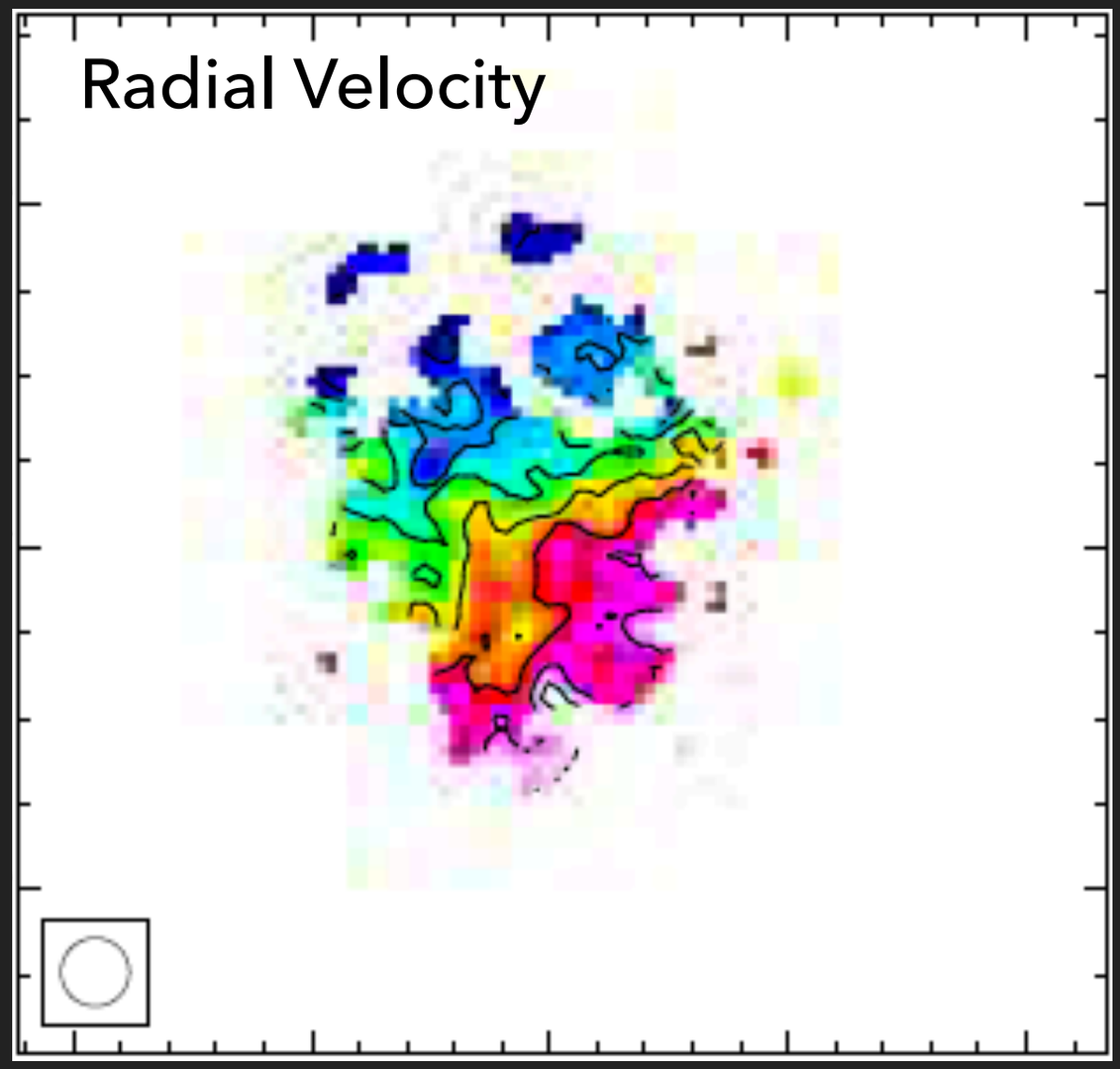

Hodge+2012

Resolved gas kinematics in an SMG merger

ALMA Cycle 3, 2.6 hr on-source, 0.2" spatial resolution, 240 GHz (band 6, z = 2.308)
CO J=7-6 @ 806.7 GHz, [C I] $^3P_2$ - $^3P_1$ @ 809.3 GHz, H_2O 2_{11} - 2_{02} @ 752.0 GHz

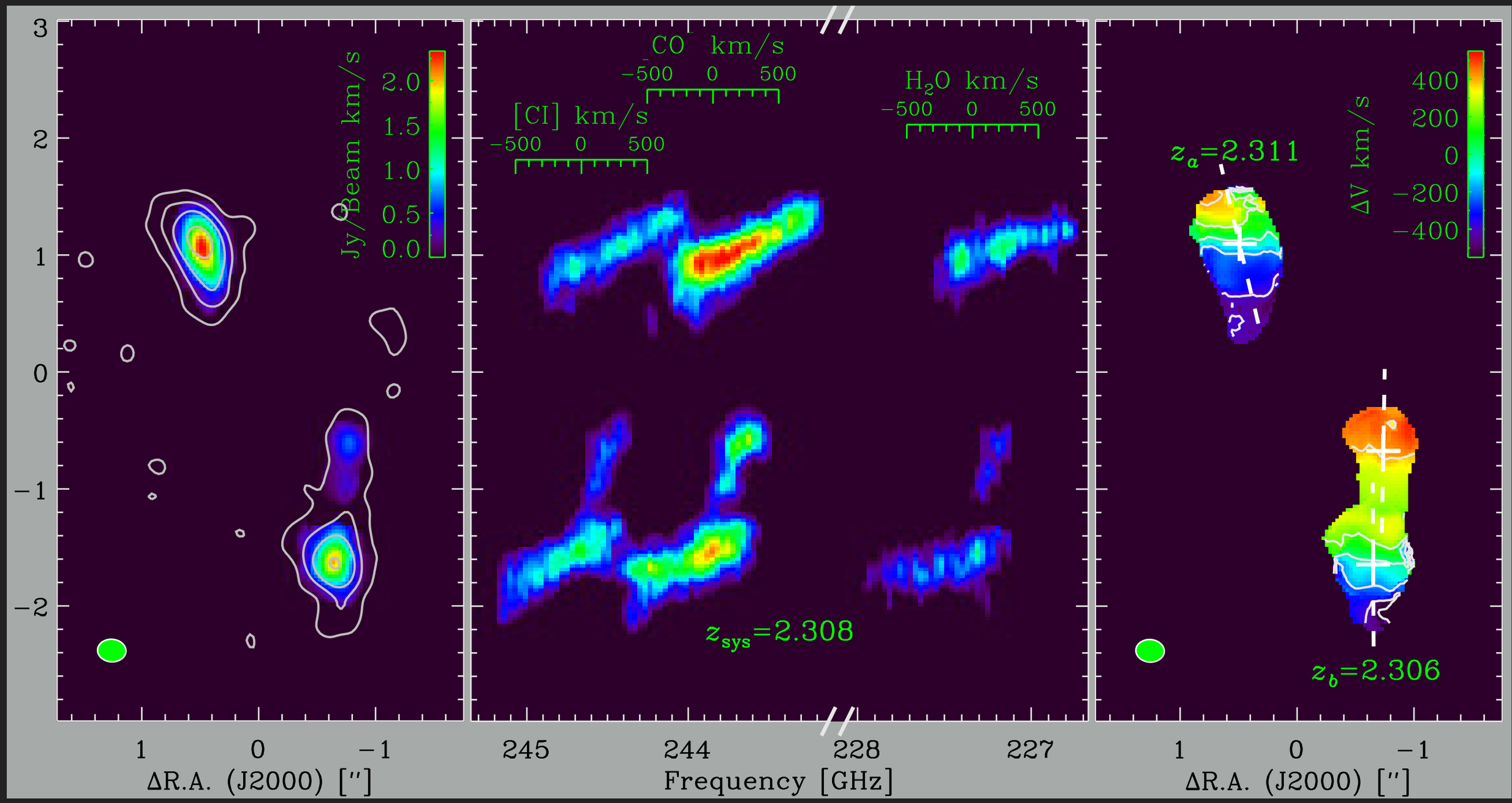

Xue, Fu+2018

Dynamical mass estimates

- Rotation velocities reach 500 km/s (inclination corrected), with a dispersion ~ 160 km/s
- Dynamical masses: M_{dyn} ~ 2x10^{11} M_{sun} within 5 kpc
- CO(1-0) luminosity: L'_{CO} ~ 1.5x10^{11} K km/s pc^2
- Upper limits on the CO-to-H2 conversion factor: M_{H2}/L'_{CO} < 1.5, much lower than the Galactic GMC value of 4.3.

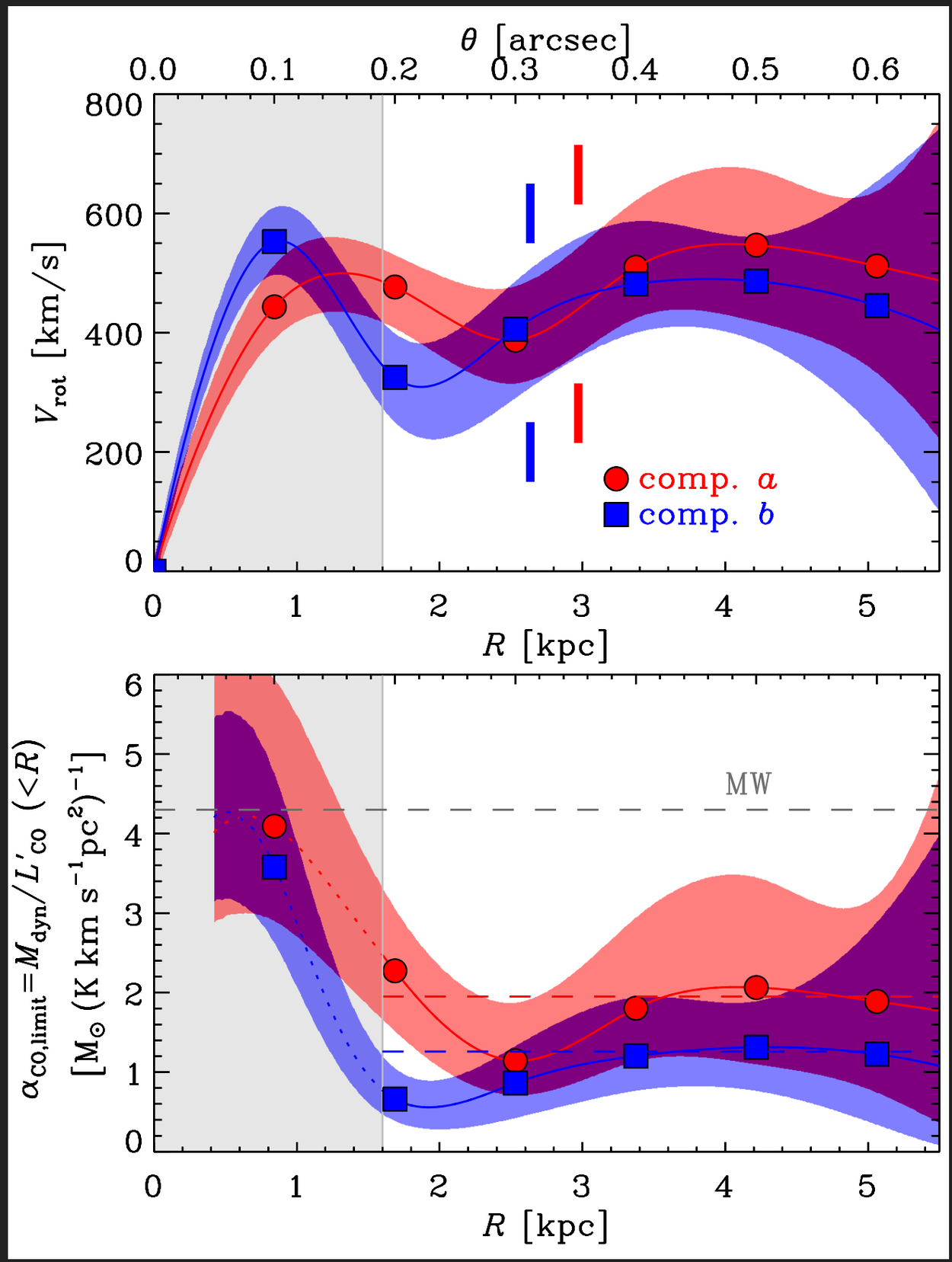

Xue, Fu+2018

The Unsustainable Growth of SMGs

- M_{gas}/SFR ~ 100 Myr
- 10x greater SFR for any given gas mass
- 10x shorter gas depletion timescale than normal star-forming galaxies
- Without continuous gas supply, SFR will decline with an e-folding timescale of ~200 Myr

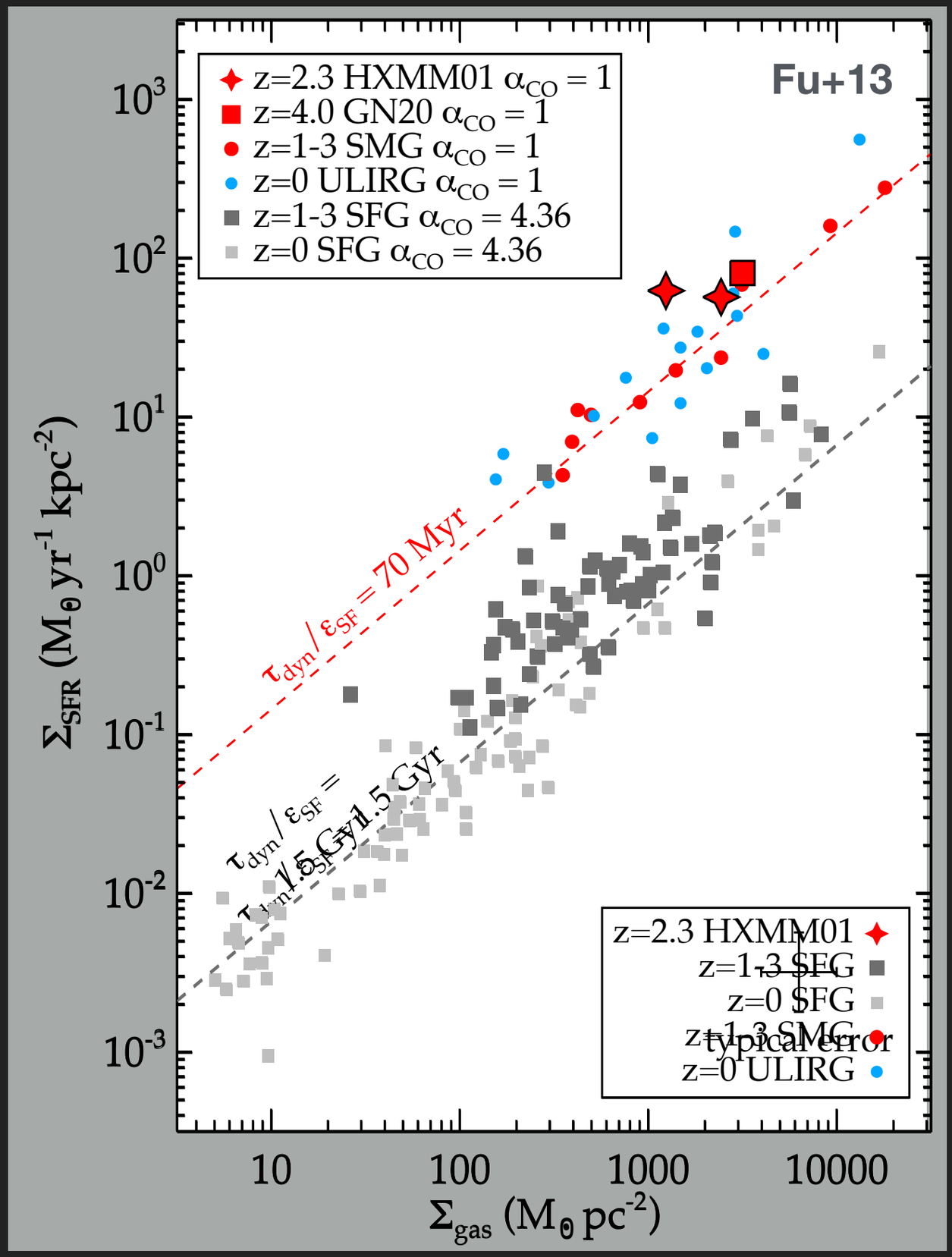

So, what's up with the SMGs?

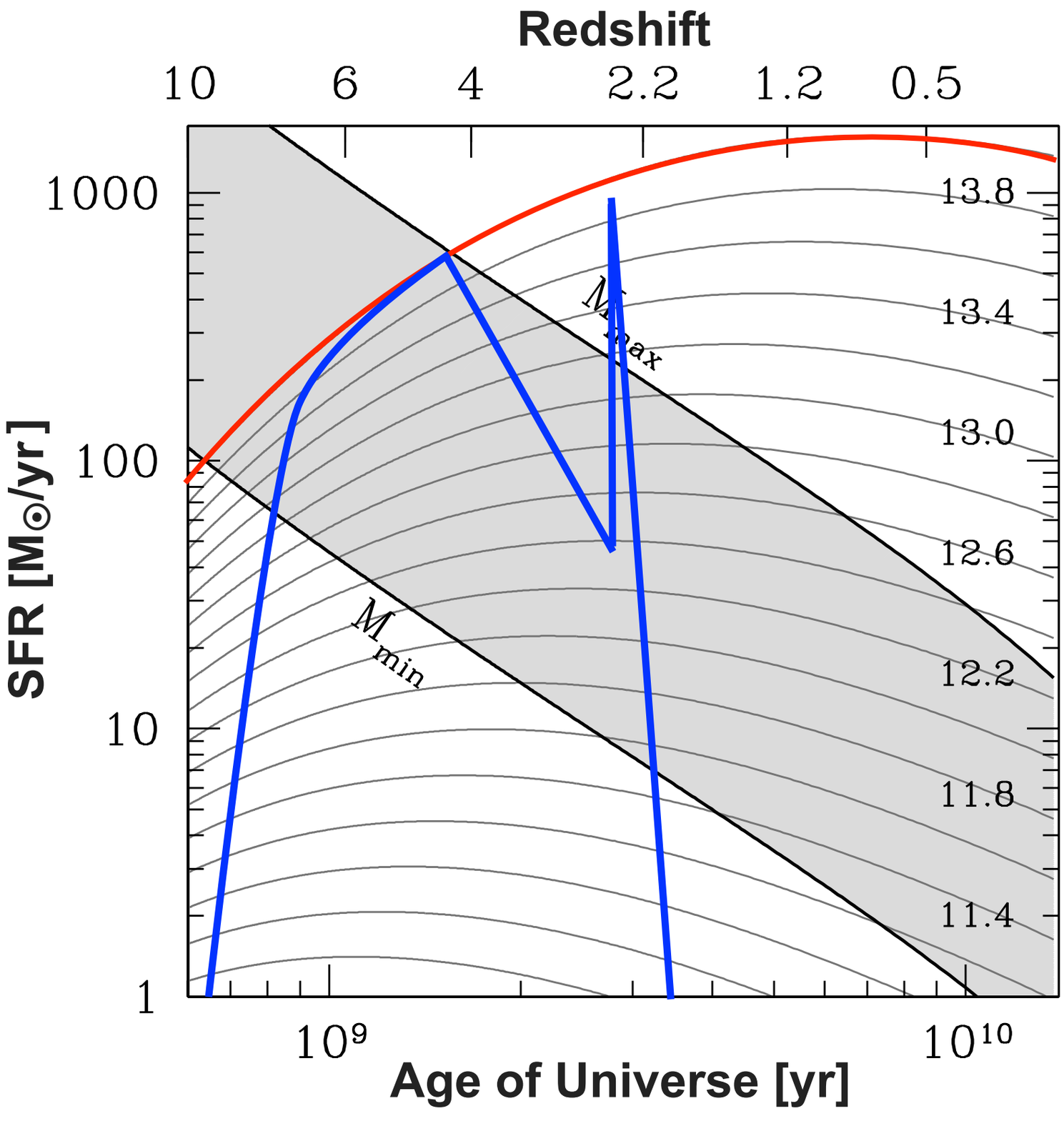

✓: Burst: Star formation efficiency increases 10x in **10^{13}** $M_\odot$ halos.

Implications:

- two distinct populations of SMGs: z > 4 and z ~ 2

- high stellar masses (~2×10^{11} M_{sun})

- relatively low gas fraction

- helps explain the early, rapid formation of massive quiescent galaxies

The early & rapid build-up of the red sequence

the evolution of the total comoving stellar mass density of quiescent galaxies

- **Early Completion**: Most of the stellar mass in the red sequence is already in place by $z = 1$
- **Rapid Build-Up**: Stellar mass density increased more than 20x in just 2.5 Gyr ($1 < z < 2$).
- *Not* observed in star-forming galaxies

Ilbert+2010

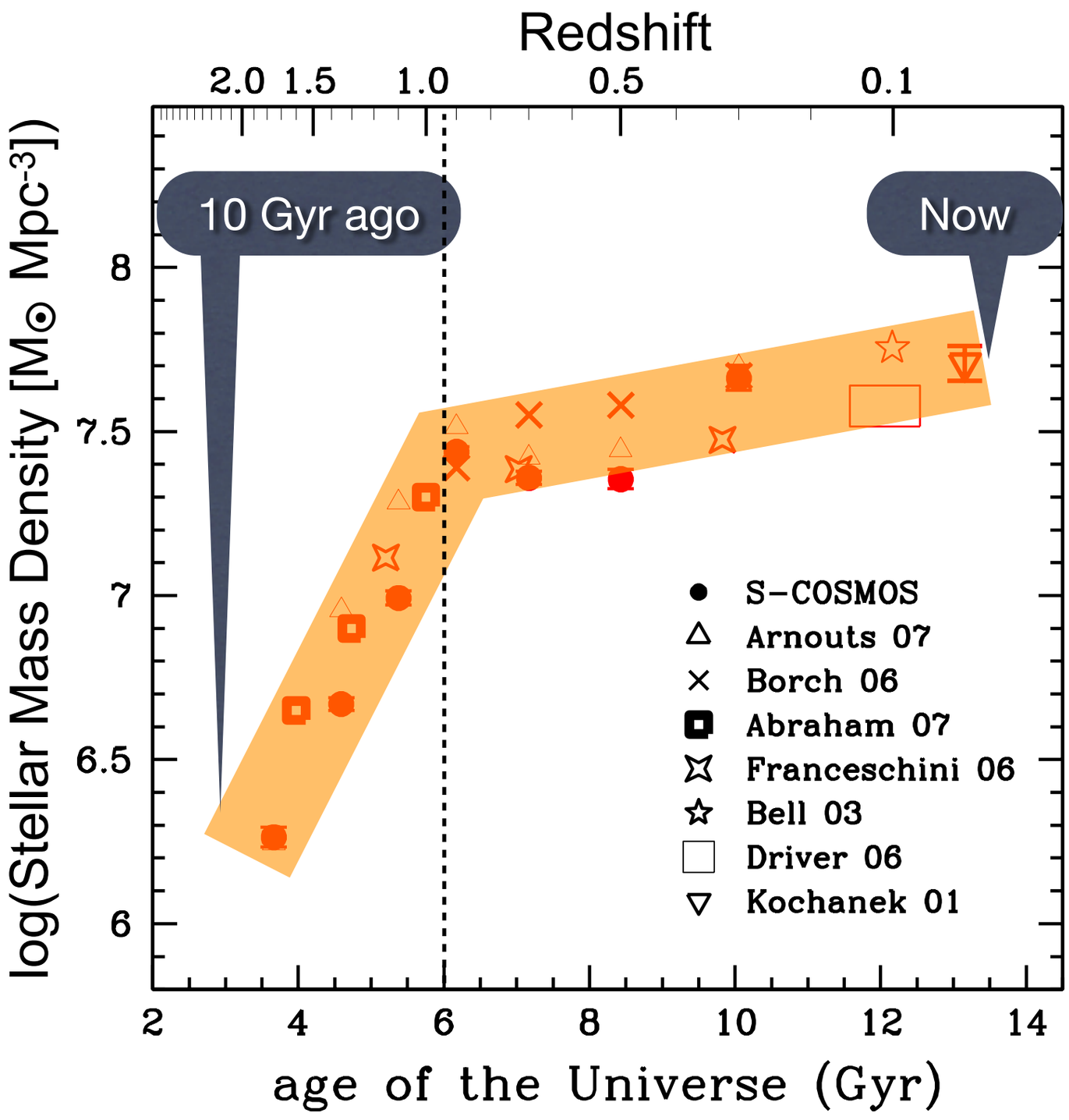

SMGs have lower gas fraction than normal SFGs?

Data Points: gas fractions measured w/ Tully-Fisher relation & $\alpha_{CO} = 1$

Curves: gas fractions inferred from sSFR(z) of different stellar masses

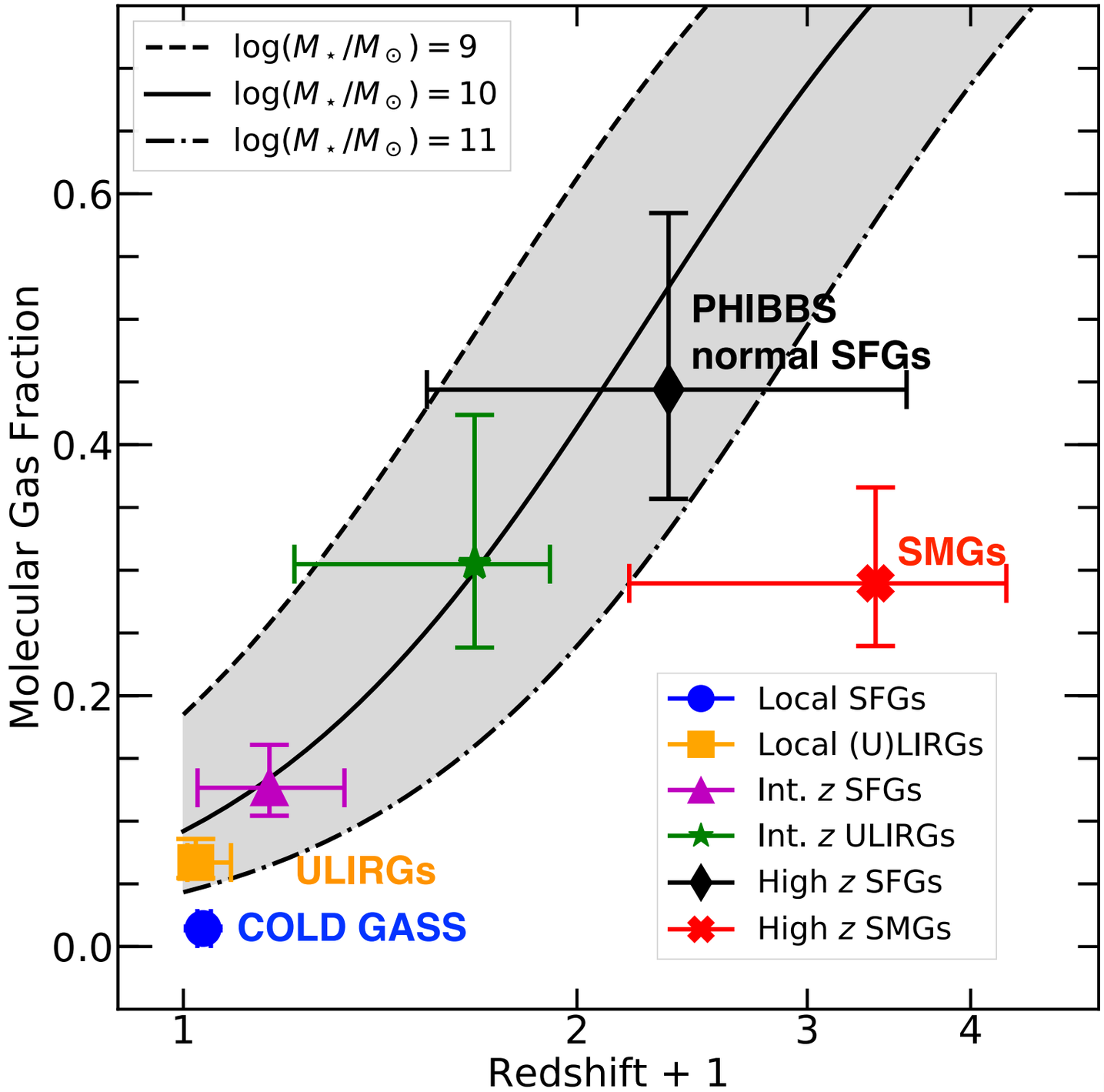

Isbell, Xue, Fu 2018

one stone two birds

- SMGs have ~10x higher SF efficiency than normal galaxies, i.e., they are massive starbursts
- Starbursts can stop star formation by rapidly exhausting the gas reservoir, providing a quenching mechanism to turn blue starforming galaxies into red passive galaxies.
- Starbursts are a universal phase in the formation of massive red galaxies. All galaxy formation models should be able to reproduce this important phase.
- *What triggers the high star formation efficiency? Why every massive galaxy goes through a burst phase?*